الجمهورية الجزائرية الديمقراطية الشعبية
République Algérienne Démocratique et Populaire
وزارة التعليم العالي والبحث العلمي
Ministère de l'Enseignement Supérieur et de la Recherche Scientifique
جامعة سعيدة الدكتور مولاي الطاهر
Université de Saida Dr MOULAY Tahar

كلية علوم الطبيعة والحياة
N° d'Ordre
Faculté des Sciences de la nature et de la Vie
قسم البيولوجيا
Département de Biologie

Mémoire pour l'obtention du diplôme de Master

En Sciences biologiques

Spécialité : Microbiologie Appliquée

Thème

Biogenic synthesis of Nanocopper particles and their applications.

Présenté par :

- Melle : **MOULAI** Rania
- Melle : **MOKHTARI** Hounaida

Soutenu le : / /2025

Devant le jury composé de :

Présidant	Mr. **Yahia Nasrallah**	Professeur Université USMT
Examinateur	Mme. **Fouzia Kheira Boukabene**	MCA Université USMT
Rapporteur	Mr. **Mohamed Amine Gacem**	MCB Université USMT

Année universitaire 2024/2025

Dedication

A special and eternal dedication goes to my beloved mother, whose love, strength, and sacrifices have been my greatest source of support. Her presence and prayers have accompanied me through every stage of my studies.

To my dear father, whose trust and encouragement have given me the courage to persevere, and to my brothers and sisters, whose affection and constant support have brightened my path — I owe you all so much.

Finally, to everyone who believed in me and contributed, even in the smallest way, to the completion of this work — I dedicate this achievement to you with heartfelt gratitude.

Rania Moulai

Dedication

I dedicate this work— the culmination of perseverance and growth— to myself, Mokhtari Hounaida, as a tribute to the strength, determination, and patience I have discovered throughout this academic journey.

With deep love and endless gratitude, I dedicate it to my beloved parents. Their unwavering support, sacrifices, and prayers have been the foundation of my success. May God protect them and reward them for their boundless love and faith in me.

To my dear family—especially my sisters, Chaimaa and Fatima, and my brother, Karim—thank you for your constant encouragement, kind words, and comforting presence, which uplifted me in moments of doubt.

To my cherished friends—Rania, Sirine, Ikram, Amira, Inas, Kouloud, Faiza, Chamsou, Mahmoud, and Walid—as well as my entire class and group of friends: your kindness, encouragement, and the laughter we've shared have made this path brighter and more meaningful. You have been my strength, and I am endlessly thankful for you.

May this dedication reflect the depth of my appreciation for all who believed in me and walked beside me throughout this unforgettable chapter.

Hounaida Mokhtari

Remerciements

This work was carried out at the Pedagogical Laboratory of the University of Saida, at the Research Center in Analytical Chemistry and Physics (CRAPC) in Laghouat, and at the Microbial Strain Collection Laboratory, Helmholtz Centre for Infection Research (HZI), Inhoffenstrasse, Braunschweig, Germany.

Before anything else, we give thanks to Almighty God for granting us the strength and patience to complete this work.

We wish to express our deepest gratitude and sincere appreciation to Dr. Mohamed Amine GACEM, from the Faculty of Natural and Life Sciences, University of Saida, for his supervision and scientific guidance. His availability, insightful advice, and the trust he placed in us were invaluable to the successful completion of this research.

Our heartfelt thanks are also extended to Mrs. Hajer, laboratory engineer at the Faculty of Natural and Life Sciences, University of Saida, for her contribution to the realization of this work and for her precious guidance, to whom we express our sincere gratitude.

We would also like to express our sincere thanks to Mr. Larbi SNOUCI, engineer at the CRAPC in Laghouat, for his assistance in the nanostructure characterization phase of this research.

We are deeply grateful to Professor Yahia NASRALLAH, from the Faculty of Natural and Life Sciences, University of Saida, for the honor he bestowed upon us by accepting to preside over the defense of this thesis.

Finally, we extend our warmest thanks to Dr. Fouzia BOUKABANE and Dr. Habiba BELGACEM, from the University of Saida, for the honor they have done us by agreeing to examine this thesis.

Table of contents.

Abreviations list

16S rRNA:	16S Ribosomal Ribonucleic Acid
ANI:	Average Nucleotide Identity
BGC:	Biosynthetic Gene Cluster
BGCs:	Biosynthetic Gene Clusters
CAT:	Catalase Activity
CFU:	Colony Forming Unit
CSA:	Casein Starch Agar
CuNPs:	Copper Nanoparticles
Cu^{2+}:	Copper Ion (Cupric Ion)
Cu^{0}:	Metallic Copper
Cu_2O:	Cuprous Oxide
Ca@CuO@Cu:	Calcium-doped Copper Oxide Nanostructures
DDH:	DNA–DNA Hybridization
DDDH:	Digital DNA–DNA Hybridization
DLS:	Dynamic Light Scattering
DNA:	Deoxyribonucleic Acid
DON:	Deoxynivalenol
DT:	Degree of Turbidity
DPPH:	2,2-Diphenyl-1-picrylhydrazyl
EtOA:	Ethyl Acetate
FTIR:	Fourier Transform Infrared Spectroscopy
FTU:	Fungal Taxonomic Unit
GC%:	Guanine–Cytosine Content
GYM:	Glucose–Yeast extract–Malt extract
GT:	Growth after Treatment
HV agar:	Humic acid–Vitamin Agar
MIC:	Minimum Inhibitory Concentration
NaCl:	Sodium Chloride
NMs:	Magnetic Nanomaterials
NPs:	Nanoparticles
NM:	Nanometer
OD:	Optical Density
PDA:	Potato Dextrose Agar
PCR:	Polymerase Chain Reaction
pH:	Potential of Hydrogen
ROS:	Reactive Oxygen Species

RNA:	Ribonucleic Acid
RPM:	Revolutions per Minute
SDS:	Sodium Dodecyl Sulfate
SD:	Standard Deviation
SEM:	Scanning Electron Microscopy
SOD:	Superoxide Dismutase
sp.	Species
SPR:	Surface Plasmon Resonance
SPSS:	Statistical Package for the Social Sciences
TEM:	Transmission Electron Microscopy
µg/mL:	Microgram per Milliliter
UPLC–MS:	Ultra-High-Performance Liquid Chromatography–Mass Spectrometry
UV–Vis:	Ultraviolet–Visible Spectroscopy
XRD:	X-Ray Diffraction

Figures list

Tables list

Abstract

This research investigates the biogenic synthesis, structural characterization, and bio-agronomic potential of calcium-doped copper nanostructures (Ca@CuO@Cu) produced via a green route mediated by the metabolites of *Streptomyces sp.* T_{003}. The study was designed to bridge microbiology, nanotechnology, and plant pathology, aiming to develop eco-friendly nanomaterials capable of replacing conventional chemical fungicides and fertilizers.The *Streptomyces* strain T_{003} was successfully revived and characterized on GYM and CSA media, showing abundant aerial and substrate mycelia, sporulation, and strong pigment diffusion typical of highly active actinobacteria. Simultaneously, three major phytopathogenic fungi *Fusarium oxysporum*, *Rhizoctonia solani*, and *Phytophthora infestans* were isolated and identified through their cultural and microscopic traits, representing the main soil-borne and foliar diseases affecting tomato crops.The green synthesis of calcium-doped copper nanostructures was visually evidenced by the characteristic color transition from blue to dark brown or black, indicating the reduction of Cu^{2+} to Cu^0/Cu_2O. UV–Visible spectroscopy revealed a broad surface plasmon resonance (SPR) band at 540– 590 nm, confirming metallic copper formation. XRD analysis showed crystalline peaks corresponding to monoclinic CuO (JCPDS 45-0937), metallic Cu (JCPDS 04-0836), and minor $CaO/CaCO_3$ reflections, demonstrating the successful formation of a hybrid Ca@CuO@Cu structure. FTIR spectra indicated the presence of hydroxyl, carbonyl, and Cu–O vibrations associated with *Streptomyces*- derived biomolecules acting as reducing and capping agents. SEM micrographs revealed irregularly shaped nanoparticles with an average size of 260–270 nm.Biological assays confirmed a multifunctional activity spectrum. Calcium-doped copper nanostructures exhibited strong antifungal effects in a dose-dependent manner, with *Phytophthora infestans* being the most sensitive, followed by *Fusarium oxysporum* and *Rhizoctonia solani*. Antioxidant activity, assessed by the DPPH assay, showed an inverse dose-response: nearly 100 % radical scavenging at 0.1 $mg \cdot mL^{-1}$ but declining at higher concentrations due to nanoparticle aggregation and possible pro-oxidant ROS generation. Insecticidal tests demonstrated time- and dose- dependent lethality, reaching 100 % mortality above 1 $mg \cdot mL^{-1}$ ($LC_{50} \approx$ 0.6–0.8 $mg \cdot mL^{-1}$ after 72 h).Agronomic experiments using tomato (*Solanum lycopersicum L.*) seedlings revealed that low to moderate calcium-doped copper nanostructures concentrations (0.5–0.75 $mg \cdot mL^{-1}$) significantly enhanced root and shoot growth, chlorophyll synthesis, and biomass accumulation, whereas higher concentrations ($\geqslant$ 1 $mg \cdot mL^{-1}$) induced phytotoxic effects through oxidative stress. In greenhouse trials, foliar spraying of Ca@CuO@Cu (0.1 $g \cdot L^{-1}$) ten days after fungal inoculation substantially reduced wilting, necrosis, and leaf blight, while improving overall plant vigor compared to both infected controls and chemically treated plants.Collectively, the results demonstrate that biogenic Ca@CuO@Cu produced by actinomycetes combine antifungal, antioxidant, insecticidal, and plant-growth-promoting properties, offering a sustainable alternative to synthetic agrochemicals and paving the way for their integration into environmentally responsible crop protection programs.

Keywords: Biogenic synthesis, Copper oxide nanoparticles, Streptomyces sp. T003, Antifungal activity, Antioxidant activity, Plant growth promotion, Nanotechnology.

Résumé

Cette recherche porte sur la synthèse biogénique, la caractérisation structurale et le potentiel bio-agronomique de nanostructures de cuivre dopées au calcium (Ca@CuO@Cu), produites par une voie verte médiée par les métabolites de *Streptomyces sp*. T_{003}. L'étude a été conçue pour établir un lien entre la microbiologie, la nanotechnologie et la phytopathologie, dans le but de développer des nanomatériaux écologiques capables de remplacer les fongicides et engrais chimiques conventionnels.La souche *Streptomyces* T_{003} a été réactivée et caractérisée sur les milieux GYM et CSA, montrant une abondante mycéliation aérienne et substratée, une sporulation active et une forte diffusion pigmentaire, caractéristiques des actinobactéries hautement actives. Parallèlement, trois champignons phytopathogènes majeurs ; *Fusarium oxysporum*, *Rhizoctonia solani* et *Phytophthora infestans* ont été isolés et identifiés à partir de leurs caractères culturaux et microscopiques, représentant les principales maladies telluriques et foliaires affectant les cultures de tomate.La synthèse verte des nanostructures de cuivre dopées au calcium a été mise en évidence visuellement par le changement de couleur caractéristique, du bleu au brun foncé voire au noir, indiquant la réduction du Cu^{2+} en Cu^0/Cu_2O. La spectroscopie UV–Visible a révélé une large bande de résonance plasmonique de surface (SPR) entre 540 et 590 nm, confirmant la formation de cuivre métallique. L'analyse XRD a montré des pics cristallins correspondant au CuO monoclinique (JCPDS 45-0937), au Cu métallique (JCPDS 04-0836) et à de faibles réflexions de $CaO/CaCO_3$, démontrant la formation réussie d'une structure hybride Ca@CuO@Cu. Les spectres FTIR ont indiqué la présence de groupements hydroxyle, carbonyle et de vibrations Cu–O, associés aux biomolécules dérivées de *Streptomyces*, jouant le rôle d'agents réducteurs et stabilisateurs. Les micrographies MEB (SEM) ont révélé des nanostructures de forme irrégulière, d'une taille moyenne comprise entre 260 et 270 nm.Les tests biologiques ont confirmé un spectre d'activités multifonctionnel. Les nanostructures de cuivre dopées au calcium ont montré de fortes activités antifongiques dépendantes de la dose, *Phytophthora infestans* étant le plus sensible, suivi de *Fusarium oxysporum* et *Rhizoctonia solani*. L'activité antioxydante, évaluée par le test DPPH, a révélé une réponse inverse à la dose : près de 100 % de piégeage des radicaux libres à 0,1 $mg \cdot mL^{-1}$, mais une diminution à des concentrations plus élevées en raison de l'agrégation des nanoparticules et de la possible génération de ROS pro-oxydants. Les essais insecticides ont montré une létalité dépendante du temps et de la dose, atteignant 100 % de mortalité au-delà de 1 $mg \cdot mL^{-1}$ ($CL_{50} \approx 0{,}6–0{,}8\ mg \cdot mL^{-1}$ après 72 h).Les expériences agronomiques menées sur des plants de tomate (*Solanum lycopersicum L.*) ont révélé que des concentrations faibles à modérées de nanostructures dopées au calcium (0,5–0,75 $mg \cdot mL^{-1}$) stimulaient significativement la croissance racinaire et caulinaire, la synthèse de chlorophylle et l'accumulation de biomasse, tandis que des concentrations plus élevées ($\geq 1\ mg \cdot mL^{-1}$) provoquaient des effets phytotoxiques liés au stress oxydatif.Lors des essais en serre, la pulvérisation foliaire de Ca@CuO@Cu (0,1 $g \cdot L^{-1}$), dix jours après l'inoculation fongique, a considérablement réduit le flétrissement, la nécrose et la brûlure foliaire, tout en améliorant la vigueur générale des plantes par rapport aux témoins infectés et aux plantes traitées chimiquement.Dans l'ensemble, les résultats démontrent que les nanostructures biogéniques Ca@CuO@Cu, produites par des actinomycètes, associent des propriétés antifongiques, antioxydantes, insecticides et

stimulatrices de la croissance végétale, offrant ainsi une alternative durable aux agrochimiques synthétiques et ouvrant la voie à leur intégration dans des programmes de protection des cultures écologiquement responsables.

Mots-clés : Synthèse biogénique, Nanoparticules d'oxyde de cuivre, Streptomyces sp. T003, Activité antifongique, Activité antioxydante, Promotion de la croissance des plantes, Nanotechnologie.

الملخص

يتناول هذا البحث التخليق الحيوي لجسيمات النحاس النانوية وتوصيفها البنيوي وتقييم إمكاناتها الحيوية في المجال الزراعي، بطريقة خضراء صديقة للبيئة اعتماداً على نواتج الأيض (Ca@CuO@Cu حيث تحضير جسيمات النحاس المطعّمة بالكالسيوم (Streptomyces sp. T003. الحيوية لبكتيريا يهدف هذا العمل إلى دمج علم الأحياء الدقيقة مع تقنيات النانو وأمراض النبات من أجل تطوير مواد نانوية مستدامة يمكن أن تمثل بديلاً فعالاً وآمناً للمبيدات الفطرية والأسمدة الكيميائية التقليدية. أظهرت سلالة Streptomyces T003 مع تكوّن الخيوط الفطرية الهوائية والسطحية وإنتاج الأبواغ وانتشار GYM و CSA نمواً جيداً على أوساط واضح للأصباغ، وهي خصائص مميزة للبكتيريا الشعاعية النشطة، وفي المقابل تم عزل وتحديد ثلاثة فطريات ممرضة للنباتات هي باعتبارها من أهم مسببات الأمراض الترابية Phytophthora infestans و Rhizoctonia solani و Fusarium oxysporum والورقية التي تصيب محصول الطماطم. تمت ملاحظة التخليق الأخضر لجسيمات النحاس النانوية المطعّمة بالكالسيوم بصرياً من إلى البني الداكن أو الأسود مما يدل على اختزال أيونات النحاس، كما أظهرت مطيافية الأشعة (Cu^{2+} خلال التغير اللوني من الأزرق (نطاق امتصاص واسع بين 540 و590 نانومتر مؤكدة تكوّن النحاس المعدني. أظهر تحليل حيود (UV–Vis فوق البنفسجية–المرئية (مع وجود انعكاسات طفيفة لأكاسيد وكربونات (CuO قمماً بلورية متوافقة مع أكسيد النحاس الأحادي ((XRD الأشعة السينية (وجود (FTIR كما بينت أطياف الأشعة تحت الحمراء (،Ca@CuO@Cu الكالسيوم مما يدل على التكوين الناجح للبنية الهجينة والتي تعمل Streptomyces المرتبطة بالجزيئات الحيوية المشتقة من Cu–O مجموعات الهيدروكسيل والكربونيل واهتزازات جسيمات نانوية غير منتظمة الشكل (SEM كعوامل مختزلة ومثبتة للجسيمات النانوية. أظهرت صور المجهر الإلكتروني الماسح (بمتوسط حجم يتراوح بين 260 و270 نانومتر. أكدت الاختبارات البيولوجية أن للجسيمات النانوية طيفاً واسعاً من الأنشطة الحيوية، Fusarium الأكثر حساسية تليها Phytophthora infestans حيث أظهرت نشاطاً مضاداً للفطريات يعتمد على التركيز وكانت نشاطاً مضاداً للأكسدة بلغ قرابة 100% عند تركيز 0.1 ملغ/مل DPPH كما أظهر اختبار ،Rhizoctonia solani و oxysporum وأثبتت الاختبارات .(ROS ثم انخفض عند التراكيز الأعلى نتيجة تكتل الجسيمات النانوية وإمكانية توليد أنواع الأكسجين التفاعلية (الحشرية فعالية عالية تعتمد على الزمن والتركيز حيث بلغت نسبة الوفيات 100% عند تراكيز 0.6–0.8 ملغ/مل بعد 72 ساعة، كما أن التراكيز المنخفضة إلى المتوسطة (0.5–0.75 (.Solanum lycopersicum L بينت التجارب الزراعية على شتلات الطماطم (ملغ/مل) حفزت نمو الجذور والسيقان وزادت من محتوى الكلوروفيل والكتلة الحيوية في حين أدت التراكيز العالية (≤1 ملغ/مل) إلى بتركيز Ca@CuO@Cu تأثيرات سمية نباتية ناتجة عن الإجهاد التأكسدي، وفي تجارب البيوت المحمية أدى الرش الورقي بمحلول 0.1 غ/لتر إلى انخفاض ملحوظ في أعراض الذبول والنخر واللفحات الورقية مع تحسن واضح في حيوية النبات مقارنة بالنباتات المصابة أو المعالجة كيميائياً، وتُظهر هذه النتائج مجتمعة أن الجسيمات النانوية الحيوية المنتجة بواسطة البكتيريا الشعاعية تجمع بين الخصائص المضادة للفطريات والمضادة للأكسدة والمبيدة للحشرات والمنشطة لنمو النباتات مما يجعلها بديلاً مستداماً وواعداً للمواد الكيميائية الزراعية الاصطناعية ويفتح آفاقاً واسعة لتطبيقها في برامج حماية المحاصيل الصديقة للبيئة.

الكلمات المفتاحية:

التخليق الحيوي، جسيمات أكسيد النحاس النانوية، النشاط المضاد للفطريات، النشاط المضاد للأكسدة، تعزيز نمو النبات، تكنولوجيا النانو، Streptomyces sp. T003.

Introduction

Introduction

The term "*nanotechnology*" was first introduced to the scientific community by Eric Drexler in his seminal book Engines of Creation (**Rajput et al., 2018**). Nanotechnology encompasses a multidisciplinary domain of research and technological innovation dedicated to the design, fabrication, and application of materials, devices, and systems at the nanoscale—typically between 1 and 100 nanometers. These nanoscale entities, whether naturally occurring or synthetically engineered, exhibit unique physicochemical characteristics attributed to their diminutive size, including high surface area-to-volume ratios, distinct optical and electronic behaviors, and enhanced chemical reactivity (**Li et al., 2011**). Such properties endow nanoparticles with remarkable potential in diverse sectors such as medicine, agriculture, energy, environmental remediation, and pharmaceuticals **(Kumar et al., 2019).**

Traditionally, nanoparticle synthesis has been achieved through chemical, photochemical, and physical techniques, which are generally categorized into two fundamental approaches: the "top-down" and "bottom-up" strategies. The top-down approach involves the mechanical or chemical breakdown of bulk materials into nanosized particles, whereas the bottom-up approach assembles nanoparticles atom-by-atom or molecule-by-molecule (**Daniel and Astruc, 2004**). Despite their widespread use, these conventional methods present several drawbacks: they are often expensive, time-intensive, and require stringent control of reaction parameters. Moreover, they may generate toxic by-products and hazardous waste, limiting their scalability and environmental compatibility (**Muhammad et al., 2016**).

To address these challenges, green synthesis has emerged as a sustainable and eco-friendly alternative for nanoparticle production. This approach employs biological systems—such as microorganisms, fungi, and plant extracts—as reducing and stabilizing agents, enabling the synthesis of nanoparticles in a biocompatible and environmentally benign manner (**Iravani, 2011**). Green synthesis offers multiple advantages, including the minimization or elimination of toxic reagents, lower production costs, and greater control over nanoparticle morphology and dispersion (**Singh et al., 2017**).

Among the diverse microbial candidates explored for nanoparticle biosynthesis, *Actinomycetes* have gained particular attention. These filamentous, Gram-positive bacteria—abundant in soil ecosystems—are renowned for their ability to produce a wide spectrum of bioactive secondary metabolites such as enzymes, antibiotics, and reducing compounds that facilitate the bioreduction of metal ions into stable nanoparticles (**Kumar et al., 2018**). The use of *Actinomycetes* in nanoparticle synthesis presents several advantages: they are easy to cultivate, possess well-characterized metabolic pathways, and can yield nanoparticles with well-defined size, morphology, and physicochemical attributes (**Patel et al., 2019**).

Nanoparticles synthesized by *Actinomycetes* exhibit wide-ranging applications. In agriculture, they can function as antimicrobial agents or plant growth enhancers (**Singh et al., 2017**). In biomedical fields, they serve as efficient vehicles for targeted drug delivery and as potential therapeutic agents against various diseases, including cancer (**Patel et al., 2019**). Environmentally, they play a pivotal role in the detoxification and remediation of contaminated soils and water through processes such as adsorption and reduction of heavy metals (**Singh et al., 2017**).

Overall, *Actinomycetes* represent a promising, sustainable, and versatile biological platform for nanoparticle production, combining environmental safety with efficiency and broad applicability (**Singh et al., 2017; Kumar et al., 2018; Patel et al., 2019**).

To achieve this objective, a comprehensive literature review was conducted as the first part of this study. It aims to compile essential information on *Actinomycetes*, including their lifestyle, ecological significance, and biotechnological importance, as well as an overview of nanoparticles particularly copper nanoparticles their biosynthesis mechanisms, additionally, a section was devoted to reporte the biological activities of copper nanoparticles.

In the second part of this study, the methodology is presented through the description of the techniques employed to conduct the experimental work, followed by the main results and their corresponding discussion. The study concludes with a general conclusion and future perspectives.

Literature Review

I. Actinomycetes

I . Actinomycetes

Actinomycetes are unique, bodacious, and appealing gram-positive filamentous bacteria that have a high G+C content (more than 55%) and precise aerial hyphae. They are members of the phylum Actinobacteria, which is one of primary taxonomic groupings among 18 major lineages that have been identified within the bacterial domain, with numerous variations within the soil category **(Farda et al., 2020).** Phylogenetic and molecular methods have also had a big impact on how they classify things when they've been used **(Devanshi et al., 2021).** On the other hand, thanks to the emergence of molecular technology, a number of creatures that were previously classified incorrectly have been reclassified**(Jagannathan et al., 2021).** However, in recent years, 16S rRNA and the use of PCR for sequencing and analysis have frequently resulted in classification of species and phylogenies **(Rathore et al., 2021)**. At the microscopic level, life cycle of actinomycetes has three distinct appearances: vegetative mycelium (growth), aerial mycelium bearing spore cuffs **(Mishra et al., 2021)**. Both culture and microscopic traits work together to help researchers organize actinomycetes until they reach a genus **(Bhattacharyya et al., 2022).** Approximately 70% to 80% of commercially available medications and antiviral active compounds have been synthesized so far **(Rajivgandhi et al., 2021).** Due to the declining success rate of discovering novel strains, A lot more work was done to look for new chemical compounds, but it didn't work out very well because actinomycetes have been improving their abilities for a long time**(Cimermanova et al., 2021)**.Actinomycetes manufacture over 80% of all rationally developed antibiotics, with Streptomyces and Micromonospora being the most common producers **(Xie et al., 2022)**. Furthermore, actinomycetes include a variety of bioactive compounds, including

anthracyclins, aminoglycosides,carbapenem, cephalosporins, quinolones, lactams, proteomics, nucleobases, hydrocarbons, polyamides, and oxytetracycline**(Raja and Prabakarana., 2011)**. Antimicrobials pure components or quasi-derived products of natural bacteria **(He et al., 2022).** The separation of secondary metabolites from novel actinomycetes remains an important endeavor for achieving this exciting isolation and characterization of novel actinomycetes from natural income **(AbdElgawad et al., 2021).** Streptomyces is most common actinobacteria strain found in the natural environment **(Dai et al., 2021)**. Actinomycetes can be antimicrobial, plant estrogens, immunomodulatory, fungicidal, antibiotic, genotoxic, antitumor, and antiviral in nature **(Rani et al., 2021).**

I. 1. History

The first documented identification of an actinomycete was by Harz (1877-1878), who isolated Actinomyces bovis from 'lumpy jaw' in cattle. Gasperini (1890, 1892) later coined the term 'actinomycetes' (ray fungi) to describe microbes that distinguished themselves from other bacteria by their ability to form a mycelium composed of narrow hyphae (approximately 1 µm in diameter) which occasionally produced spores of a similar size. These initial studies were primarily based on clinical sample observations. The groundbreaking research of Krainsky (1914) and Waksman & Curtis (1916) revealed that actinomycetes were widespread saprophytes in the soil, and further investigations (1919-1920) provided key insights into the distribution and functions of actinomycetes, such as Streptomyces, Micromonospora, and Thermoactinomyces **(Williams, 1990).**

I. 2. Definition

Actinomycetes are typically filamentous, branched bacteria that form circular colonies composed of hyphae, which expand centrifugally from the center of growth. They occupy an intermediate position between fungi and true bacteria in terms of morphology and physiology. Notably, their ability to secrete antibiotics renders them capable of engaging in diverse biochemical reactions and synthesizing a wide range of bioactive compounds **(Bourguignon and Bourguignon, 2015).**

These actinobacteria thrive in environments with near-neutral pH levels, generally between 6.0 and 7.5 **(Soltner, 2005),** and are widely distributed in nature. They can be found in soil, air, freshwater and marine environments, compost, plant debris, pollen, melliferous plants, lichens, and numerous other substrates **(Henri, 1969 ; Goodfellow and Williams, 1983).**

A recent synthesis highlights that arid soils exhibit a higher abundance of actinobacteria and a lower prevalence of Proteobacteria, Cyanobacteria, and Planctomycetes when compared to the microbiomes of non-arid soils **(Javiera et al., 2020).**

I. 3. Characteristics of actinomycetes

I. 3. 1. Morphology of actinomycetes

The morphology of actinomycetes exhibits significant diversity, ranging from simple bacillary forms to highly complex mycelial structures. Some species develop a vegetative or substrate mycelium that grows within or on the surface of the culture medium, while others produce aerial mycelium that extends above the substrate. These filamentous structures may generate spores that are either solitary, arranged in chains, or enclosed within specialized structures such as sporangia or conidia, which release spores of various shapes and surface textures, including smooth or wrinkled appearances. Certain actinomycetes produce a non-persistent mycelium that rapidly transforms into irregular, bacteroid-like forms. In contrast, others exhibit only rudimentary mycelial development. When cultivated on solid media, actinomycetes form characteristic colonies resulting from the accumulation of branched hyphae rather than discrete cells, as observed in non-filamentous bacteria. The diameter of these colonies typically ranges between 1 and 4 mm. The colonies are typically compact, dry, and exhibit a surface that can be smooth or rough, often resembling a cauliflower shape with either smooth or lobed edges. They are frequently pigmented in various colors such as white, cream, yellow, violet, pink, or grey **(Boudemech, 2007).**

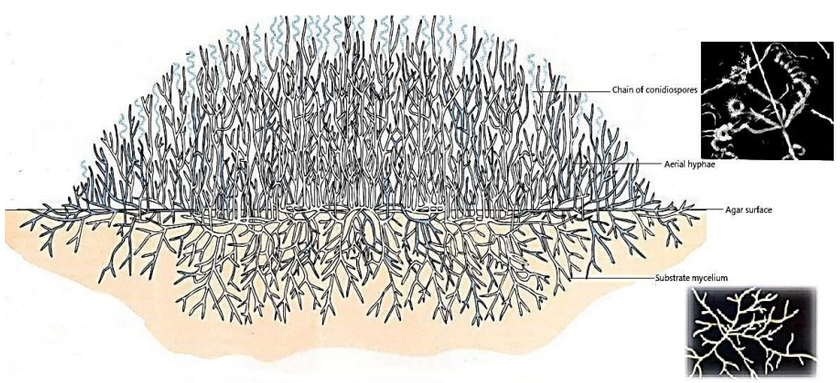

Figure 1. Actinomycetes colony growing on agar (common morphology of actinomycetes, the cross section of an actinomycete colony showing the substrate mycelium and aerial mycelium with chains of conidiospores)

I. 3. 2. Physiology

Actinomycetes are generally Gram-positive bacteria **(Locci, 1976 ; Williams et al., 1993; Sanglier and Trujillo, 1997).** They are predominantly aerobic organisms with an oxidative metabolism, although some species exhibit fermentative metabolism under anaerobic conditions. Most species are heterotrophic; however, certain strains are capable of chemolithoautotrophic growth. These organisms often require specific nutrients, such as vitamins and essential amino acids, for optimal growth. Actinomycetes are commonly found colonizing insoluble substrates such as coal and are capable of degrading complex organic compounds including proteins, cellulose, paraffin, and plant residues in the soil **(Crawford al., 1993 ; Lacey, 1997).**

I. 3. 3. Chemical characteristics

I. 3. 3. 1. Cell wall composition

The cell wall of actinomycetes lacks chitin and cellulose. Instead, it is composed of glycoproteins that may contain lysine (in fermentative forms) or diaminopimelic acid (in oxidative forms). Cytologically, actinomycetes exhibit typical bacterial features; they lack a nuclear membrane and possess flagellar organelles similar to those found in other bacteria. Most actinomycetes are sensitive to lysozyme and antibacterial agents. Notably, the diameter of their hyphae is smaller than that of fungi **(Gottlieb, 1973 ; Mariat and Sebald, 1990).**

I. 3. 3. 2. DNA Structure

The nuclear chromosome composition is a key determinant in the classification of actinomycetes families. One of the primary criteria used is the GC content, also known as the Chargaff coefficient, which represents the percentage of guanine and cytosine base pairs per 100 base pairs of DNA **(Larpent & Sanglier, 1989);** In actinomycetes, the GC content typically ranges from 63% to 76%.

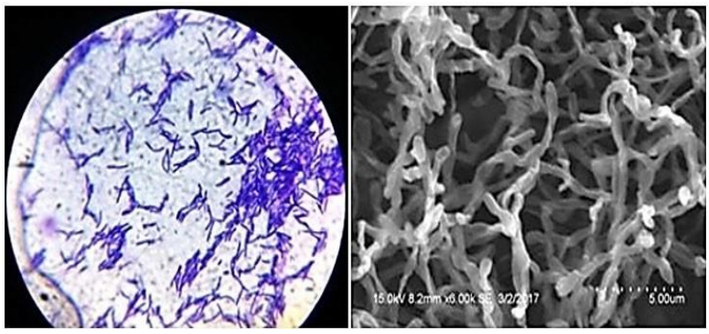

Figure 2. Gram staining (a) and Scanning Electron Microscope (b) morphology of actinomycete isolate AA1 **(Maria et al., 2018)**

I. 4. Ecology and distribution of actinomycetes

Actinomycetes are ubiquitous microorganisms commonly found in a wide range of natural substrates **(Waksman, 1959).**

I. 4 .1. Actinomycetes in Soil

Actinomycetes are widely distributed across all soil types, except in environments subjected to extreme conditions. They are particularly abundant in the layer ranging from the soil surface down to approximately 2 meters in depth, known as the rhizosphere. Among the various genera,

Streptomyces is the most predominant in soil, accounting for about 95% of all isolated actinomycete strains **(Nonomura, 1969).**

I. 4. 2. Actinomycetes in Marine

Actinomycetes have also been reported in marine environments. However, the notion that actinomycetes can colonize such habitats remains highly controversial. Some researchers argue that the actinomycete strains isolated from marine environments are merely terrestrial forms that have adapted to the saline conditions of seawater. In contrast, others suggest the existence of a distinct actinomycete community specific to marine sediments, characterized by barotolerance, halophilicity, and a preference for low optimal temperatures **(Weyland, 1981).**

I. 4. 3. Actinomycetes in Air

Air does not serve as a natural habitat for actinomycetes but rather functions as a vehicle for their dispersal. The spores produced by actinomycetes are significant environmental contaminants. Exposure to these airborne spores may lead to adverse health effects **(Gazenko et al., 1998 ; Reponen et al., 1998 ; Suutari et al., 2002).**

I. 4. 4. Thermophilic actinomycetes

Actinomycetes have been isolated at temperatures ranging from 40°C to 60°C from various substrates such as diverse soils, manure, compost, hay, and forage. These isolates are generally considered thermotolerant rather than truly thermophilic **(Lacey, 1997).**

I. 4. 5. Pathogenic Actinomycetes

Several species of Actinomycetes are known to be pathogenic to plants, animals, and humans **(McNeil, 1994; Boiron, 1995).** Notable examples include:

- Streptomyces scabies, the causative agent of potato scab;
- Actinomyces bovis, responsible for actinomycosis in cattle;
- Mycobacterium tuberculosis, the agent of tuberculosis, and Mycobacterium leprae, the causative agent of leprosy;
- Nocardia asteroides, associated with human nocardiosis;
- Micropolyspora faeni, which can cause allergic pneumonitis in humans.

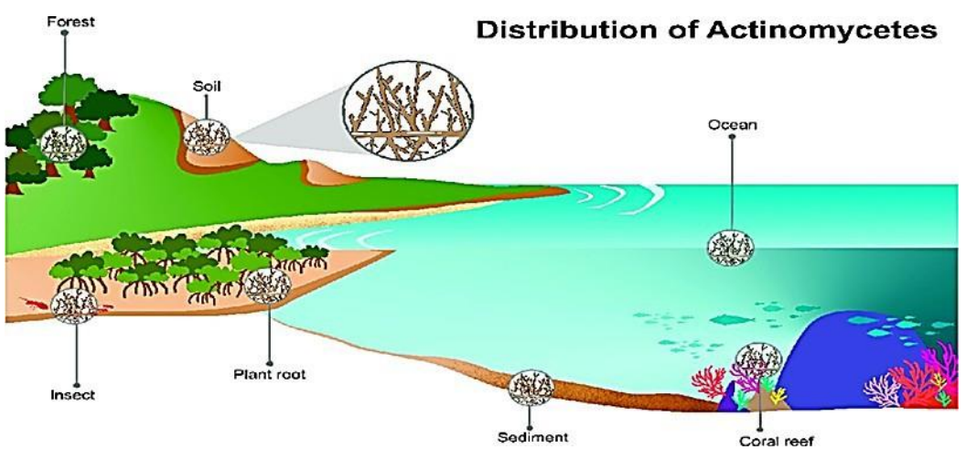

Figure 3. Diversity of actinomycetes habitats (**Ngamcharungchit et al., 2023**).

Actinomycetes are predominantly found in various ecological habitats e.g., marine ecosystems (of water bodies, coral reefs, seawater, mangrove forest), and terrestrial ecosystems (soil and plants, and insects).

I. 5. Isolation methods of actinomycete

Selective techniques for the isolation of actinomycetes are fundamental for understanding their ecological roles and for identifying strains with potential industrial applications. These methods typically involve the use of selective culture media—often supplemented with antibiotics—to inhibit the growth of non-target microorganisms. Pretreatment procedures are also essential to increase the recovery of actinomycetal strains while suppressing competing flora **(Hayakawa, 2008).**

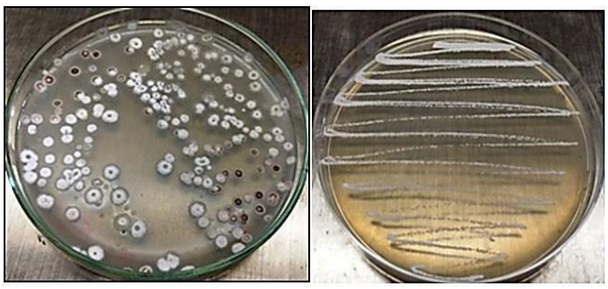

Figure 4. Colony morphology of actinomycete isolate AA1 on Starch casein agar **(Maria et al., 2018).**

Table 1. Selected techniques for the isolation of actinomycetes from soil samples **(Hayakawa, 2008).**

Type of Treatment	Pretreatment Details	Culture Medium	Isolated Genera
Physical	Heating at 120°C for 1 hour	HV agar ± nalidixic acid and trimethoprim	*Streptomyces*, rare actinomycetes (*Spirilliplanes*)
Chemical	0.05% SDS + 5% yeast extract	HV agar + nalidixic acid	*Streptomyces* and other genera
Physical + Chemical	Heating at 110°C for 1 hour + 1% phenol	HV agar + kanamycin, josamycin, lysozyme, nalidixic acid	*Actinomadura viridis*
Enrichment	Rehydration at 30°C for 90 min + centrifugation (1500×g, 20 min), incubation in moisture and drying	HV agar + nalidixic acid and trimethoprim	*Actinoplanes*, *Actinosynnema*, *Actinokineospora*, *Kineosporia*, *Streptomyces*, and others

I. 6. Identification of actinomycetes

The taxonomy of actinomycetes is based on a combination of morphological, chemical, physiological, and molecular criteria. It has undergone four major phases, each contributing significantly to the understanding and classification of these microorganisms.

During the first phase, identification relied solely on macromorphological and micromorphological characteristics. Key features such as the presence, abundance, and arrangement of hyphae in both aerial and substrate mycelium, the presence and morphology of spores (including their number, motility, shape, and positioning on hyphae), as well as the occurrence of sporangia, were used to differentiate between genera **(Waksman and Henrici, 1943).**

The second phase marked the emergence of chemotaxonomy, which, when combined with morphological criteria, greatly enhanced the differentiation of various genera—for example, distinguishing Streptomyces from Nocardia (Becker et al., 1964). Chemical markers enabled the

identification of various cell wall types based on cellular constituents in actinomycetes. In this context,

Nonomura (1974) proposed a classification approach for actinomycetes, especially the genus Streptomyces, based on morphological, physiological, and biochemical features. The most frequently used characteristics include:

- Color of the aerial mycelium (various series: white, gray, red, green, blue, or violet);
- Production of melanoid pigments (greenish-brown or dark brown);
- Production of soluble pigments (red, orange, green, yellow, blue, or violet);
- Color of the substrate mycelium;
- Carbohydrate assimilation patterns;
- Spore chain morphology (e.g., Rectiflexibles [RF], Retinaculiaperti [RA], or Spirales [S])
- Spore surface characteristics (smooth, warty, spiny, or hairy).
- Presence or Absence of Specific Structures:

Identification may also include observation of specific structures such as sclerotia, synnemata, and sporangia **(Nonomura, 1974).**

The third phase in the development of actinomycete taxonomy was marked by the introduction of numerical taxonomy in the 1970s. This approach combined computer-assisted analysis with a large number of biochemical and physiological tests. As a result, dendrograms were generated, allowing the classification and identification of species across various genera of actinomycetes. These included Actinomyces and Rothia **(Holmberg and Hallander, 1973),** Arachnia **(Holmberg and Nord, 1975),** Actinomadura **(Goodfellow and Alderson, 1979)**, Nocardia **(Orchard and Goodfellow, 1980),** Streptomyces **(Williams et al., 1983)**, Actinomadura and Nocardiopsis **(Athalye et al., 1985),** and Actinoplanes **(Goodfellow et al., 1990).**

The fourth and most recent phase has been defined by the use of genetic and molecular analysis methods. These techniques have provided unprecedented clarity in the classification of actinomycetes by enabling the reconstruction of their phylogeny **(Stackebrandt and Kroppenstedt, 1987).**

I. 7. Nutritional aspects of actinomycetes

Early studies on actinomycetes focused on pathogenic species, which were slow-growing, anaerobic or microaerophilic, and required complex media and specific conditions for growth. However, the discovery of saprophytic, aerobic actinomycetes, especially Streptomyces, in soils led to the development of simple media like Conn's agar and Kuster-Williams agar, which effectively isolated these organisms by limiting bacterial growth. While Streptomyces species are easily cultured, other actinomycetes, which grow slower or in smaller numbers, require special methods to reduce competition and provide necessary growth factors. Recent research has focused on isolating and preserving these rarer actinomycetes for biotechnological exploration, improving our understanding of their physiology and nutritional needs**(Srinivasan et al., 1991).**

I. 8. Taxonomy and classification of actinomycetes

Initial taxonomic systems for actinomycetes were primarily based on observable phenotypic traits, such as the color of spores, substrate mycelium, soluble pigments, and melanin production **(Anderson and Wellington, 2001 ; Ngamcharungchit et al., 2023)**Although morphological characteristics remain useful in describing taxa, they often lack the resolution to differentiate between many genera. To address this limitation, polyphasic taxonomy was developed, offering more reliable

identification through a combination of genotypic, phenotypic, and chemotaxonomic data **(Citarella and Colwell., 1970).**

Genotypic techniques typically focus on nucleic acid analysis (DNA or RNA), while chemotaxonomic methods assess proteins, cellular structures, and other phenotypic features. Each approach provides varying degrees of resolution at different taxonomic levels. Techniques like DNA base composition analysis and DNA–DNA hybridization (DDH) are commonly used for bacterial characterization, whereas more complex and labor-intensive methods, such as amino acid sequencing, are only necessary for specific taxa **(Vandamme et al., 1996).**

Currently, actinomycete taxonomy is significantly informed by 16S rRNA gene sequencing and whole-genome-based phylogenetic analysis. DDH remains an important tool for determining species relatedness, with a threshold value of 70% suggested for defining distinct species **(Wayne et al., 1987).** Digital DDH (dDDH), which estimates genomic similarity through melting temperature and sequence comparison, offers a more accurate genome-wide distance. Alongside dDDH, average nucleotide identity (ANI) based on high-scoring segment pairs (via BLAST and other tools) provides enhanced resolution, correlating better with 16S rRNA sequences and presenting a lower error margin. The accepted species delimitation thresholds are approximately 95–96% for ANI and 70% for dDDH **(Meier-Kolthoff et al., 2013).**

In addition, molecular taxonomy, microscopic morphology, and chemotaxonomic profiles—particularly those involving cell wall composition, whole-cell sugar patterns, phospholipid types, and menaquinone profiles—are essential for taxonomic investigations at the family and genus levels **(Tindall et al., 2010)**. Actinomycetes exhibit significant morphological diversity, especially in terms of the presence or absence of substrate or aerial mycelium, pigmentation, and spore structure **(Barka et al., 2016).** These features, in conjunction with polyphasic approaches, have facilitated the discovery of novel actinomycete species in various habitats, including Actinokineospora bankokensis, Saccharopolyspora rhizosphaerae **(Intra et al., 2019)**, Streptosporangium jomthongense **(Intra et al., 2014),** Saccharomonospora colocasiae **(Wattanasuepsin et al.,2017),** Amycolatopsis iheyensis **(Ngamcharungchit et al., 2023),** and Micromonospora pelagivivens **(Intra et al., 2020).**

Table 2. Taxonomy of Actinomycetes (2nd Edition of Bergey's Manual of Systematic Bacteriology) **(Goodfellow et al., 2012).**

Order	Suborder	Family	Genera
Actinomycetales	*Actinomycineae*	*Actinomycetaceae*	*Actinomyces* *Actinobaculium* *Arcanobacterium* *Mobiluncus*
	Corynebacterineae	*Mycobacteriaceae*	*Mycobacterium*
		Nocardiaceae	*Nocardia* *Rhodococcus*
	Micromonosporaceae	*Micromonosporaceae*	*Micromonospora* *Actinoplanes* *Catellatospora* *Couchioplanes* *Dactylosporangium* *Pilimelia* *Spirilliplanes* *Verrucosispora*

	Pseudonocardineae	*Pseudonocardiaceae*	*Pseudonocardia* *Saccharomonospora*
		Actinosynnemataceae	*Saccharothrix*
	Streptomycineae	*Streptomycetaceae*	*Streptomyces* *Kitasatospora* *Streptoverticillium*
	Streptosporangineae	*Streptosporangiaceae*	*Streptosporangium* *Microtetraspora*
		Nocardiopsaceae	*Nocardiopsis* *Thermobifida*
		Thermomonosporaceae	*Thermomonospora* *Actinomadura* *Spirillospora*

I. 9. Role of actinomycette

I. 9. 1. Antibiotic production

Actinomycetes are a major source of antibiotics used in human medicine. Species of the genus Streptomyces produce a wide range of clinically important antimicrobial agents, including streptomycin. These bacteria naturally synthesize secondary metabolites that inhibit or kill other microorganisms **(Genilloud, 2018).**

I. 9. 2. Ecological role

Actinomycetes play a pivotal role in soil ecosystems by decomposing complex organic matter, such as cellulose and lignin, thereby contributing to nutrient cycling and enhancing soil fertility.Their enzymatic capabilities enable them to break down recalcitrant compounds, making them essential in the biodegradation of organic pollutantsMoreover, certain species have demonstrated potential in bioremediation efforts, including the degradation of hydrocarbons and detoxification of heavy metals ,thus aiding in the restoration of contaminated environments **(Bhatti et al., 2017 ; Thangaraj et al., 2023).**

I. 9. 3. Medical Impact

While many Actinomycetes are beneficial, certain species such as Actinomyces can be pathogenic. Actinomyces israelii, for instance, is responsible for actinomycosis, a chronic granulomatous disease that leads to abscess formation and tissue damage **(Kumar et al., 2023).**

I. 9. 4. Industrial uses

Beyond antibiotic production, Actinomycetes are employed in industrial settings for their ability to produce a variety of enzymes (e.g., cellulases, amylases) and bioactive compounds. They are also used in wastewater treatment due to their ability to degrade complex organic pollutants **(Thangaraj et al., 2023).**

I. 9. 5. Unique biological features

Actinomycetes are Gram-positive bacteria with filamentous growth, resembling fungi in morphology. They exhibit a branching hyphal structure and are capable of forming spores, a rare characteristic among bacteria **(Williams et al., 1989).**

I. 9. 6. Agricultural applications

Certain species of Actinomycetes play a crucial role in sustainable agriculture by improving soil health and suppressing plant diseases. Their antimicrobial properties help reduce the need for chemical pesticides, thereby promoting eco-friendly farming practices **(Kumar et al., 2023).**

I. 9. 7. Ongoing research

Current research on Actinomycetes is intensifying, focusing on the discovery of novel bioactive compounds, particularly antibiotics, to combat the rising threat of multidrug-resistant pathogens. Advancements in genomic and metabolomic technologies have facilitated the exploration of previously uncultivable Actinomycetes, unveiling a plethora of new species with unique biosynthetic pathways

Marine-derived Actinomycetes, for instance, have emerged as a promising source of novel antimicrobial agents, expanding the horizons of pharmaceutical applications **(Subramani and Sipkema, 2019 ; Barka et al., 2016).**

I. 10. Developmental cycle of actinomycetes

The life cycle of many actinomycetes involves the formation of filamentous cells known as hyphae, as well as the production of spores (Figure 5) **(Prescott et al., 2010)**. Actinomycetes typically exhibit a two-layered mycelial structure:

- The first layer consists of aerial mycelium.
- The second layer is composed of substrate mycelium.

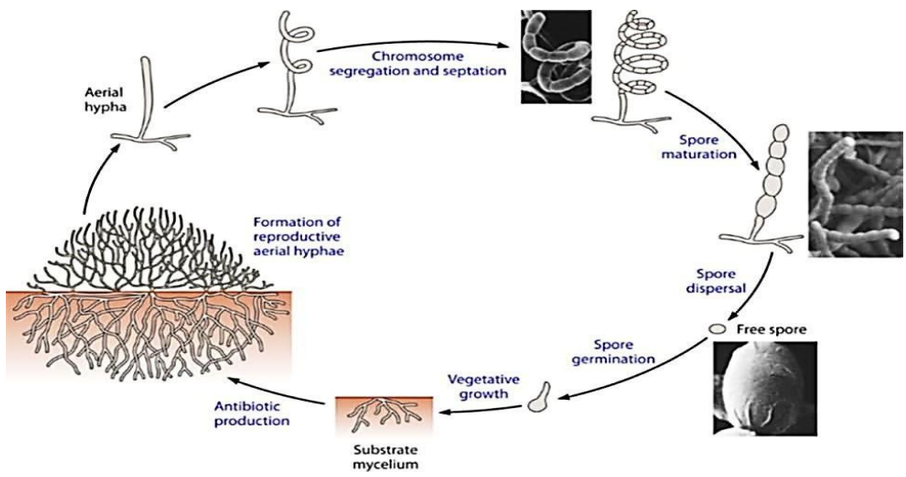

Figure 5. Schematic representation of the lifecycle of sporulating actinomycetes **(Barka et al., 2016).**

I. 10. 1. Aerial mycelium

The aerial mycelium is often thicker than the substrate mycelium and represents a significant level of differentiation. Several isolates are capable of being grouped based on similar morphological characteristics under specific conditions. This differentiation forms the basis for the classification of the genus Streptomyces into species. The aerial mycelium is typically characterized by a cottony, velvety, or powdery texture. Additionally, the formation of concentric zones, pigmentation, or ring patterns is commonly observed.

I. 10. 2. Substrate mycelium

The substrate mycelium, also referred to as the "primary" or "vegetative" mycelium, develops

from the germination tube of spores. When hyphae grow on a solid substrate such as soil or agar,

actinomycetes form a branched network of hyphae. These hyphae extend inward into the substrate, creating a dense mat known as vegetative mycelium. In many actinomycetes, the vegetative hyphae differentiate into upward-growing hyphae that give rise to the aerial mycelium, which rises above the surface **(Prescott et al., 2010).**

- Spore germination occurs as part of this developmental process.
- Spore Germination Process in Actinomycetes
- Spore germination in actinomycetes occurs in four distinct stages: activation, initiation, emergence of the germ tube, and germ tube elongation.

In these bacteria, the substrate mycelium exhibits considerable variability in size, shape, and thickness. Additionally, it shows a wide range of pigmentation, varying from white or nearly colorless to shades of yellow, brown, red, pink, orange, green, or even black **(Prescott et al., 2010)**

I. 11. Metabolism of actinobacteria

Actinobacteria are generally heterotrophic organisms with minimal nutritional requirements. They derive their energy from a wide range of nitrogenous and carbonaceous substrates, which contributes to their widespread distribution in nature. Many species exhibit strong proteolytic and amylolytic activities **(Hsu and Lockwood, 1975).**

Actinomycetes are often bacteriolytic due to their production of hydrolytic enzymes capable of degrading peptide components of bacterial cell walls. Their antimicrobial properties are well-documented, and numerous antibiotics are synthesized during their growth. The enzymatic arsenal of actinomycetes is highly diverse, underpinning their significant ecological role. Their abundance and diversity are influenced by various environmental factors such as pH, organic matter content, seasonal variations, and agricultural practices. Moreover, actinomycetes play an important role in aquatic environments, including freshwater bodies such as rivers and streams.

Ii. 12. Future perspectives on actinomycetes

Actinomycetes are prolific producers of a wide array of bioactive metabolites, many of which serve as valuable therapeutic lead compounds. Consequently, the continued exploration of these microorganisms presents a vast potential reservoir of pharmacologically active substances **(De Simeis and Serra, 2021 ; Mast and Stegmann, 2019 ; Jose and Jha, 2016).**These bacteria inhabit a broad spectrum of ecological niches, including both terrestrial and marine environments, and can be isolated from various sources such as soil, aquatic systems, sediments, plants, and insects **(Betancur et al., 2017 ; Gadelhak et al., 2005 ; Vijayabharathi et al., 2014).** Despite their significant contribution to commercially available therapeutic agents, a substantial proportion of actinomycetes and their secondary metabolites—with potentially high therapeutic value—remain insufficiently studied **(Jose and Jha, 2016)**

The discovery of new genera and species within this group is particularly promising for the identification of novel bioactive secondary metabolites. Thus, a deeper understanding of actinomycete biodiversity, combined with targeted isolation and taxonomic characterization, is essential for optimizing the production of these compounds**(Tiwari and Gupta, 2012 ; Ding et al., 2019 ; Lazzarini et al., 2000)**.Screening strategies focused on novel strains with potential biosynthetic capabilities should be prioritized.

Furthermore, genomic analyses have revealed the presence of numerous biosynthetic gene clusters (BGCs), many of which are transcriptionally silent under standard laboratory conditions. Reactivating these silent clusters could lead to the discovery of new metabolites **(Choi et al., 2015 ; Peng et al., 2018)**. Preliminary whole-genome sequencing enables the assessment of strain biodiversity and facilitates the identification of BGCs. Genome mining, particularly when focused on detecting silent BGCs, offers a promising approach to uncover hidden metabolic potential **(Lee et al., 2020)**

Genetic engineering techniques—such as cloning and heterologous expression of entire BGCs—represent alternative strategies for activating these cryptic pathways **(Liu et al., 2021 ; Gomez-Escribano and Bibb, 2011 ; Salcedo et al., 2016)** . Additionally, co-cultivation with other microorganisms, including bacteria and fungi, has been shown to trigger the expression of silent gene clusters **(Yu et al., 2019 ; Hoshino et al., 2018)** . This interaction, driven by competition for nutrients or the presence of signaling molecules, can stimulate the production of novel metabolites. However, co-cultivation can also lead to the repression of other gene clusters, making the selection of suitable microbial partners a critical challenge. Therefore, a deeper understanding of the molecular signals involved in silent BGC activation is essential to unlock the full biosynthetic potential of actinomycetes.

II. Biogenic synthesis of copper Nano and their application

II. Biogenic synthesis of copper nanoparticles and their applications

Nanotechnology is an innovative and rapidly advancing field that has gained significant attention due to its remarkable versatility and broad range of applications. One of the major driving forces behind this progress is the development of metal nanoparticles, such as copper nanoparticles (CuNPs). Nanoparticles are nanoscale entities composed of clusters of atoms ranging from 1 to 100 nanometers in size.

In recent years, biogenic synthesis has emerged as a sustainable alternative to conventional chemical synthesis methods. This approach is preferred for its environmental friendliness, reliability, sustainability, and low energy requirements (**Díaz et al., 2023**). Biogenic synthesis relies on biological agents—including microorganisms and plant extracts—as reducing and stabilizing agents in nanoparticle formation. Compared to traditional chemical methods, this green synthesis route is eco-friendlier and more cost-effective, and it offers potential for scaling up production processes (**Luque et al., 2023**).

This environmentally conscious approach has demonstrated promising applications in medicine, pharmaceuticals, food processing, and agriculture. Over the past decade, numerous studies have investigated the biogenic synthesis of copper nanoparticles. However, a comprehensive and organized review summarizing their properties and potential applications has been lacking.

Therefore, this systematic review aims to evaluate research conducted over the past ten years concerning the antioxidant, antitumor, antimicrobial, dye removal, and catalytic activities of biogenically synthesized copper nanoparticles, employing a big data analytics framework. The review focuses on copper nanoparticles synthesized using plant extracts and microorganisms (bacteria and fungi) as biological agents. Our objective is to assist the scientific community in better understanding and identifying valuable insights for future research and application development (**Luque et al., 2023**).

II.1. Historical background

The term “nano” originates from the Greek word meaning dwarf or extremely small, representing one-billionth of a meter (10^{-9} m). It is important to distinguish between nanoscience and nanotechnology. Nanoscience refers to the study of structures and molecules on the nanometer scale (1–100 nm), while nanotechnology involves the practical application of this knowledge in developing devices and systems at the nanoscale (**Mansoori et al., 2005**).

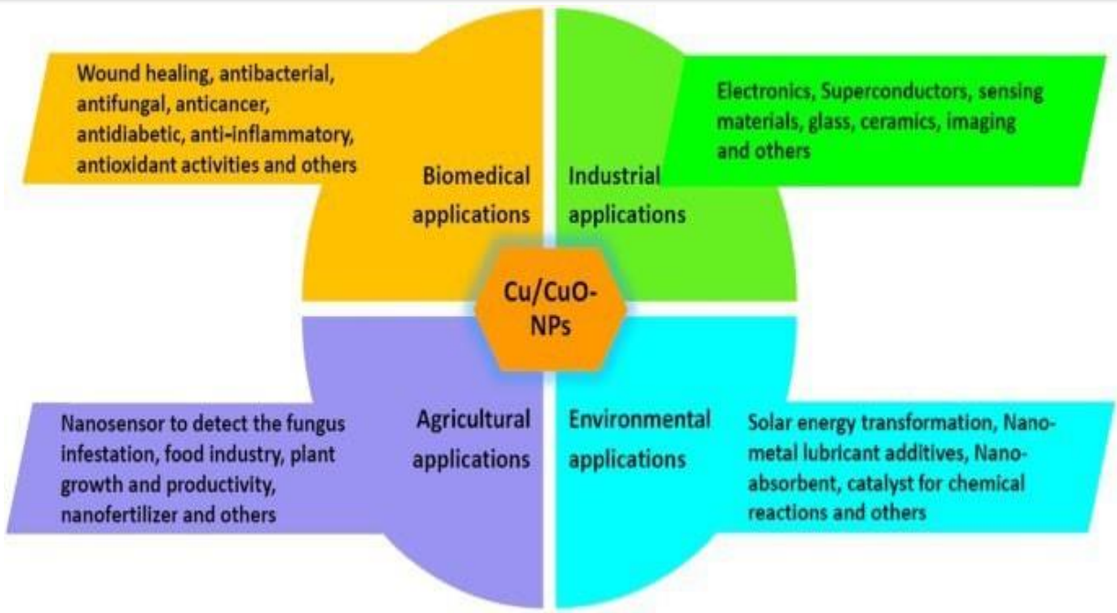

Figure 06. Fields of application of copper nanoparticles synthesized via green methods (**Siddiqi et al., 2018**).

II.2. Rationale for biogenic production of copper nanoparticles

II.2.1. Eco-friendly and sustainable

Biogenic synthesis eliminates the use of toxic chemical reducing agents such as sodium borohydride and hydrazine, which are commonly used in conventional chemical synthesis. Instead, it employs renewable biological resources—including plants, bacteria, fungi, and algae—making it a safer and more sustainable alternative. Moreover, this method produces minimal hazardous waste, thereby reducing environmental pollution and protecting ecosystems (**Pérez et al., 2021**).

II.2.2. Cost-effective and simple

Biogenic production relies on inexpensive and readily available materials, such as plant extracts and microbial cultures. The process does not require costly equipment or high-energy inputs typically associated with physical or chemical synthesis methods, making it an economically viable and scalable approach (**Parikh et al., 2021**).

II.2.3. Biocompatibility

Nanoparticles synthesized through biological methods are naturally bio-capped with organic molecules such as proteins, flavonoids, and polysaccharides. These natural coatings enhance nanoparticle stability, prevent aggregation, and improve biocompatibility, thereby making them suitable for medical, agricultural, and environmental applications (**El-Deeb et al., 2020**).

II.2.4. Tunable properties

Different biological systems—plants, fungi, and bacteria—can produce copper nanoparticles with diverse shapes, sizes, and surface chemistries. This variability allows researchers to optimize nanoparticle properties for specific applications such as antimicrobial, antioxidant, or catalytic functions.

II.2.5. Dual functionality of biomolecules

During green synthesis, biological molecules serve a dual role:

- As reducing agents, they convert copper ions (Cu^{2+}) into elemental copper (Cu^{0}).

- As capping agents, they stabilize the newly formed nanoparticles, preventing agglomeration.

This dual function simplifies the overall synthesis process while enhancing nanoparticle stability and performance (**Javed et al., 2022**).

II.2.6. Scalability and broader applications

The use of microbial fermentation and plant extracts facilitates easy scale-up for industrial production. Biogenically synthesized copper nanoparticles show immense potential across diverse sectors—pharmaceuticals, agriculture (as antifungal and antibacterial agents), wastewater treatment (for dye degradation), and catalysis (**Lithi et al., 2025**).

II.3. Microorganism-mediated synthesis of copper nanoparticles

II.3.1. Mechanism

- **Enzymatic Reduction:**

Microbial enzymes such as nitrate reductase, hydrogenase, and oxidoreductases catalyze the reduction of copper ions ($Cu^{2+} \rightarrow Cu^{0}$) (**Antonio et al., 2023**).

- **Extracellular synthesis:**

Microorganisms secrete enzymes and metabolites into the surrounding culture medium, which reduce copper ions outside the cell, resulting in the formation of extracellular nanoparticles (**Antonio et al., 2023**).

- **Intracellular Synthesis:**

Copper ions can enter microbial cells and are subsequently reduced by intracellular enzymes and proteins, leading to the nucleation and growth of nanoparticles within the cell (**Antonio et al., 2023**).

- **Capping and stabilization:**

Microbial biomolecules such as proteins, peptides, and polysaccharides act as capping agents, preventing nanoparticle aggregation and enhancing stability (**Antonio et al., 2023**).

II.3.2. Selection of biological agents for green biosynthesis

The concept of green chemistry underpins the biosynthesis of copper nanoparticles, emphasizing environmentally friendly and sustainable practices. Biological entities such as bacteria, fungi, plants, and actinomycetes are widely used due to their ability to reduce and stabilize metal ions, producing nanoparticles with unique characteristics. Both unicellular and multicellular organisms participate effectively in these syntheses.

- Plant-**mediated synthesis**

Plants act as natural “chemical factories,” providing a low-cost, low-maintenance, and renewable source for nanoparticle synthesis. They possess remarkable abilities to detoxify and accumulate heavy metals, making them ideal for eco-friendly nanoparticle production (**Singh et al., 2019**).

Magnolia leaf extract has been used to produce CuNPs with sizes ranging from 40–100 nm. Leaf extracts of Brassica juncea, Medicago sativa, Helianthus annuus, and Tridax procumbens have successfully reduced Cu^{2+} ions to Cu^{0}, forming stable nanoparticles (**Abdul Hameed, 2012**). Gum karaya, a natural hydrocolloid, served as both reducing and capping agent, yielding nanoparticles as small as 4.8 ± 1.6 nm. The medicinal plant Ocimum sanctum has also been employed, where its alkaloids, glycosides, tannins, and saponins contribute to reduction and stabilization (**Kulkarni et al., 2013**).

- **Bacteria-mediated synthesis**

Bacteria have demonstrated strong potential for nanoparticle production due to their short generation time, ease of culture, mild experimental conditions, and extracellular synthesis capabilities (**Jadoun et al., 2021**). They survive in toxic metal environments by converting harmful ions into non-toxic metal oxides (**Sheini et al., 2017**). Serratia sp. isolated from insect midguts was used to synthesize CuO nanoparticles (**Hasan et al., 2008**). Morganella morganii RP42 and Morganella psychrotolerans produced CuNPs measuring 15–20 nm (**Suresh et al., 2011**). Pseudomonas stutzeri generated spherical CuNPs (8–15 nm) via rapid biological synthesis (**Varshney et al., 2010**). Streptomyces sp. synthesized CuO nanoparticles for antimicrobial textile coatings (**Usha et al., 2010**). Escherichia coli and Pseudomonas stutzeri produced nanoparticles with variable morphologies, including cubical CuNPs (50–150 nm) from electroplating wastewater (**Varshney et al., 2011**).

- **Fungi-mediated synthesis**

Fungi are excellent candidates for nanoparticle biosynthesis owing to their abundant enzyme secretion and ease of handling (**Sahayaraj et al., 2011**). Penicillium species (P. aurantiogriseum, P. citrinum, P. waksmanii) have been shown to synthesize CuNPs extracellularly (**Honary et al., 2012**). Fusarium oxysporum produced CuNPs at room temperature, even using copper recovered from electronic waste.

Hypocrea lixii generated spherical CuNPs (~24.5 nm) stabilized by protein amide groups (**Marcia R. et al., 2013**). Marine brown algae Bifurcaria bifurcata synthesized CuNPs through diterpenoids, which served both reducing and stabilizing roles (**Abboud et al., 2013**).

Table 03. Some biological cells involved in the green biosynthesis of CuNps.

Biological entity	Species	Parts used	Size	References
Bacteria	*Escherichia coli*	_	_	(**Singh et al., 2010**)
	M.psychrotolerans and M. morganii RP42	_	15-20 nm	(**Ramanathan et al., 2011**)
	Pseudomonas sp	_	84-130 nm	(**Majumder, 2012**)
	Pseudomonas stutzer	_	8-15 nm	(**Varshney et al., 2010**)
	Pseudomonas stutzeri	_	50-150 nm	(**Varshney et al., 2011**)
	Serratia	_	_	(**Hasan et al., 2008**)
	Streptomyces sp.	_	_	(**Usha et al., 2010**)
Fungi	*Fusarium oxysporum*	_	93-115 nm	(**Majumder, 2012**)
	Hypocrea lixii	_	average of 24.5 nm	(**Salvador et al., 2013**)
	Penicillium aurantiogriseum, Penicillium citrinum Penicillium waksmanii	_	_	(**Honary et al., 2012**)

Algae	*Bifurcaria bifurcata*	_	5–45 nm	(**Abboud et al., 2013**)
Angiospermic Plant	*Calotropis procera L.*	Latex	15 ± 1.7 nm	(**Harne et al., 2012**)
	Euphorbia nivulia	Latex	_	(**Lee et al., 2013**)
	Gum karaya	Gum	4.8 ± 1.6 nm	(**Černík., 2013**)
	Helianthus annus	_	_	(**Hameed et al., 2012**)
	Lantana camara	_	Average of 20 nm	(**Majumder, 2012**)
	Magnolia	Leaves	40-100 nm	(**Lee et al., 2011**)
	Magnolia kobus	Leaves	average size 37 - 110 nm	(**Lee et al., 2013**)
	Medicago sativa	_	_	(**Hameed et al., 2012**)
	Ocimum sanctum	leaves	77 nm	(**Kulkarni and Kulkarni, 2013**)
	Soy beans	seed	_	(**Guajardo-Pacheco et al., 2010**)
	Syzygium aromaticum	Flower Buds	40-45 nm	(**Ipsa subhankari and Nayak, 2013**)
	Tridax procumbens	_	_	(**Hameed et al., 2012**)
	Zingiber officinale	Rhizome	40 and 25 nm	(**Ipsa subhankari and Nayak, 2013**)

II .4. Characterizations of copper nanoparticles

Table 04. Characterization of copper nanoparticles (**Rani et al., 2017**).

Technique	**Principal**	**Purpose in CuNP**	**Outcome**
UV–Visible Spectroscopy (UV–Vis	Measures surface plasmon resonance (SPR) absorption of CuNPs |	Confirms nanoparticle formation and estimates stability	Peak around 560–600 nm indicates CuNPs
Fourier Transform Infrared Spectroscopy (FTIR)	Detects vibration of functional groups	Identifies phytochemicals/proteins responsible for reduction and capping	Shows functional groups (–OH, –NH, –C=O) involved in stabilization
X-ray Diffraction (XRD	Measures diffraction of X-rays through crystalline material	Determines crystallinity, size, and phase composition	Confirms crystalline nature and average particle size (using scherrer's equation
Transmission Electron Microscopy (TEM)	Electron beam transmitted through thin sample	Provides detailed morphology and size distribution	High-resolution images of nanoparticles (1–100 nm)
Scanning Electron Microscopy (SEM	Uses electron beam scanning to image surfaces	Analyzes morphology and surface topography	Reveals shape (spherical, cubic, irregular) and surface texture
Energy Dispersive X-ray Spectroscopy (EDX/EDS)	Coupled with SEM/TEM to detect emitted X-rays	Confirms elemental composition	Detects presence of copper along with other capping elements
Dynamic Light Scattering (DLS)	Measures scattering of light by particles in suspension	Determines hydrodynamic particle size and polydispersity index	Gives average particle size in colloidal form

Zeta Potential Analysis	Measures electrostatic potential at particle surface	Evaluates surface charge and stability in suspension	High absolute zeta value indicates better stability
Thermogravimetric Analysis (TGA))	Measures weight change with temperature	Studies thermal stability and organic content on CuNPs	Provides info about decomposition and capping molecules

II.5. Optimization of physico-chemical factors for the biosynthesis of copper nanoparticles

The biosynthesis of metallic nanoparticles (NPs) using plant extracts requires careful optimization of reaction parameters. Key factors include the concentration and ratio of plant extract to metal salt, as well as pH, reaction time, and temperature. Adjusting these variables allows control over nanoparticle size, shape, and yield.

An increase in plant extract concentration can influence nanoparticle morphology and size, while longer reaction durations tend to enhance NP production. In contrast, elevated temperatures often lead to a decrease in both nanoparticle size and overall yield. Furthermore, the interaction between metal ions and biomolecules in plant extracts is highly dependent on pH. At varying pH levels, nanoparticles of different morphologies—tetrahedral, hexagonal, spherical, rod-shaped, or irregular—can be synthesized. Generally, higher pH values result in smaller nanoparticles (**Dikshit et al., 2021**).

II.51. Effect of pH

Adjusting pH plays a crucial role in determining the shape, size, and efficiency of metallic nanoparticles. These morphological features can be optimized by controlling experimental parameters such as reaction time, reactant concentration, temperature, and the ratio of plant extract to metal salt.

In acidic conditions, larger nanoparticles are generally formed, while more alkaline environments favor smaller, well-dispersed nanoparticles. For instance, during Avena sativa biomass-mediated synthesis, smaller gold nanoparticles were observed at pH 3.0–4.0 compared to pH 2.0, likely due to enhanced nucleation promoted by functional groups at higher pH levels (**Dikshit et al., 2021**).

At low pH values, silver ions (Ag^{+}) interact with amino and sulfhydryl groups, leading to reduction into Ag^{0}. This reduction process is favored around pH 8, where positively charged functional groups promote ionic bonding. At higher pH, increased bioreduction and nanoparticle dispersion occur, often accompanied by negative zeta potentials, which result in larger NP sizes (**Rahuman et al., 2022**).

Similarly, in the biosynthesis of copper nanoparticles using Punica granatum fruit rind extract, pH significantly influenced the bioreduction of copper sulfate. Lower pH values produced smaller crystallite sizes due to faster nucleation rates (**Kumari et al., 2018**).

II.5.2. Effect of temperature

Temperature is another critical factor influencing nanoparticle formation. For example, extracts of hawthorn berries used in the synthesis of copper and silver nanoparticles produced a light

brownish color at 20°C, which darkened to reddish-brown at higher temperatures, indicating nanoparticle formation. Increasing temperature generally results in smaller nanoparticle sizes when aqueous plant extracts are employed (**Długosz et al., 2020**).

At around 60°C, uniformly small metallic nanoparticles are typically obtained, regardless of the salt used. In general, nanoparticle size is inversely proportional to temperature. For instance, silver nanoparticles synthesized using olive leaf extracts exhibited faster reduction of Ag^+ ions and uniform nucleation at elevated temperatures, producing smaller, spherical particles. High temperatures promote rapid reduction rates and limit secondary reduction to the surface of preformed nuclei. Conversely, lower temperatures tend to yield polydisperse nanoparticles ranging from 5 to 300 nm (**Khan et al., 2022**).

II.5.3. Effect of reaction time

The reaction time also has a pronounced effect on nanoparticle synthesis efficiency and yield. Using Punica granatum plant extracts, optimal copper nanoparticle production was achieved within 2 hours (**Kumari et al., 2018**). Ficus hispida leaf extracts showed an increased surface plasmon resonance (SPR) intensity after 1 hour of reaction, confirming active nanoparticle formation (**Ramesh et al., 2018**). In another study, Saudi date extracts yielded the highest production of platinum nanoparticles after 10 hours (**Al-Radadi., 2019**). These findings highlight the importance of determining the optimal reaction time for each biological source to ensure efficient nanoparticle synthesis.

II.5.4. Effect of CuSO4 concentration

The concentration of copper sulfate (CuSO4) directly influences nanoparticle formation. Experiments using CuSO4 concentrations of 318.4, 750, and 1000 ppm revealed that control samples (without biological agents) showed no characteristic absorption peaks in the 550–650 nm region typical of CuNPs.

When cell-free microbial supernatant was added to 750 and 1000 ppm CuSO4 solutions, absorption peaks appeared above 700 nm, confirming nanoparticle formation. Specifically, adding 10 mL of cell-free supernatant to a 318.4 ppm CuSO4 solution produced a clear absorption peak, indicating that this amount was sufficient for complete reduction of copper ions. Increasing the supernatant volume to 40 mL for 1000 ppm CuSO4 led to peak sharpening and nanoparticle aggregation, suggesting over-reduction and particle clustering (**Shantkriti and Rani, 2014**).

II.6. Biological and catalytic activities

II.6.1. Antioxidant activity

Copper nanoparticles (CuNPs) have been widely reported to exhibit strong antioxidant potential due to their ability to scavenge free radicals and reduce oxidative stress. Their high surface-area-to-volume ratio enhances electron transfer, enabling the effective neutralization of reactive oxygen species (ROS).

For example, **Kareem** et al. (**2022**) demonstrated that green-synthesized CuNPs using Terminalia chebula fruit extract exhibited dose-dependent antioxidant activity in the DPPH radical scavenging assay, with an EC_{50} value of 44.65 µg/mL, indicating significant free radical quenching

capability. These findings highlight the potential of CuNPs as effective antioxidant agents with possible applications in biomedical, agricultural, and food systems (**Kareem et al., 2022**).

II.6.2. Antitumor activity

Copper nanoparticles (CuNPs) have shown promising antitumor properties through multiple mechanisms, including ROS generation, oxidative stress induction, mitochondrial dysfunction, and activation of apoptosis pathways in cancer cells. Their nanoscale size facilitates efficient cellular uptake, enabling selective cytotoxicity toward tumor cells while sparing normal cells at controlled concentrations.

Vidya et al. (**2020**) reported that biosynthesized copper oxide nanoparticles induced dose-dependent cytotoxicity in human breast cancer (MCF-7) and colon cancer (HT-29) cell lines through ROS-mediated apoptosis. The nanoparticles disrupted mitochondrial membrane potential and activated caspase-dependent pathways, confirming their potential as cost-effective nanotherapeutics for cancer treatment, particularly when synthesized via eco-friendly biological routes (**Vidya et al., 2020**).

II.6.3. Antimicrobial activity

Copper nanoparticles (CuNPs) exhibit broad-spectrum antimicrobial activity against Gram-positive and Gram-negative bacteria, as well as various pathogenic fungi. Their antimicrobial mechanism is primarily attributed to the generation of reactive oxygen species (ROS), disruption of microbial membranes, leakage of intracellular contents, and binding to proteins and nucleic acids, thereby impairing vital cellular processes.

For instance, **Usman** et al. (**2013**) reported that green-synthesized CuNPs displayed strong antibacterial activity against Escherichia coli, Staphylococcus aureus, and Pseudomonas aeruginosa. The nanoparticles effectively inhibited bacterial growth by damaging cell walls and inducing oxidative stress, confirming their potential as eco-friendly antimicrobial agents in biomedical and agricultural applications (**Usman et al., 2013**).

II.6.4. Antifungal activity

Copper nanoparticles (CuNPs) have demonstrated significant antifungal activity against a wide range of pathogenic fungi. Their antifungal action results from ROS generation, membrane disruption, and interference with essential enzymatic processes. Due to their small size, CuNPs interact directly with fungal spores and hyphae, leading to structural deformation and growth inhibition.

Ramesh et al. (**2014**) showed that biosynthesized CuNPs exhibited potent antifungal effects against Fusarium oxysporum, Aspergillus niger, and Candida albicans. The study reported a marked reduction in spore germination and hyphal elongation, attributed to oxidative stress and membrane damage. These results indicate that CuNPs are promising eco-friendly antifungal agents for use in agriculture and medicine (**Ramesh et al., 2014**).

II.6.5. Antibacterial activity

Copper nanoparticles (CuNPs) possess remarkable antibacterial efficacy against a wide variety of pathogenic microorganisms. Their mechanism of action includes penetration of bacterial cell walls,

generation of ROS, and interference with key metabolic pathways. Their nanoscale dimensions allow intimate interaction with bacterial membranes, leading to protein denaturation, membrane disintegration, and cytoplasmic leakage.

Usman et al. (**2013**) reported that biosynthesized CuNPs exerted strong antibacterial effects against both Gram-negative (Escherichia coli, Pseudomonas aeruginosa) and Gram-positive (Staphylococcus aureus) bacteria. Electron microscopy revealed visible cell wall disruption in treated bacteria, confirming the nanoparticles' potential as efficient antimicrobial agents for biomedical and environmental applications (**Usman et al., 2013**).

II.6.6. Antiviral activity

Copper nanoparticles (CuNPs) also display potent antiviral activity by directly interacting with viral particles, disrupting surface proteins, and producing reactive oxygen species (ROS) that damage viral nucleic acids. Their strong redox behavior enables them to inactivate both DNA and RNA viruses, reducing infectivity and replication rates.

For instance, **Hang** et al. (**2015**) reported that copper oxide nanoparticles significantly inhibited the replication of Herpes simplex virus type 1 (HSV-1) by binding to viral glycoproteins and blocking entry into host cells. Similarly, CuNPs have been shown to reduce the infectivity of influenza and other enveloped viruses, demonstrating their potential as antiviral agents for biomedical and environmental applications, such as surface coatings, disinfectants, and protective materials (**Hang et al., 2015**).

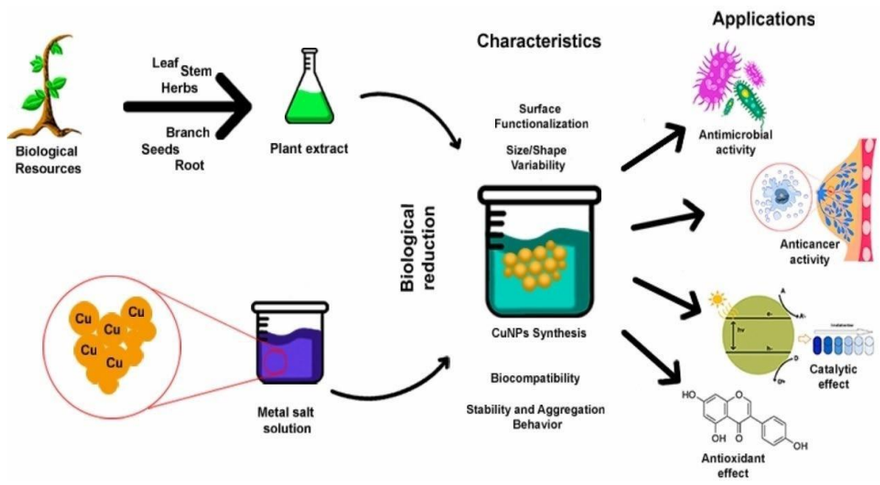

Figure 07. Schematic representation of the different activities of copper nanoparticles.

II.6.7. dye removal and environmental remediation

Copper nanoparticles (CuNPs) have shown great promise in environmental remediation, particularly in the removal of toxic dyes from industrial wastewater. Their high surface-area-to-volume ratio and strong catalytic redox properties make them highly effective in degrading synthetic dyes such as methylene blue, methyl orange, and rhodamine B.

CuNPs function as efficient catalysts in advanced oxidation processes (AOPs) by enhancing electron transfer and accelerating the breakdown of dye molecules into less harmful or colorless byproducts.

For example, **Rajeshkumar** and **Naik** (2018) reported that green-synthesized CuNPs exhibited excellent catalytic activity in the degradation of methylene blue and Congo red, achieving significant decolorization within a short reaction time. These results highlight the potential of CuNPs as eco-friendly and cost-effective nanomaterials for wastewater treatment and environmental remediation (**Rajeshkumar et al., 2018**).

II.7. Mechanisms of action of copper nanoparticles

Copper nanoparticles (CuNPs) exhibit a wide range of biological and catalytic activities owing to their unique physicochemical properties at the nanoscale. Their mechanisms of action can be categorized into several interconnected pathways, involving both redox activity and molecular interactions with biological components.

II.7.1. Generation of reactive oxygen species (ros)

CuNPs undergo continuous redox cycling between Cu^0, Cu^+, and Cu^{2+} oxidation states, leading to the generation of reactive oxygen species (ROS) such as hydroxyl radicals (•OH), superoxide anions (O2•–), and hydrogen peroxide (H2O2). These oxidative species induce lipid peroxidation, protein oxidation, DNA fragmentation, and ultimately cell death in both microbial and cancer cells (**Usman et al., 2013**).

II.7.2. Disruption of cell membranes

CuNPs interact electrostatically with negatively charged microbial or cancer cell membranes. This interaction increases membrane permeability, resulting in leakage of intracellular components, disruption of ion balance, and eventual structural collapse of the cell (**Ruparelia et al., 2008**).

II.7.3. Interaction with proteins and enzymes

CuNPs bind to thiol (–SH) and amino groups of proteins, leading to the inactivation of key metabolic and enzymatic systems involved in cellular respiration, replication, and repair. Such interactions disrupt essential biochemical pathways, thereby inhibiting microbial growth and tumor cell proliferation (**Dizaj et al., 2014**).

II.7.4. DNA and RNA damage

Copper ions released from CuNPs can intercalate with nucleic acids, causing DNA strand breaks, base modifications, and replication inhibition. These interactions interfere with both DNA transcription and RNA translation, resulting in genetic mutations or cell death. This mechanism plays a crucial role in the antimicrobial and antiviral activities of CuNPs (**Hang et al., 2015**).

II.7.5. Catalytic redox reactions

In environmental remediation and organic synthesis, CuNPs function as efficient heterogeneous catalysts. Their surface provides active redox sites that facilitate oxidation, reduction, and coupling reactions. These catalytic processes are vital for applications such as dye degradation, pollutant detoxification, and chemical synthesis (**Nasrollahzadeh et al., 2015**).

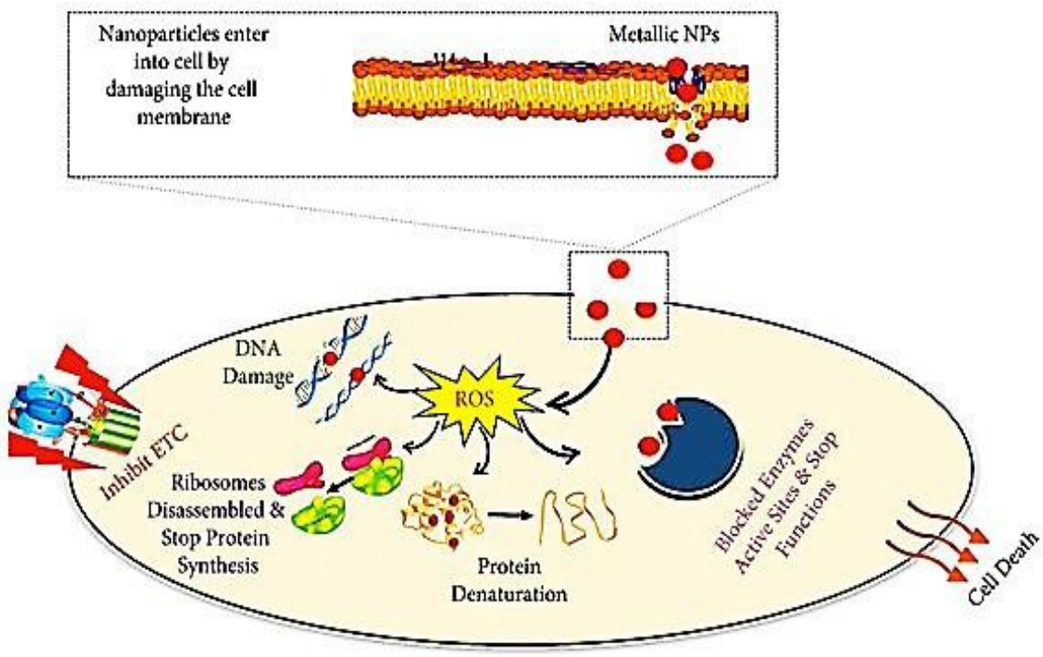

Figure 08. Schema of mechanism action of copper nanoparticle (**Yin et al., 2023**).

II.8. Application of copper nanoparticles in agriculture and their insecticidal activity

Copper nanoparticles (CuNPs) have found applications across various fields due to their diverse physicochemical and biological properties. In agriculture, they are utilized to enhance crop growth, yield, and quality (**Hernández-Hernández et al., 2019**). In medicine, CuNPs exhibit potent antioxidant, antibacterial, and anticancer activities (**Mehdizadeh et al., 2020**), while in environmental science, they serve as effective decontamination and remediation agents (**Abbas et al., 2020**). Additionally, CuNPs are increasingly employed in several technological applications, including sensors, catalysis, and material engineering (**Huang et al., 2019**).

Recent studies in the agricultural sector have particularly emphasized the significance of CuNPs in promoting plant health and controlling insect pests, highlighting their potential as eco-friendly alternatives to conventional agrochemicals.

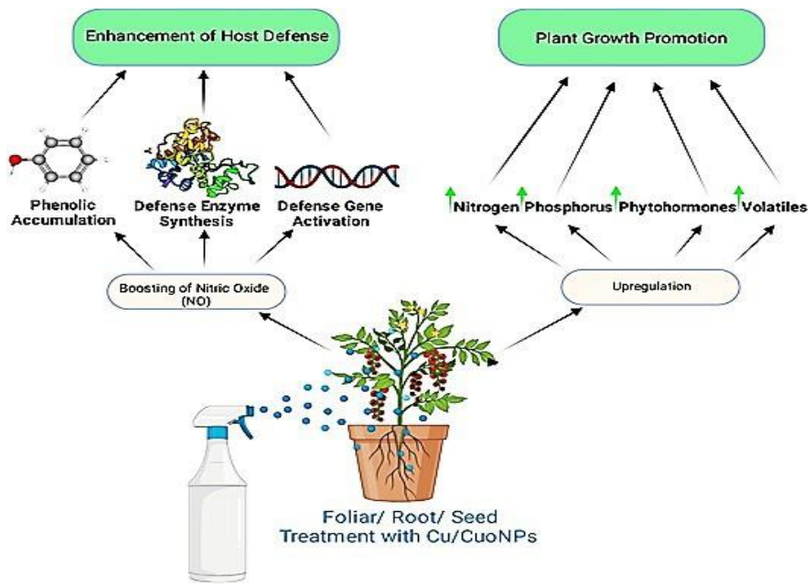

Figure 09. Application of copper nanoparticles in agriculture (growth of plants).

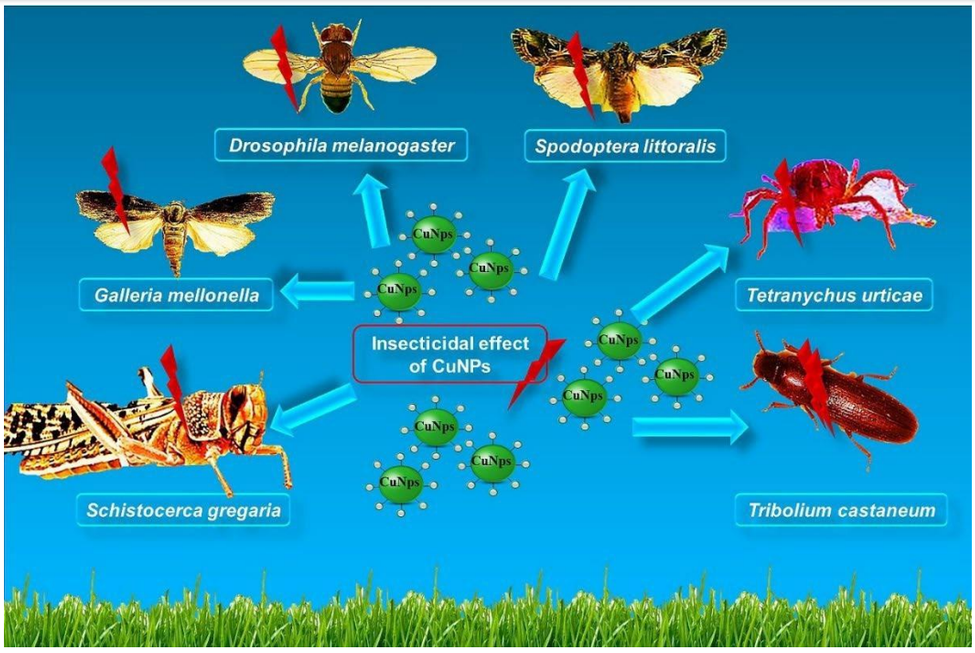

Figure 10. Top insects managing by CuNPs in the agricultural field.

Green synthesized of CuNPs show good effect against *Anopheline mosquitoes*, the highest larval mortality (100.0%) was obtained with 140 and 20 ppm of *Lantana camara* extract alone or mixed with CuNPs, respectively (**Hassanain et al., 2019**). The above results are proved by a more recent study. The authors reported that CuNPs synthesized by *Pseudomonas fluorescens* MAL2, similar to *Pseudomonas fluorescens* DSM 12442^{T}, demonstrate 100% mortality against *Tribolium castaneum* (the little mealworm) in the presence of 300 µg mL^{-1} of NPs (**El-Saadony et al., 2020**). Green synthesis of CuONPs from the leaves of *Tridax procumbens* and evaluation of its larvicidal activities against *Aedes aegypti* revealed high mortality (**Selvan et al., 2018**). The remarkable insecticidal activity of CuNPs compared to plant extracts is strongly attributed to the small particle size. The CuNPs can penetrate and cross the larval cell membrane and bind to proteins and DNA. Damage is possible after the interaction of NPs with cellular proteins and nucleic acids. Consequently, the alterations induce a rupture of the cell membrane and disrupt the driving forces of the protons. It involves a breakdown of cell functions and ultimately cell death (**Parthiban et al., 2018**). The insecticidal effect may also be attributed to the ability of CuNPs to cross the barrier of epithelial and endothelial cells by transcytosis (**El-Saadony et al., 2020**). The NPs can reach the circulatory system and attack potentially sensitive target sites such as the nervous system (**Ramadan et al., 2020**).

In other equally important crops, CuNPs have displayed a remarkable insecticidal effect. For example, in common bean cultivation (*Phaseolus vulgaris* L.) widely cultivated in the world, copper nanocapsules (alginate/chitosan/copper oxide nanoparticle) sprayed during the simultaneous appearance of the first flower buds demonstrated a significant reduction in the population of *Tetranychus urticae* (**Dorri et al., 2018**). Copper oxide NPs (CuONPs) showed high mortality rates in *Spodoptera littoralis* larvae (the cotton leafworm). NPs affect eggs laid in females and modify the sex ratio of females and males. However, the combination of CuNPs with the methomyl pesticide minimizes the toxic potency of the pesticide in the insects, the reduction of the toxic effect is due to the photodegradation of pesticide by CuNPs (**Shaker et al., 2016**). For other NPs, the insecticidal activity can be further enhanced by combining NPs with other chemical agents, citing as an example the combination of silver NPs with malathion. The resulting combination clearly showed its high

insecticidal efficacy against *T. castaneum* (**Alif Alisha and Thangapandiyan, 2019**), in *S. litura*, the use

of CuONPs enhances the activity of β-cypermethrin against the insect (**Lu et al., 2019**).

The incorporation of CuONPs and silver-doped copper oxide nanosheets into the diet of *S. littoralis* demonstrated high larval mortality. Copper NPs are more effective than doped with silver. The mortality rate is proportional to the concentration of NPs, the exposure time, and the larval stages. CuO nanostructures have a significant effect on the timing of living larval development. Deformities of pupae and malformations in adults are also recorded (**Atwa et al., 2017**). In *Galleria mellonella*, whose larvae are a problem for beekeepers, CuONPs induce a significant oxidative stress. The accumulation of NPs in the midgut and fat body tissues of the insect larvae significantly increases the activity of glutathione S-transferase in the fat body. The CuONPs concurrently increase catalase activity (CAT) in the midgut and fat body. However, superoxide dismutase activity (SOD) is weakened (**Sezer Tuncsoy et al., 2019**). In the same insect, the diets containing 10 and 100 mg L^{-1} of CuNPs induce a significantly higher increase in the total number of hemocytes, while the diets containing 1000 mg L^{-1} of CuNPs induce an opposite effect (**Sezer Tuncsoy and Ozalp, 2017**).

In Drosophila or vinegar fly (*Drosophila melanogaster*), CuNPs induce genotoxicity in larval hemocytes. Toxicity is characterized by DNA damage, reduced larval count, and delayed development of adult larvae (**Carmona et al., 2015**). In *Schistocerca gregaria*, treatment by CuNPs revealed acute toxicity. Pupal mortality is initially observed in the 4^{th} stage of development (**Ramadan et al., 2020**). It should be noted that the insect mortality rate is proportional to the increase in the concentration of CuNPs and to the exposure time (**El-Saadony et al., 2020**). It is also noted that the nanometric level of the Cu nanoparticles is important for attenuating the targets and inducing toxicity. **(Karlsson et al., 2009**). **Table 6** demonstrates some insecticidal effects of CuNPs.

Table 05. Insecticidal activity of some copper nanoparticle.

Nanoparticle	Size	Structure	Insecticidal activity against	Lethal dose	References
CuNPs	240.88 ± 62.66 nm		*Euwallacea fornicatus*		**(Cruz et al., 2021)**
CuNPs	10-70 nm	Spherical	*Tribolium castaneum*	300 µg mL^{-1}	**(El-Saadony et al., 2020)**
Cellulose/nanocrystal ZnO/CuO Nanostructure			*Anopheles stephensi*		**(Elfeky et al., 2020)**
CuONPs	20-40 nm	Spherical	*Anopheles subpictus mosquito larvae*	80 ppm for 48h	**(Velsankar et al., 2020)**
CuNPs	11.5-13.5 nm	Rods in shape	*Schistocerca gregaria*		**(Ramadan et al., 2020)**
Cu/NiNPs			*Culex quinquefasciatus*	83,96; 258.83 and 331.50 mg L^{-1}	**(Danbature et alH., 2020)**
CuNPs	11-17.8 nm	Spherical	*Anopheline mosquitoes*	20 ppm	**(assanain et al., 2019)**
CuONPs	33.0±8.3 nm)	Spherical	*Galleria mellonella*	10 µg L^{-1}.	**(Tuncsoy et al., 2019).**
Cu_2O nano capsules	Less than 50nm		*Tetranychus urticae*	5.5 g L^{-1}	**(Dorri et al., 2018)**
CuONPs	16 nm	Monoclinic structure	*Aedes aegypti*	10 mg mL^{-1}	**(Selvan et al., 2018)**
Ag-doped CuO nanostructures	~ 10 nm		*Spodoptera littoralis*	300 mg/150 mL	**(Atwa et al., 2017)**
CuONPs-Ag					
CuO nanostructures	24-52.4 nm		*Spodoptera littoralis*	1 g L^{-1}	**(Shaker et al., 2016)**

CuONPs	29.84 ± 15.28 nm	Spherical	*Drosophila melanogaster*	0.24–7.5 mg mL^{-1}	(**Carmona et al., 2015)**

II.8.1. Mode of interaction of copper nanoparticles against insects

Despite the recommendations encouraging the application of NPs in agriculture for pest control, knowledge of the mode and mechanism of action is essential to predict the toxicological consequences arising from the use of CuNPs as pesticides. Several types of researches have illustrated the mechanism of action of CuNPs in bacteria (**Chatterjee et al., 2014; Varympopi et al., 2020; Aguilera-Correa et al., 2021**). For others, they confirmed the toxicity in rats (**Xu et al., 2018; Tang et al., 2018; Zhou et al., 2019).** However, illustrations of the mode and mechanism of action of CuNPs against insects are strictly limited, and only a few studies have focused on possible mechanisms of action (**Sezer Tuncsoy et al., 2019; Carmona et al., 2015**). Due to the lack of information regarding the mechanism of action of CuNPs at the molecular level in insects, the paragraphs below discuss the most likely mechanism of toxicity by which CuNPs extinguish insects. **Figure 10** illustrates the likely mechanism of action of CuNPs against insect pest.

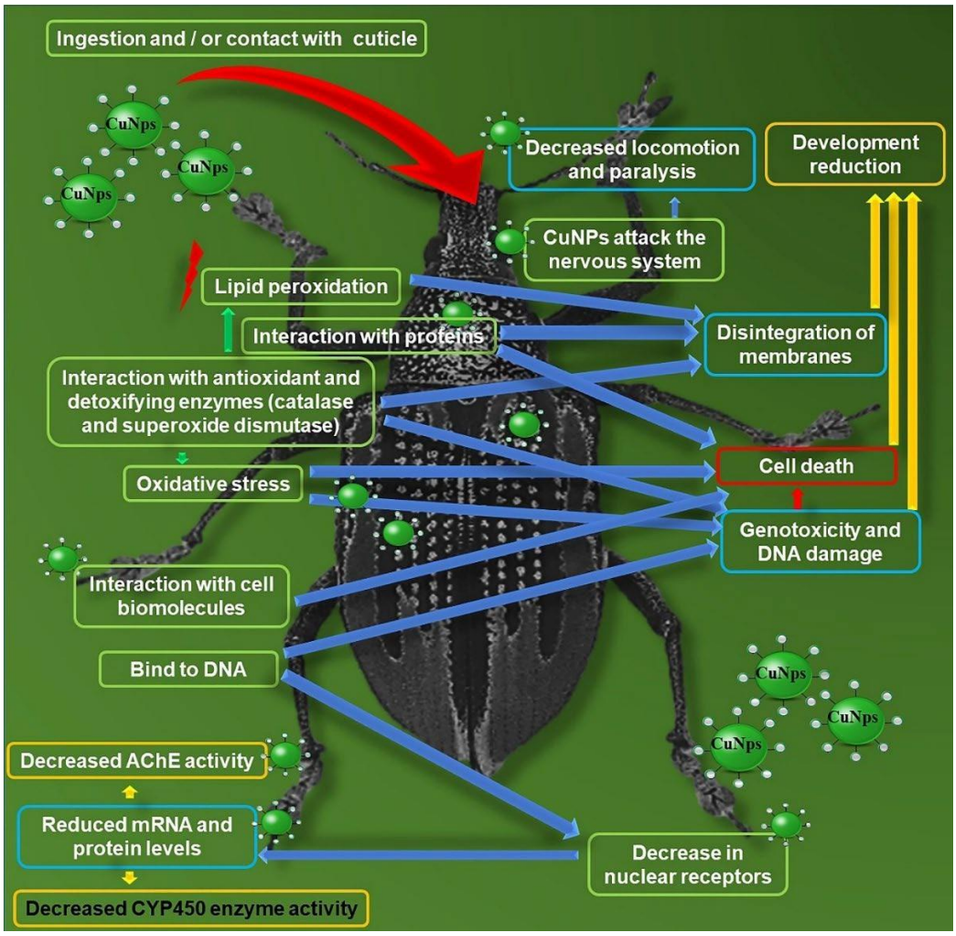

Figure 11. Proposed mechanism of action of CuNPs against insect pest.

In general, several probable mechanisms illustrating the mode and mechanism of action of NPs against insects are accepted. Oxidative stress triggered by NPs in the target tissues is the most discussed mechanism (**Angelé-Martínez et al., 2017**). In addition, toxicity may also be due to the penetration of nanoparticles orally inside the digestive tract and then into the circulation (**Atwa et al., 2017**). As demonstrated in the intracellular space of human cells (cell line A549), CuNPs can interfere with DNA and as a result, they induce oxidative damage and DNA damage (**Karlsson et al., 2009**). The interaction of NPs with the membrane components is also possible, and as a consequence, it damages the membrane (**Karlsson et al., 2013**).

In insect, DNA is considered the primary target of CuNPs, in addition, DNA is sensitive to stress and oxidative damage. As clearly shown in human cells (alveolar epithelial cell line R3/1), CuNPs release reactive oxygen species (ROS) and induce the formation of H_2O_2 that cause cell death (**Vanwinkle et al., 2009**). In insects, CuNPs are well known for their genotoxic properties with several mechanisms controlling their ability to promote DNA damage. In the larval hemocytes of *D.melanogaster*, CuNPs induce remarkable toxicity. CuNPs cause dose-dependent DNA strand damage and breaks (**Carmona et al., 2015**). Oxidative stress is proposed as the main mechanism of the alteration. The ROS generated in the intracellular environment potentially cause oxidative damage to DNA by a radical attack (**Ahamed et al., 2010**). DNA damage is also possible by interaction with malondialdehyde formed by the breakdown of lipid peroxidation products. In *D. melanogaster* treated with CuNPs, the induction of oxidative stress via lipid peroxidation is not an intrinsic characteristic effect of CuNPs, but it is attributed to copper (**Carmona et al., 2015**). In the human lung epithelial cell line (A549), cells surviving the actions of CuNP demonstrated cell cycle arrest. The blocked cell cycle is attributed to Cu ions released by CuNPs in the medium (**Hanagata et al., 2011)**.

CuNPs can alter the activities of antioxidant enzymes. As demonstrated in *G. mellonella* larvae exposure to CuNPs, the accumulation of copper in the midgut and fat body of the larvae causes a reduction of SOD in the fat body. However, CAT activity increases in the midgut and fat body. For glutathione S-transferase, an increase is noted in the fat body, while for acetylcholinesterase (AChE), a decrease is noted in the midgut (**Tuncso et al., 2019**). In *S. gregaria*, treatment with copper NPs also induced a decrease in the enzymatic activity of AChE (**Ramadan et al., 2020**). The affinity of copper for sulfur-donor groups may induce AChE inhibition by binding to its thiol residues (**Gomes et al., 2011**). Treatment of *S. littoralis* larvae (2^{nd} instar) by CuNPs resulted in malformations and morphological changes through adsorption of nanoparticles. Low levels of SOD are also noted (**Abd El Wahab and Anwar, 2014**). During the study of the enzymatic activity in *Daphnia magna*, the glutathione content and the activities of CAT and SOD are inhibited when the insect was exposed to CuNPs (**Liu et al., 2014**). This strongly suggests that the destabilization of the cellular functionalities is due to the strong oxidative stress induced by CuNPs.

CuNPs can reach the nervous system and induce severe toxicities. As demonstrated in *S. gregaria*, CuNPs cause paralysis, decreased locomotion, and tremors of the abdominal segments **(Ramadan et al., 2020**). The pervious result suggests that excessive copper levels can be harmful to the nervous system (**Gromadzka et al., 2020**). Otherwise, astrocytes can accumulate copper oxide nanoparticles and copper ions. When the accumulation exceeds the threshold tolerated by the cells, accelerated production of ROS is noted (**Bulcke and Dringen, 2016**). The gradual accumulation of copper causes brain damage and neurological symptoms. In rat astrocytes, the excess copper decreases the activity of glutathione reductase and increases the activity of nitric oxide. The destabilization of enzymatic activities aggravates oxidative stress **(Scheiber et al., 2014),** and causes a severe loss of cell viability (**Joshi et al., 2019**). CuNPs also induce mitochondrial dysfunctions and plasma membrane disintegration (**Minocha and Mumper, 2012**).

II.9. Nanomaterials as detoxification tools in feeds

Nowaday, the elimination and detoxification of mycotoxins has become a challenge for the food industry. Indeed, a large number of control and prevention strategies are applied. Despite the success recorded for conventional methods of detoxification in its early tages, the limitations noted

and the requirements demanded proved the failure of these methods. these methods suffer from disadvantages, such as the generation of toxic residues for humans and the environment, moreover the biological methods require selection and a long period of growth without neglecting the high cost during their applications. The inability of conventional methods to remove mycotoxins has prompted research to innovate more potent techniques capable of destroying toxigenic fungal cells and/or blocking their mycotoxin biosynthetic pathways. In recent years, several studies have reported the advantage of NMs in the detoxification of mycotoxins, several types of NMs have been the subject of a fungicide capable of inhibiting toxigenic molds and/or their toxin. In this part of the chapter several types of nanomaterials are reported.

II.9.1. Detoxification by targeting mycotoxinogenic molds or adsorption of mycotoxins

The treatment of corn with zinc oxide nanoparticles (ZnO-NPs) under the experimental conditions described by Hernández-Meléndez and his team in 2018 demonstrated that at 100 µg/g of ZnO-NPs, significant inhibition of the growth of *A. flavus* and mycotoxin synthesis are recorded. The untreated grains presented a fungal invasion of 67%, on the other hand, the treated grains presented a moderate fungal invasion (30%). Aflatoxin production in control and treated grains was 45 ng/g and 14 ng/g, respectively (**Hernández-Meléndez et al., 2018**). In a more recent study, the antiaflatoxinogenic efficacy of ZnO-NPs was 93.80% in stored maize grains, this result is recorded in the presence of 1.13 µg/kg of AFB_1 (**Yousif et al., 2019**). Similar results were observed with 100µg/ml of ZnO-NPs, a more than three-fold reduction (12ng/l of AFB_1) is observed on treated samples compared to controls (46 ng/l) (**Nabawy et al., 2014**). It should be noted that the reducing agents used in the synthesis of ZnO-NPS play a very important role in the efficiency of NPs, the ZnNPs derived from the reducing agent NaOH exert a large antifungal potential and high efficiency in DNA disintegration of maize fungal pathogens (**Kalia et al., 2021**). In liquid culture medium, ZnO-NPs prepared from *Syzygium aromaticum* demonstrated their efficacy in the regression of DON and ZEA of *F. graminearum* (**Lakshmeesha et al., 2019**). Anti-aflatoxigenic activity is highly dependent on reactive oxygen species (ROS) generation, Zn^{2+} release, hyphal damage, lipid peroxidation and antioxidant response (**Zhang et al., 2021**).

Silver nanoparticles (Ag-NPs) are also effective in inhibiting AFB_1 synthesis, Ag-NPs can gain access inside the fungal cell and alter genes responsible for mycotoxin biosynthesis. Deabes and his team confirmed this principle, Real Time-polymerase chain reaction (qRT-PCR) proved that Ag-NPs alter O-methyltransferase gene (*omt-A*) in the gene cluster responsible for the biosynthesis of AFB_1 (**Deabes et al., 2018**). Damage to genes responsible for mycotoxin biosynthetic pathways leads to downregulation or complete blockage of mycotoxin synthesis

Copper trace elements are essential in cereal crops. Cu deficiency may be the cause of higher *Fusarium* incidence on wheat. The treatment of wheat kernel with powdered CuO-NPs prepared as a superabsorbent polymer demonstrated that at a dose of 200 g/ha Cu, the NPs are able to imbibe water and slowly release nutrients. This result suggests that the Cu uptake capacity of the plants has improved. CuO-NPs improve the fat, crude fiber and cellulose content of wheat grain. Note that an absence of DON was recorded on the samples treated with CuO-NPs **(Kolackova et al., 2021**). In another study, the ion-exchanged zeolites with Li^+ and Cu^{2+} demonstrated an excellent antifungal effect against *A. flavus* and inhibition capacity of AFB_1 (**Savi et al., 2017**). However, the use of CuO-NPs can be toxic to agricultural crops, Rajput et al demonstrated that the application of CuO-NPs

cause toxicity in barley (*Hordeum sativum distichum*), harmfulness is characterized by the formation of electron-dense materials in the intercellular space of cells and a reduction in root length (**Rajput et al., 2018**).

Some polymers are also considered as fungicides, chitosan is among the most studied polymers, this compound has very good antifungal and antimycotoxinogenic activity. When applied alone, chitosan nanoparticles of with an average size of 3.00 ± 0.70 nm are able to inhibit AFB_1, chitosan is able to adsorb AFB_1 by interacting the positive charges of the amino group, with the negative charges of the oxygen atoms of the aflatoxins (**Cortés-Higareda et al., 2019**). Chitosan also has the ability to incorporate metallic NPs and other fungicides, the resulting NMs have an excellent antifungal and antimycotoxigenic potential. Copper-chitosan nanocomposite-based chitosan hydrogels (Cu-Chit/NCs hydrogel) prepared using a metal vapor synthesis exhibits an excellent antifungal activity against *A. flavus* associated with peanut meal and cotton seeds. The activity depends on the fungal strain and the concentration of NPs (**Abd-Elsalam et al., 2020**). Application of these NPs at different concentrations in maize grains (under laboratory conditions and incubated at 28°C for 28 days) inhibited *F. graminearum* growth and DON and ZEA synthesis. The encapsulation of the essential oil in NPs gives it an excellent stabilization by increasing the lifetime antifungal activity of CMEO by gradual release of antifungal constituents of Ce-CMEO-NPs (**Kalagatur et al., 2018**). In another study, Chitosan nano biopolymer entrapped *Coriandrum sativum* essential oil (Ce-CSEO-NPs) with a size ranging between 57–80 nm exerts good antifungal activity against several stored rice contamination molds, complete inhibition is recorded against *A. flavus, A. niger, A. fumigatus, A. sydowii, A. repens, A. versicolor, A. luchuensis, Alternaria alternata, Penicillium italicum, P. chrysogenum, P. spinulosum, Cladosporium herbarum, F. poae, F. oxysporum* Chitosan nanoemulsion showed insignificant inhibition of AFB_1 secretion (13.06%) (**Das et al., 2019**). Other essential oil encapsulates in Ce-NPs have also proven to be effective in inhibiting mycotoxin synthesis. Fumigation of two samples of maize (150g) with 1.0 µL/mL and 2.0 µL/mL of Origanum majorana essential oil encapsulated into chitosan nanoemulsion (Ce-OmEO-NPs) and inoculated with 10^6 spores/mL of *A. flavus* demonstrated relevant results, a total absence of AFB_1 is recorded in the two maize samples after a storage period of 6 months, however, the controls recorded contamination of approximately 26.17 µg/Kg and 25.37 µg/Kg (**Chaudhari et al., 2020).** Propolis known for its medicinal properties can also be incorporated into chitosan, the application of coatings based on chitosan and propolis on figs under semi-commercial conditions has shown encouraging results. After 12 to 15 days of storage of figs infected with spores of A. flavus and treated with NPs, a decrease in aflatoxin synthesis of <20 ppb is obtained compared to the control which recorded a level of 250 ppb, The sensory quality was acceptable, however, the antioxidant activity increased (**Aparicio-García et al., 2021**).

Carbon-based nanostructures have impressive advantages in the fight against mycotoxins, Graphene oxide GeO is among one of these promising materials, it has excellent adsorption property. In vitro tests have demonstrated that GeO (10 µg/mL) is capable of adsorbing AFB_1, ZEA and DON, The maximal removal efficiency was attained at 65% for 25 ng/g DON and 90% for 6 and 0.5 ng/g of ZEA and AFB_1, respectively. The adsorption capacity of GeO was 1.69 mg/g, 0.53 mg/g, 0.045 mg/g for DON, ZEA, and AFB1, respectively (**Horky et al. 2020**). Reduced graphene oxide-gold nanoparticle (rGO-AuNP) also exhibits good capacity and selectivity in the adsorption of AFB_1,

AFB_2, AFG_1, AFG_2, AFM_1 and AFM_2 from wheat and maize samples, the recovery of mycotoxins is related to the concentration of the nanocomposite, it increased from 48.5% to 106.6% when the quantity of rGO-AuNPs increased from 5 to 15 mg. However, a decrease in recoveries is recorded above 15 mg of rGO-AuNPs (**Guo et al., 2017**).

The application of magnetic nanomaterials in the removal of mycotoxins in food matrices could be attractive, these types of NMs have good adsorption and separation ability due to magnetic susceptibility (**Targuma et al., 2021**). These types of NMs are used in the detection of mycotoxins in food samples, suggesting their ability in the removal of mycotoxins. Iron oxide carbon nanocomposites prepared from for bagasse with a size range of 60–300 nm has an excellent capacity in adsorbing AFB_1, for 200 ppm, the equilibrium time was 115 min and 150 min at pH 3 and pH 7, respectively. According to the researchers, the prepared adsorbent can be used as an alternative to activated carbon to detoxify poultry feed (**Muhammad and Khan, 2018**). Magnetic carbon nanocomposites prepared from maize wastes has good capacity in the removal of AFB_1. Nearly 90% removal of AFB_1 was achieved, the equilibrium time is depend on pH, it is 96 and 180 min at pH 7 and 3, respectively **(Zahoor and Khan, 2016**). In another study performed on oil system with an initial concentration (0.2 µg/mL) of AFB1, magnetic mesoporous silica prepared from rice husk is able to adsorb 94.59% of mycotoxin (**Li et al., 2020b**). Magnetic nano-zeolite (MZNC) can adsorb mycotoxins better than the natural zeolite, 50 mg of the nanocomposite removed >99% of Afs, 50% of OTA, 22% of ZEA, and 1.8% of the DON from the contaminated sample **(Karami-Osboo et al., 2020).**

II.9.2. Detoxification of mycotoxins by photocatalysis

The photocatalytic nature of NMs enabled these materials to be involved in the degradation of mycotoxins. The process of degradation of mycotoxins by photocatalytic reactions as oxidation technology is very encouraging, this process is characterized by its low cost and respect for the environment. The process of photocatalysis involves a chemical reaction after absorption of photons, the reaction is based on the process of generating pairs of electrons (e^-) and holes (h^+) in the NM (photocatalyst) exposed to light. The electrons and the holes formed lead to reduction and oxidation reactions of the molecules adsorbed on the surface of the NMs. Along with this process, it is observed that during photocatalytic degradation, other reactive oxygen species (ROS) can also form, it is superoxide ($O_2^{\cdot -}$), hydroxyl radical ($OH^{\cdot}$), and hydrogen peroxide (H_2O_2) (**Murugesan et al., 2021**).Formation of ROS speciesis shownin **Figure12**.

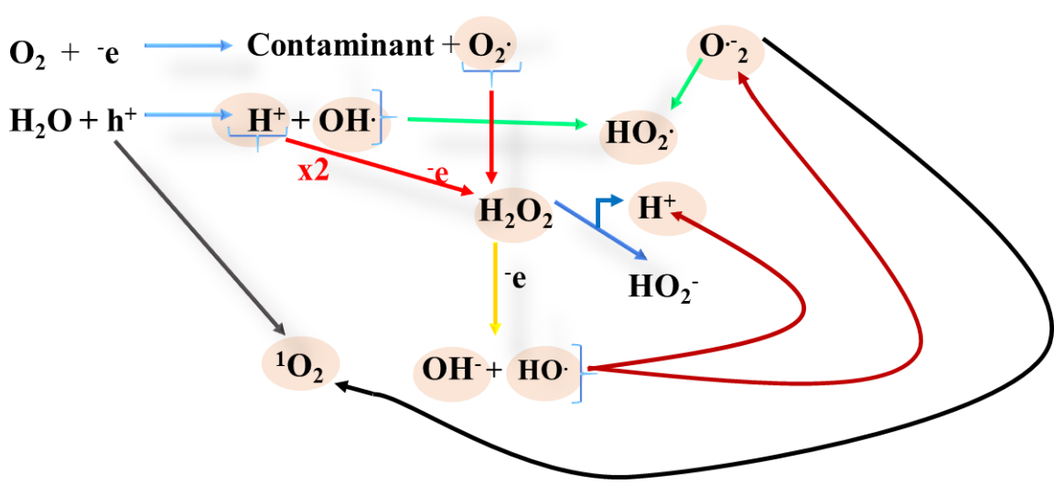

Figure 12. Formation of ROS species.

Notably, He et al. developed a novel and highly efficient nanomaterials of cerium (Ce) doped titanium dioxide (TiO_2) (Ce-TiO_2) with an enhanced photocatalytic activity for the DON in aqueous solution under ultraviolet light irradiation (λ = 254 nm). Different levels of Ce doping on pure TiO_2 demonstrated different Ce-TiO_2 photocatalytic degradation effects. The degradation rate can reach 96% using 0.5Ce-TiO_2 after 240 min. The exploration of the main ROS active in the process of DON degradation indicate that the hole plays a crucial role in the photocatalytic reaction than OH•. Moreover, the small CeO_2 particles produced on the TiO_2 particles caused by Ce doping play a co-catalytic effect on DON degradation following the generation $O_2^{\bullet-}$. The two possible degradation intermediate products are $C_5H_8O_3$ and $C_{17}H_{18}O_6$ (**He et al., 2021**). The degradation of DON in aqueous solution by the photocatalytic activities of the dendritic-like α-Fe_2O_3 under visible light irradiation (λ > 420 nm) demonstrated that dendritic-like α-Fe_2O_3 could adsorb more DON than that of commercial α-Fe_2O_3. Degradation rate is estimated at 90.3% in 2 h at initial concentration of 4.0 μg/mL of DON. During the photoreaction over α-Fe2O3, the morphology of the dendritic-like α-Fe_2O_3 absorbs more sunlight and provides more electrons and the holes, these lead to the formation of active radicals such as $O_2^{\bullet-}$and OH• which could react with the active site of DON and form two intermediate products (**Wang et al., 2019**), in another study, three degradation products were identified, namely $C_{15}H_{20}O_8$, $C_{15}H_{20}O_7$ and $C_{15}H_{20}O_5$ under simulated sunlight using UCNP@TiO_2 (6 mg/mL). OH·, h^+ and $O_2^{\cdot-}$ are the main ROS produced in the photocatalytic reaction. The application of UCNP@TiO_2 in the reduction of DON in wheat demonstrated a decrease in the detoxification compared to that of standard DON. It may be due to the combination of mycotoxin with starch, protein and other macromolecules of wheat, on the other hand, the light cannot be evenly diffused on the contaminated wheat, which also affect the degradation efficiency **(Wu et al., 2020b).**

A recent study investigated the photocatalytic activity of ZnO-NPs in the degradation of AFB_1 in aqueous solution under UV light. A complete removal of AFB_1 (10 μg/L) by 0.10 mg/mL of NPs has been recorded after 60 min under UV irradiation. Application NP in soymilk (5 mg ZnO-NPs to 50 mL soymilk with 10 μg/L of AFB_1) completely removed AFB_1 (91.53%) after 60 min under UV irradiation with no significant effect on its overall acceptability, which suggests its application in liquid foodstuffs (**Raesi et al., 2022**). Similarly, the study of the effect of ZnO-NPs on fumonisin accumulation by *F. proliferatum* both in vitro and in situ demonstrated a significative result. With ZnO-NPs concentrations of 0.8 and 8 g L-1 at 25 °C, 21 days and under darkness or photoperiod incubation, a high reduction (84–98%) occurred after 14 days under photoperiodic incubation. Under the in-situ assay, the evaluation of the effect of ZnO-NPs on FB_1, FB_2 and FB_3 rates on irradiated maize grains (adjusted to 0.995, 0.98 and 0.97 aW) in darkness at 25 °C during 21 days demonstrated a reduction of FBs rates. At 0.8–2 g kg−1 and 0.98–0.995 aW, ZnO-NPs reduce total FBs accumulation by 71–99%, suggesting that ZnO-NPs could be applied in maize grains to control phytopathogenic and toxigenic fungi such as *F. proliferatum* and to reduce fumonisins accumulation (**Pena et al., 2022).** The photocatalytic graphitic carbon nitride (g-C_3N_4) could induce photocatalytic effect on ZEA UV lamp (λ = 254 nm). Under experimental conditions, g-C3N4 degrades a rate of 50% of ZEA in real powder samples (**Li et al., 2021**). Patulin degradation in aqueous solution is also possible by nitrogen-doped chitosan-TiO_2 nanocomposite under UV, 500 μg/kg was completely degraded within 35 min. This improved degradation compared to TiO_2 nanoparticles and chitosan-TiO_2 nanocomposite is linked to the reduction of the average particle size of TiO_2 nanoparticles due to : (1) the introduction of nitrogen and chitosan, the structure obtained facilitates the movement of -

e from the structure to the surface, thereby reducing the probability of recombination with holes, (2) the introduction of nitrogen and chitosan increase the surface of the nanocomposite which is beneficial to the adsorption of toxin, (3) the introduction of nitrogen and chitosan improved the photoresponse ability of TiO_2 nanoparticles and enhanced its photocatalytic activity (**Huang and Peng, 2021**). Activated carbon supported TiO_2 catalyst (AC/TiO_2) has an excellent efficiency for degradation of AFB_1 under UV–Vis light in comparison with TiO_2. OH• and *h*+ play an important role in the degradation of AFB1 **(Sun et al., 2019**). Magnetic graphene oxide/TiO_2 nanocomposite ($MGeO/TiO_2$) is able to reduce AFB_1 in corn oil, the quality of the nanocomposite-treated oil was acceptable after 180 days of storage (**Sun et al., 2021**).

Experimental part

I. Material and methods

I. Material and methods

I .1.Actinomycetes

I.1.1. Reactivation of a preserved strain (T_{003})

The Actinomycete strain used in this study, designated T_{003}, belongs to the microbial collection of **Dr. Gacem Mohamed Amine**. The strain had previously been preserved at –20 °C in a 50% (v/v) glycerol solution.

For reactivation, a small aliquot of the frozen culture was taken using a sterile needle and inoculated onto Casein Starch Agar (CSA) medium. The plates were incubated at 30 °C for 3–5 days. Characteristic Actinomycete colonies gradually appeared, exhibiting filamentous morphology and distinctive pigmentation that varied according to the strain.

I.1.2. Purification of the strain

Purification is a crucial step to ensure that each culture represents a single, genetically uniform organism. This was achieved by repeated sub-culturing on CSA medium and GYM medium. Each colony showing distinct coloration or morphology was isolated and cultured separately. After incubation at 30 °C for 3–5 days, homogeneous colonies were selected and considered as pure isolates.

I.1.3. Preservation of the purified strain

To ensure long-term viability and genetic stability of the purified strain T_{003}, preservation was carried out in 50% (v/v) glycerol. Sterile tubes were prepared by filling them with equal volumes of sterile distilled water and glycerol, followed by autoclaving for sterilization.

After cooling, aliquots of the pure culture were aseptically transferred into the tubes. The preparations were then stored at –20 °C for short-term maintenance or at –80 °C for long-term preservation. The tubes used for glycerol preservation are known as cryovials or freezing vials.

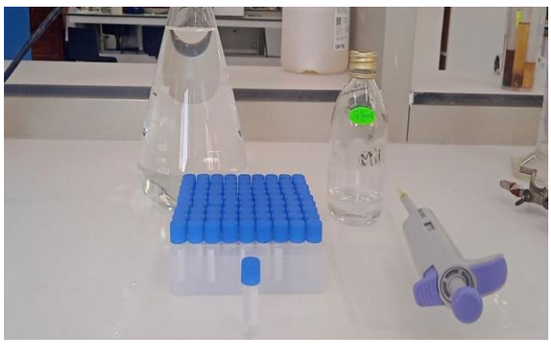

Figure 13. Preservation of T_{003} strain in glycerol 50%.

I.2. Fungal strains

I.2.1. Isolation and preparation of fungal strains

In this study, three phytopathogenic fungal strains were used: *Fusarium oxysporum, Rhizoctonia solani*, and *Phytophthora sp*. *Fusarium oxysporum* strain was obtained from the microbial collection of **Dr. Gacem Mohamed Amine**, while *Rhizoctonia solani* was isolated from infected tomato tissues, and *Phytophthora sp*. was isolated from infected potato leaves exhibiting symptoms of late blight.

Small fragments of the infected plant tissues were aseptically placed onto Potato Dextrose Agar (PDA) medium in sterile Petri dishes. All plates were incubated at 30 °C for 7 days to allow fungal growth and colony development.

I.2.2. Purification of fungal isolates

After initial growth, each fungal strain was purified to obtain a single, genetically uniform culture. This was achieved by sub-culturing individual colonies with distinct morphological characteristics onto fresh PDA plates. The purified colonies were incubated at 30 °C for 7 days to confirm their purity.

I.2.3. Identification of *Fusarium, Rhizoctonia,* and *Phytophthora*

Following purification, the fungal strains were identified based on their morphological and microscopic characteristics using the microculture method:

- ***Fusarium oxysporum*** forms cottony colonies ranging from white to pink. Microscopically, it produces crescent-shaped macroconidia with multiple septa.
- ***Rhizoctonia solani*** develops flat, brown, felt-like colonies without spore formation; its hyphae branch at right angles and may produce dark sclerotia.
- ***Phytophthora sp***. develops creamy, fluffy colonies, and microscopic examination reveals coenocytic hyphae typical of oomycetes.

Described by **Haris** (**1989**), the microculture technique involves inoculating fungal spores onto a slide containing small squares of acidified PDA medium, which are then covered with a coverslip. The spores are placed along the peripheral edges of the medium to provide a high oxygen potential, promoting germination. The entire assembly is incubated in a sterile, humid chamber at 25 ± 2 °C for 7 days (Figure).

After incubation, the coverslips with attached mycelium are transferred onto other sterile slides containing a few drops of lactophenol. Microscopic observations are then performed at ×10, ×40, and ×100 magnifications. Fungal genera are determined based on their cultural and microscopic characteristics, referring to the manual of **Barnett** and **Hunter** (**1972**).

This workflow ensures that the identification is performed only on pure, uncontaminated cultures, providing reliable characterization before further experimentation.

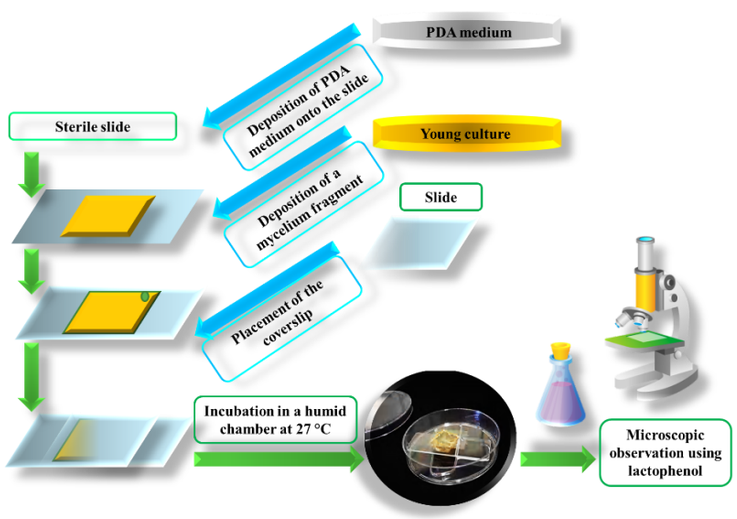

Figure 14. Microculture of fungi for microscopic identification.

I.3. Submerged pre-culture of actinomycetes in gym liquid medium for fermentation preparation

The submerged pre-culture stage aims to promote the growth and multiplication of Actinomycetes isolates in a nutrient-rich liquid medium before the main fermentation. In this step, sterile Erlenmeyer flasks containing 150 mL of liquid Gym medium are prepared. Small agar squares cut from solid Gym medium with actively growing Actinomycetes (T03) are inoculated into the flasks. The cultures are incubated under agitation at 28–30 °C for 7 to 10 days to ensure sufficient aeration and microbial

development. This submerged culture technique, carried out in a liquid medium under continuous shaking, offers significant advantages such as higher biomass yield and enhanced production of bioactive metabolites within a shorter period (**Singh et al., 2016**). The resulting pre-culture provides abundant microbial biomass that serves as the inoculum for the subsequent fermentation or metabolite production stage (Figure 05: Gym liquid medium used for the pre-fermentation stage).

Figure 15. Gym liquid medium used for pre-fermentation stage.

I.4. Extraction process of secondary metabolites produced by actinomycetes.

To prepare the crude extracts, 20 ml of ethyl acetate (Sigma-Aldrich, USA) was mixed with 20 ml of bacterial culture from the previously prepared selected isolate (culture incubated under agitation for 10 days in liquid media, namely: 5294). The mixtures were agitated for 12 min, and then the media were separated by centrifugation at 6000 rpm for 10 min. The solvent containing the metabolites was subsequently transferred to a rotavapor (Heidolph, Germany) in order to evaporate it completely. Once evaporation was completely achieved, the weight of the extract is calculated and then recovered in 1 ml of methanol (figure).

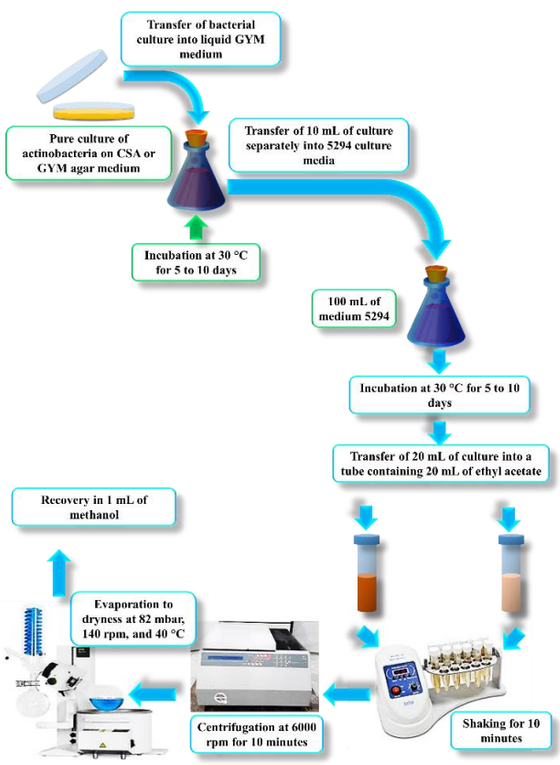

Figure 16. Extraction process of secondary metabolites produced by actinomycetes.

I.5. Biosynthesis of copper nanoparticles and characterization

I.5.1. Biosynthesis and recovery of copper nanoparticles (CuNPs) from actinomycete culture

The culture medium 5294 containing Actinomycetes was collected in an Erlenmeyer flask and subjected to thermal treatment in a water bath at 60–70 °C for one hour to induce cell lysis. This

process facilitates the release of intracellular bioactive compounds and the potential formation of biogenic nanoparticles.

Following lysis, the lysate was distributed into 50 mL centrifuge tubes and centrifuged at 6000 rpm for 10 minutes. The resulting supernatant, containing soluble metabolites and extracellular biomolecules, was retained for nanoparticle precipitation experiments.

To each supernatant sample, an aqueous copper sulfate ($CuSO_4$) solution was added as a source of Cu^{2+} ions. The mixtures were then incubated in a water bath at 60–70 °C for 15–20 minutes to promote the bioreduction of copper ions and the subsequent formation of bio-capped copper nanoparticles (CuNPs). Subsequently, NaOH was added dropwise until the solution reached an alkaline pH (8), favoring the reduction and precipitation of copper nanoparticles.

After the bioreduction step, the samples were centrifuged again at 6000 rpm for 10 minutes. The resulting pellet, containing the biosynthesized CuNPs, was collected, whereas the supernatant—containing residual copper ions and other impurities—was discarded.

For purification, the pellet was washed repeatedly with distilled water followed by centrifugation until the blue or green coloration, indicative of unreacted copper species, disappeared completely. A final wash with ethanol was performed to remove organic impurities (**Iravani, 2011 ; Rajeshkumar and Bharath, 2018**).

The purified nanoparticle pellet was then dried either at room temperature or in a low-temperature oven. The dried CuNPs were stored in sterile containers for subsequent physicochemical characterization, including UV–Vis spectrophotometry, Fourier-transform infrared spectroscopy (FTIR), and electron microscopy (SEM/TEM), to confirm their formation, morphology, and stability.

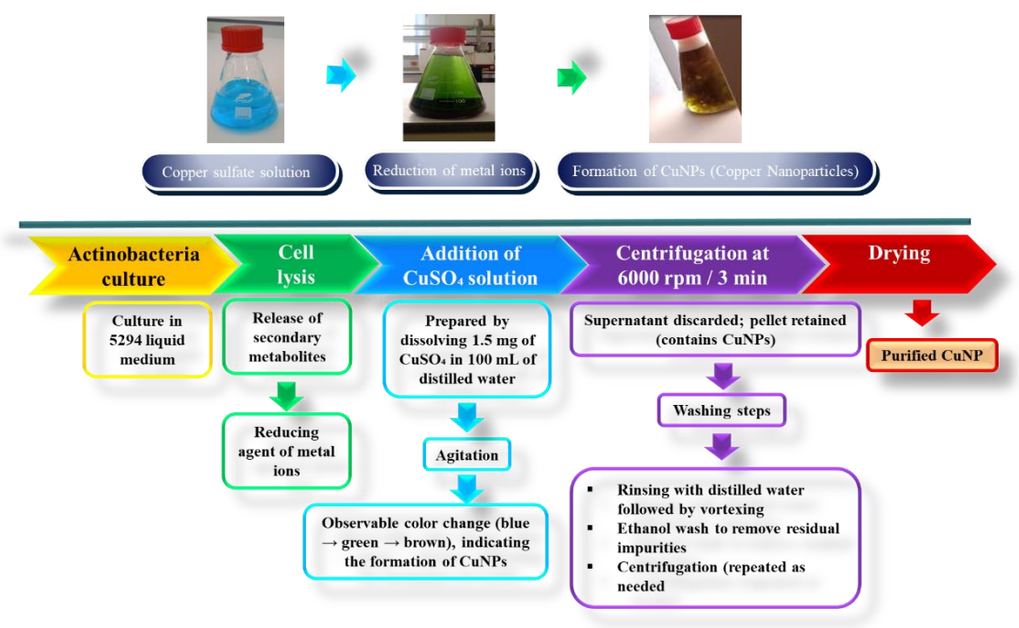

Figure 17. Preparation of biogenic copper nanoparticle.

I.5.2. Characterization of copper nanoparticles (CuNPs)

The synthesized copper nanoparticles (CuNPs) were subjected to comprehensive physicochemical characterization using several analytical techniques to determine their structural, morphological, and optical properties.

- **The UV–Visible spectroscopy** analysis was carried out using a spectrophotometer in the wavelength range of 200–800 nm to confirm nanoparticle formation through surface plasmon resonance (SPR) absorption, typically observed around 560–580 nm for CuNPs.
- **The Fourier Transform Infrared Spectroscopy (FTIR)** analysis was performed in the spectral range of 400–4000 cm^{-1} to identify the functional groups present on the nanoparticle surface and to confirm the presence of organic biomolecules responsible for capping and stabilization.
- **The X-Ray Diffraction (XRD)** analysis was conducted using Cu Kα radiation (λ = 1.5406 Å) to determine the crystalline nature, phase purity, and average crystallite size of the CuNPs, which was calculated using the Debye–Scherrer equation.
- **The Transmission Electron Microscopy (TEM)** analysis provided detailed insights into the morphology and particle size distribution, revealing spherical and well-dispersed nanoparticles with average diameters typically below 50 nm.

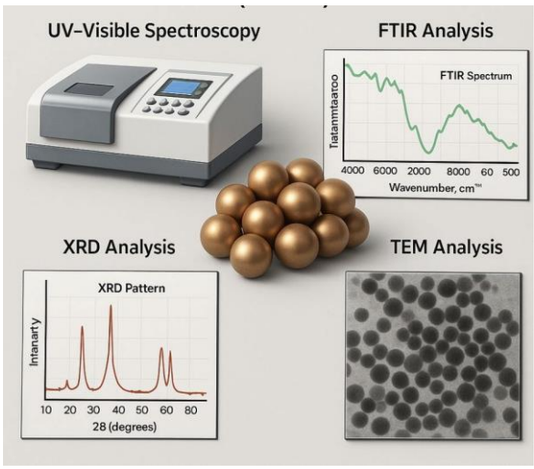

Figure 18: Physicochemical characterization of copper nanoparticles (CuNPs).

Together, these complementary techniques confirmed the successful synthesis of stable, crystalline, and uniformly distributed CuNPs with properties suitable for biological and antifungal applications.

I.6. Measurement of antifungal activity

I.6.1. Measurement of antifungal activity of crude extract

The antifungal activity was evaluated using the agar well diffusion method on Potato Dextrose Agar (PDA) plates. Young fungal cultures were first prepared, and the inoculum was adjusted to the desired optical density using a spectrophotometer to ensure standardized spore concentration. PDA plates were inoculated uniformly by flooding with 100 µL of the prepared fungal inoculum (106 UFC). After solidification, wells were aseptically perforated in the agar using a sterile cork borer. Each well was then filled with 30 µL of the crude extract. The plates were incubated at 27 °C for 5 days to allow fungal growth and diffusion of the extract.

Following incubation, the antifungal activity was determined by measuring the diameter of the inhibition zones around each well. The results were expressed in millimeters (mm) as an indication of the antifungal potential of the tested sample.

This method is a well-established and widely used technique for assessing the antimicrobial or antifungal efficacy of bioactive compounds (Balouiri et al., 2016).

I.6.2. Measurement of antifungal activity of copper nanoparticles

The antifungal potential of copper nanoparticles (CuNPs) was assessed using the agar well diffusion method on Potato Dextrose Agar (PDA) medium. Wells were aseptically perforated into the solidified and inoculated PDA using a sterile cork borer. Each well was subsequently filled with 30 µL of CuNP suspensions prepared at different concentrations: 2, 1.5, 1.0, 0.75, 0.5, 0.25, and 0.1 mg/mL.

The inoculated plates were incubated at 27 °C for 5 days under static conditions to allow fungal growth and diffusion of the nanoparticles into the medium. After incubation, the antifungal activity was evaluated by measuring the diameter of the inhibition zones surrounding each well. The inhibition zone was expressed in millimeters (mm) as an indicator of the antifungal efficacy of the copper nanoparticles (**Balouiri et al., 2016**).

All treatments (extract and CuNP concentrations) were performed in triplicate to ensure the reliability and reproducibility of the results.

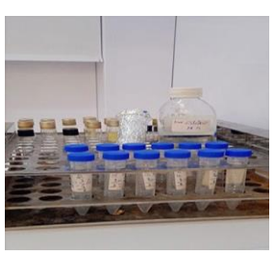

CuNP concentrations

Crude extract

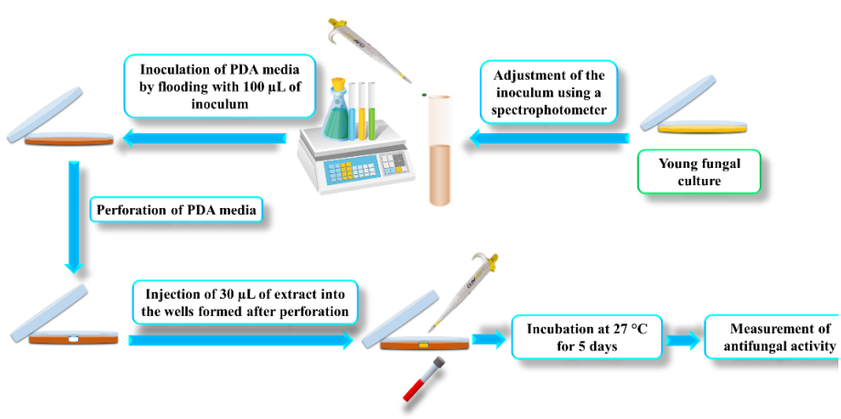

Figure 19. Schematic representation of the antifungal activity assay of crude extract and copper nanoparticles by the agar well diffusion method.

I.7. Antioxidant test by DPPH radical scavenging assay

The 2,2-diphenyl-1-picrylhydrazyl (DPPH) assay is among the most widely employed methods for the rapid and reliable assessment of antioxidant activity, owing to the stability of the DPPH radical and the simplicity of the procedure. DPPH exhibits a characteristic absorption maximum at 517 nm within the visible spectrum. In this study, the evaluation of free radical scavenging activity was performed following the method of **McCune** and **Johns** (**2002**), with slight modifications as described by **Dosseh** et al. (**2014**) and adopted by **Evenamede** et al. (**2017**).

An amount of 0.025 g of copper nanoparticles was accurately weighed and transferred into a clean test tube. Subsequently, 12.5 mL of hydrochloric acid (HCl) was added, and the mixture was vortexed thoroughly until a homogeneous suspension was obtained. This stock solution served as the basis for preparing the different working concentrations used in the assay.

From the stock solution, a series of dilutions was prepared to obtain the following concentrations: 2, 1.5, 1.0, 0.75, 0.5, 0.25, and 0.1 mg/mL (or as specified according to the experimental design).

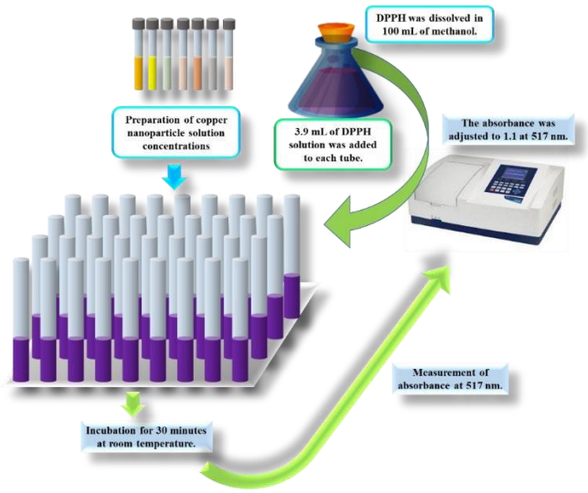

Figure 20. Schematic representation of the DPPH radical scavenging assay procedure for evaluating the antioxidant activity of copper nanoparticles.

To each test tube, add 3 mL of DPPH solution and 1 mL of nanoparticle solution at the desired concentration. Mix the contents thoroughly and incubate the tubes in the dark at room temperature for 30 minutes to prevent photodegradation of DPPH. After incubation, measure the absorbance at 517 nm using a UV–Visible spectrophotometer, with methanol serving as the blank.

I.8. Evaluation of insecticidal activity

The insecticidal activity of copper nanoparticles (CuNPs) was evaluated using the leaf-dip method described by **Bhattacharyya** et al. (**2016**), with some modifications adapted for tomato leaves.

A colony of aphids was maintained on healthy tomato plants to obtain a homogeneous population of insects for bioassays. The experiments were conducted using tomato leaves collected from both healthy and naturally infested plants.

The selected leaves were carefully washed three times with distilled water and then air-dried at room temperature. They were subsequently immersed for 5 minutes in CuNPs solutions prepared at different concentrations: 0.1, 0.25, 0.5, 0.75, 1, 1.5, and 2 mg/mL. Each concentration was prepared by dilution in sterile distilled water.

After immersion, the leaves were placed in Petri dishes (90 × 14 mm) lined with moistened filter paper and left to dry at room temperature. Once dry, 10 live aphids were gently transferred onto each leaf using a fine brush.

Two control groups were prepared:

- Positive control: infested but untreated leaves.
- Negative control: 10 aphids placed in a Petri dish with moistened filter paper (without leaf or treatment).

Each experimental condition was performed in triplicate. The number of dead aphids was recorded every 3 hours until complete mortality was achieved. Death was confirmed by the absence of movement upon stimulation of legs and antennae using a fine brush.

The mortality rate and corrected mortality rate were calculated according to **Abbott's** formula (1925):

Corrected mortality (%) = [(Treatment mortality − Control mortality)/ (100 − Control mortality)] x 100

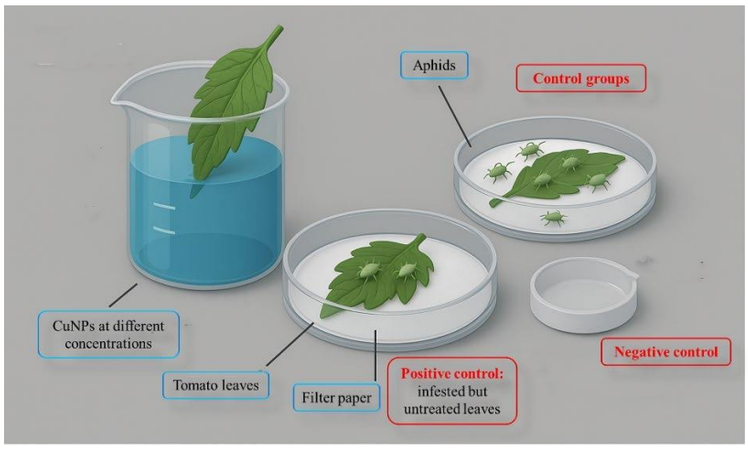

Figure 21. Experimental design illustrating the evaluation of copper nanoparticle treatments (0.1–2 mg/mL) on tomato plants infested with aphids.

I.9. Evaluation of the effect of copper nanoparticles on tomato seed germination and pigment content

I.9.1. Experimental design for germination assay

To evaluate the phytotoxic or stimulatory effects of copper nanoparticles on tomato (*Solanum lycopersicum*) seed germination, seven different nanoparticle concentrations were prepared using distilled water acidified with HCl: 2, 1.5, 1, 0.75, 0.5, 0.25, and 0.1 mg/mL.

For each concentration, ten tomato seeds were placed in sterile test tubes containing the respective nanoparticle suspensions and soaked for three hours under controlled conditions. After treatment, the seeds were transferred into pots containing sterilized soil and covered with a thin layer of the same soil.

Two control tests were also conducted: the first with untreated seeds (seeds alone) and the second with seeds soaked only in the HCl-acidified solution without nanoparticles (**Adhikari, et al., 2012**).

All pots were maintained under identical environmental conditions and regularly irrigated with tap water. Germination percentage and early seedling development were monitored for two weeks.

I.9.2. Determination of chlorophyll and photosynthetic pigments in tomato seedlings

The quantification of photosynthetic pigments, including chlorophylls (a and b) and carotenoids, was performed spectrophotometrically after pigment extraction from 15-day-old fresh tomato seedling leaves, following the classical methods of **Arnon** (**1949**) and **Lichtenthaler** and

Wellburn (**1983**). This procedure allows for the evaluation of the physiological effects of copper nanoparticles on the photosynthetic efficiency of the treated plants.

For sample preparation, approximately 0.3 g of fresh tomato leaves were carefully weighed after gently removing surface moisture. The leaves were then finely chopped using a sterile scalpel to facilitate pigment extraction. The chopped plant material was transferred into a clean mortar, and 10 mL of acetone (80% or 90%) was added for every 0.1 g of plant tissue. The mixture was thoroughly ground until a homogeneous bright green extract was obtained, indicating the release of chlorophylls and other pigments. The homogenate was then filtered through Whatman filter paper or centrifuged at 3000 g for 10 minutes to obtain a clear supernatant containing the dissolved pigments (Figure).

Spectrophotometric quantification of chlorophylls and carotenoids was carried out by transferring an aliquot of the clear extract into a clean quartz cuvette and measuring absorbance using a UV–Visible spectrophotometer. Absorbance readings were taken at 663 nm for chlorophyll a, 647 nm for chlorophyll b, and 470 nm for total carotenoids, with a baseline correction at 750 nm to eliminate turbidity interference. The concentrations of the different pigments were then calculated using the equations proposed by Lichtenthaler and Wellburn (1983), allowing the determination of total chlorophyll content and the relative pigment composition in tomato seedlings.

Figure 22. Preparation of chlorophyll extract from tomato leaves using acetone.

I.10. Evaluation of the effect of copper nanoparticles on fungal growth and tomato plant health under greenhouse conditions

I.10.1. Preparation and transplantation of tomato seedlings for growth experiments

During this stage, tomato seeds were first sown in small pots, with five seeds per pot. A thin layer of soil was added to cover the seeds. A total of 80 pots were prepared and maintained under controlled watering and care conditions to promote germination and initial growth.

After three weeks, when the seedlings were sufficiently developed, they were carefully transferred to a pre-prepared soil bed. The soil had been conditioned and well-aerated to facilitate root development. To organize the planting area and separate the experimental groups, plastic films were used as barriers between the rows. In addition, a wooden stake was placed next to each plant to provide structural support during the growth of the tomato plants, as illustrated in the corresponding figure.

The planting bed was divided into three rows per section, with six tomato plants per row, to ensure better organization and optimal monitoring. After transplantation, each plant was irrigated with 200 mL of water containing NPK fertilizer at a concentration of 0.5 g/L, once a week for two months. This nutrient solution contributed to strengthening root establishment and promoting healthy vegetative growth.

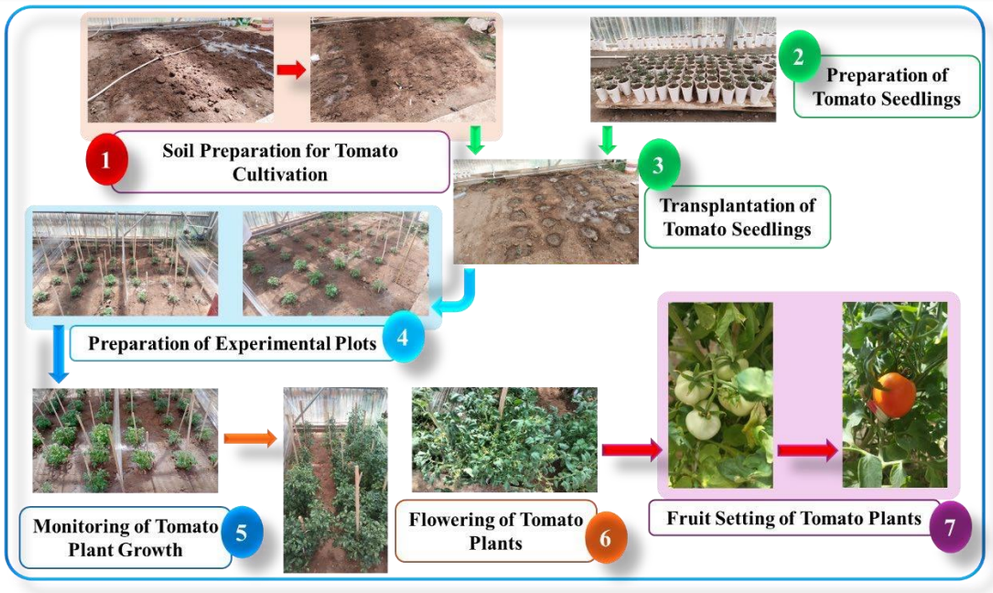

Figure 23. Evaluation of the effect of copper nanoparticles on fungal growth and tomato plant health under greenhouse conditions

I.10.2. Tomato fruit development

During the growth period, tomato plants were regularly monitored to document the morphological and physiological progression of fruit development. Following flowering and pollination, the fertilized ovaries initiated the fruit set process, marking the onset of fruit formation. The growth of the tomatoes occurred in distinct phases: an initial stage of rapid cell division, followed by a phase of cell expansion leading to the gradual increase in fruit size.

Over time, the fruits exhibited a gradual color transition from green to orange and finally to deep red, corresponding to the degradation of chlorophyll and the accumulation of carotenoid pigments, particularly lycopene and β-carotene. This chromatic evolution reflects the physiological stages of ripening, during which significant biochemical changes also occur, such as sugar accumulation, reduction in acidity, and softening of fruit tissues.

Visual and photographic observations conducted throughout this period clearly illustrate these developmental stages and confirm a uniform and healthy fruit maturation, favored by optimal cultivation conditions in terms of irrigation, nutrient availability, and light exposure.

I.10.3. Fungal inoculation procedure

For the fungal infection experiment, four distinct plots were established, each consisting of three rows of tomato plants.

- The first plot served as the negative control, with no fungal inoculation, to observe normal plant growth.
- The second plot, used as the positive control, was infected only with the pathogenic fungi without any treatment.
- The third plot was infected and treated with a copper-based nanosolution, while
- The fourth plot was infected and treated with a commercial chemical fungicide (Metraz).

The fungal inoculum was prepared from preserved fungal cultures maintained in slanted tubes. Using a sterile swab, a portion of each pathogenic strain (Fusarium, Phytophthora, and Rhizoctonia)

was transferred into sterile distilled water and thoroughly homogenized. The resulting suspension was then analyzed using a spectrophotometer. When the absorbance value ranged between 0.8 and 1.0, the suspension was considered suitable for inoculation.

Once the fungal suspensions were ready, they were transferred into sterile spray bottles. A volume of 10 mL of each fungal suspension was uniformly sprayed onto the tomato plants in the corresponding plots, targeting both the foliage and the fruits. This quantity was chosen to ensure a consistent inoculation while avoiding excessive moisture that could alter experimental conditions.

This spraying method ensured direct contact between the fungal pathogens and their preferred infection sites, thereby simulating natural infection conditions under controlled experimental settings.

I.10.4. Treatment and comparative evaluation

One week after fungal inoculation, two distinct treatments were applied to two of the four experimental plots to evaluate the effectiveness of different antifungal agents.

The first infected plot was treated with a commercial chemical fungicide (Metraz), prepared according to the manufacturer's instructions and applied uniformly to the infected tomato plants.

The second infected plot received a biological treatment based on a copper nano-solution, prepared under precise experimental conditions. The nano-solution was obtained by accurately dissolving 0.1 g of nanoparticle powder in one liter of distilled water, followed by vigorous stirring to ensure a homogeneous and stable dispersion of the nanoparticles. During preparation, the pH of the solution was measured and adjusted to 8.1, which was considered optimal for application on tomato plants.

Both treated plots were maintained under identical environmental conditions (temperature, humidity, and watering), and the plants were regularly monitored to compare their physiological and pathological responses.

This experimental setup, which also included a negative control plot (non-infected) and a positive control plot (infected but untreated), was designed to assess and compare the efficacy of a synthetic fungicide and a copper-based nanotechnological treatment in controlling fungal diseases caused by Fusarium, Phytophthora, and Rhizoctonia.

II. Results and discussion

II. Results and discussion

II.1. Biogenic Formation of nanostructures mediated by *Streptomyces* strain

II.1.1. Revivification de la souche T_{003}

GYM medium

Figure 24. Colony morphology of *Streptomyces* sp T_{003} on GYM (Glucose–Yeast extract–Malt extract) and CSA (Casein Starch Agar) medium after 10 days of incubation.

The strain *Streptomyces sp* T_{003}, cultivated on GYM (Glucose–Yeast extract–Malt extract) medium, exhibited abundant growth characteristic of the genus *Streptomyces*. The substrate mycelium appeared dense, well-adhered, and deeply embedded in the agar, showing a brown to dark red coloration that indicates the production of phenolic or melanin-like diffusible pigments. The aerial mycelium was fine, powdery to chalky in texture, and ranged from whitish to pale grayish-pink depending on the stage of maturation. The colony surface was dry and friable, reflecting good sporulation. Microscopic observation revealed thin, branched hyphae forming a compact network, with long, flexible spore chains arranged in spirals, which are typical morphological traits of Streptomyces species. This overall morphological and physiological behavior demonstrates the strain's intense metabolic activity, favored by the rich nutrient composition of GYM medium, which provides optimal conditions for the revival and morphological differentiation of actinobacteria.

On CSA (Casein Starch Agar) medium, the strain *Streptomyces* T_{003} exhibited a vigorous and well-developed growth, forming dense colonies with a striking pigmentation. The substrate mycelium appeared compact, firmly attached to the agar, and showed an intense orange to deep red coloration, indicating the production of diffusible pigments associated with secondary metabolism. The aerial mycelium was moderately developed, dry and powdery in appearance, with a whitish to pale orange tone that contrasted with the strongly pigmented substrate layer. The pigmentation diffused slightly into the surrounding agar, producing a reddish halo that suggests the secretion of soluble metabolites or antibiotic compounds. Microscopically, the strain displayed thin, branched hyphae with well-formed spore chains arranged in irregular spirals, typical of *Streptomyces* morphology. The growth pattern on CSA medium demonstrates the strain's ability to utilize complex carbon and nitrogen sources such as starch and casein, confirming its strong proteolytic and amylolytic potential. Overall, the CSA medium supports good differentiation and pigment production, making it suitable for studying the metabolic activity and secondary metabolite synthesis of *Streptomyces* T_{003}.

II.1.2. Fungal strain isolation

II.1.2.1. Isolation and identification of *Fusarium oxysporum*

The fungal strain isolated from the microbial collection of **Dr. Gacem Mohamed Amine** developed rapid, cottony growth on Potato Dextrose Agar (PDA) medium after 7 days of incubation at 30 °C. The colonies initially appeared white and fluffy, later turning pink to violet as pigmentation accumulated within the mycelium and diffused slightly into the surrounding agar. The colony margin was regular, and the reverse of the plate displayed a pale pink coloration.

Microscopic observations revealed the typical morphological structures of *Fusarium oxysporum* (**Figure 25**). The fungus produced both macroconidia and microconidia. The macroconidia were hyaline, multicellular, slightly curved (canoe-shaped), and possessed 3–5 septa, measuring approximately 20–40 µm in length. The microconidia were single-celled, oval to ellipsoidal, and borne on short, simple conidiophores. In addition, chlamydospores were observed, appearing as thick-walled, round cells formed singly or in pairs within the hyphae, indicating the fungus's ability to survive under adverse conditions.

Based on both cultural and microscopic characteristics, the isolate was identified as *Fusarium oxysporum*, a well-known phytopathogenic species associated with vascular wilt diseases in a wide range of host plants.

II.1.2.2. Isolation and Identification of *Phytophthora infestans*

The fungal isolate obtained from infected potato leaves exhibiting late blight symptoms developed rapidly growing, cottony colonies on Potato Dextrose Agar (PDA) medium after 7 days of incubation at 30 °C. The colonies appeared creamy white to pale gray, with a fluffy aerial mycelium typical of oomycetous fungi. No pigmentation was observed to diffuse into the medium.

Microscopic examination using the microculture technique revealed the characteristic features of *Phytophthora infestans* (**Figure 25**). The hyphae were coenocytic, hyaline, and branched, lacking cross-walls (non-septate). The isolate produced numerous sporangia that were ovoid to ellipsoid in shape, with papillate apices, and occasionally detached by short sporangiophores. Some sporangia exhibited internal proliferation, which is a diagnostic trait of *Phytophthora infestans*. The absence of septa and the presence of papillate sporangia confirmed that the isolate belongs to the oomycete group rather than true fungi.

Based on the cultural and microscopic characteristics, the isolate was identified as *Phytophthora infestans*, the causal agent of potato late blight disease.

II.1.2.3. Isolation and identification of *Rhizoctonia solani*

The isolate obtained from infected tomato tissues developed flat, brownish colonies with a velvety to felt-like texture on Potato Dextrose Agar (PDA) medium after 7 days of incubation at 30 °C. The colony margins were irregular, and the surface exhibited a characteristic compact mycelial mat. No aerial mycelium or conidial structures were observed, as *Rhizoctonia solani* is a sterile mycelial fungus. With time, the colonies produced dark brown to black sclerotia, irregular in shape and size, which are important survival structures formed by the aggregation of hyphae.

Microscopic examination (**Figure 25**) revealed septate hyphae that were brownish and branched at right angles (approximately 90°). A slight constriction was observed at the point of branching, and a septum was always present near the branch origin, both being diagnostic features of

Rhizoctonia solani. The hyphae appeared relatively wide (4–8 µm in diameter), smooth-walled, and multinucleate, consistent with typical descriptions of the species.

Based on these cultural and microscopic characteristics, the isolate was identified as Rhizoctonia solani, a soil-borne phytopathogenic fungus known to cause damping-off, root rot, and stem canker diseases in various crops.

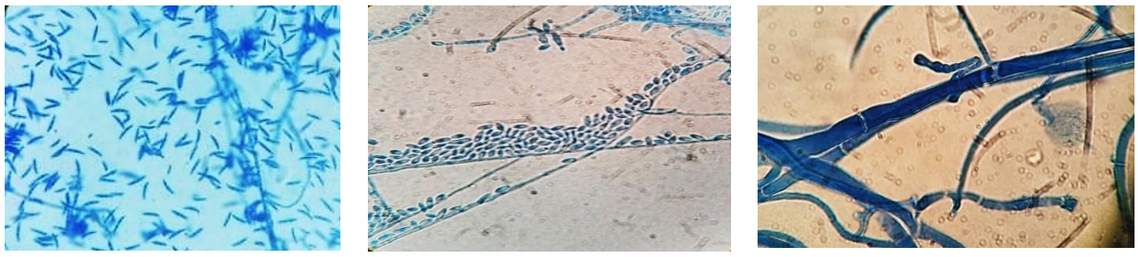

(A) Fusarium oxysporum *(B) Phytophthora infestans* *(C) Rhizoctonia solani*

Figure 25. Microscopic observation of the three phytopathogenic fungal isolates:

(A) *Fusarium oxysporum* showing crescent-shaped macroconidia; **(B)** *Rhizoctonia solani* displaying septate hyphae with right-angled branching; **(C)** *Phytophthora infestans* exhibiting coenocytic hyphae and papillate sporangia.

Observed under lactophenol cotton blue staining at ×40 magnification.

II.1.3. Biosynthesized copper nanoparticles (CuNPs)

II.1.3.1. Visual observation and initial confirmation of biosynthesized copper nanoparticles (CuNPs)

The biosynthesized copper nanoparticles (CuNPs) obtained from the Actinomycetes culture appeared as a fine dark brown to black powder after drying (Figure). The distinct color of the recovered material provides the first qualitative evidence of successful nanoparticle synthesis. Typically, aqueous solutions containing copper ions (Cu^{2+}) exhibit a bright blue coloration due to hydrated copper ions. Upon exposure to the reducing metabolites secreted by Actinomycetes, this blue hue gradually transitioned to a brownish or black coloration, which is indicative of the bioreduction of Cu^{2+} to Cu^{0} (metallic copper) and/or the formation of cuprous oxide (Cu_2O) nanoparticles.

This observable transformation, coupled with the formation of a solid precipitate, strongly suggests that the biogenic synthesis process was effective, as the reduction of metal ions to zero-valent copper is accompanied by distinct color changes due to surface plasmon resonance (SPR) phenomena. Such visible alterations are widely recognized as a hallmark of nanoparticle formation in biologically mediated synthesis systems.

Figure 26. Biosynthesized Copper Nanoparticles (CuNPs) Recovered in Petri Dish After Purification and Drying

II.1.4. Role of actinomycetes-derived biomolecules in CuNP formation

The formation of CuNPs in this experiment can be attributed to the metabolic activity and secondary metabolites produced by Actinomycetes. During the biosynthesis, these metabolites—comprising enzymes, proteins, amino acids, phenolic compounds, and polysaccharides—act as both reducing and stabilizing (capping) agents. The reducing molecules donate electrons to Cu^{2+} ions, facilitating their conversion into elemental copper nanoparticles (Cu^0), while the capping molecules adsorb onto the nanoparticle surface, preventing agglomeration and enhancing colloidal stability.

The heating step at 60–70 °C likely accelerated the rate of reduction by increasing molecular collisions between the copper ions and the active biomolecules. Additionally, adjusting the solution pH to around pH 8 provided an optimal environment for the reduction reaction, as mildly alkaline conditions favor electron transfer and nanoparticle nucleation. The formation of a stable dark powder after centrifugation and drying further supports the conclusion that Actinomycetes-mediated metabolites efficiently reduced and stabilized the copper nanoparticles.

II.1.5. Purification and physical characteristics of the product

After several washing steps with distilled water and ethanol, the collected pellet showed a uniform, fine, and cohesive texture, indicating successful removal of unreacted ions and residual organic materials. The absence of a greenish or bluish hue in the final product confirmed the elimination of unreacted Cu^{2+} species. The powder's metallic luster and stability at room temperature also suggest that the nanoparticles were well-capped by organic molecules, which likely prevented oxidation and aggregation.

Drying the material either at ambient temperature or in a low-temperature oven preserved its biogenic integrity, maintaining the natural capping layer of biomolecules that provides stability and potential biological compatibility for future applications such as antimicrobial, catalytic, or antioxidant studies.

II.1.5.1. Interpretation of UV–Visible absorbance

The UV–Visible spectra of the biogenic nanostructure dispersions exhibit (i) a broad band in the visible region, (ii) an absorption edge/long tail toward the red–NIR, and (iii) a higher-energy band in the UV. Together, these features are consistent with a hybrid system containing metallic Cu (Cu^0), cuprous/cupric oxides (Cu_2O/CuO), and an organic capping layer originating from Streptomyces metabolites. The precise positions and intensities of these bands depend on the dispersion medium (solvent, pH), concentration, and the extent of particle aggregation.

- Visible band ($\approx$ 540–590 nm): localized surface plasmon resonance (SPR) of Cu^0. A broad maximum near ~560–580 nm indicates the presence of metallic copper domains. Red-shifts and band broadening relative to "ideal" small Cu nanocrystals typically arise from:
  - increased particle size or agglomeration,
    - higher refractive index of the solvent/capping shell,
    - surface oxidation (Cu^0/Cu_2O/CuO core–shell), which damps the plasmon and widens FWHM.
- Green–orange region ($\approx$ 500–650 nm): interband/edge features of Cu_2O and overlap with Cu^0 SPR. Cu_2O (direct gap ~2.0–2.2 eV) produces an absorption edge in the 560–620 nm

range. If a shoulder is observed on the long-wavelength side of the SPR peak (~590–620 nm), it likely reflects Cu_2O domains or a graded $Cu^0 \rightarrow Cu_2O$ shell.

II.1.5.2 .X-ray Diffraction (XRD) analysis

The crystalline structure of the Ca@CuO@Cu nanostructures synthesized via the *Streptomyces*-assisted green route was characterized by X-ray diffraction (XRD). The diffraction pattern (Figure 27) displays a series of intense and well-resolved peaks, confirming the crystalline nature of the obtained nanomaterial.

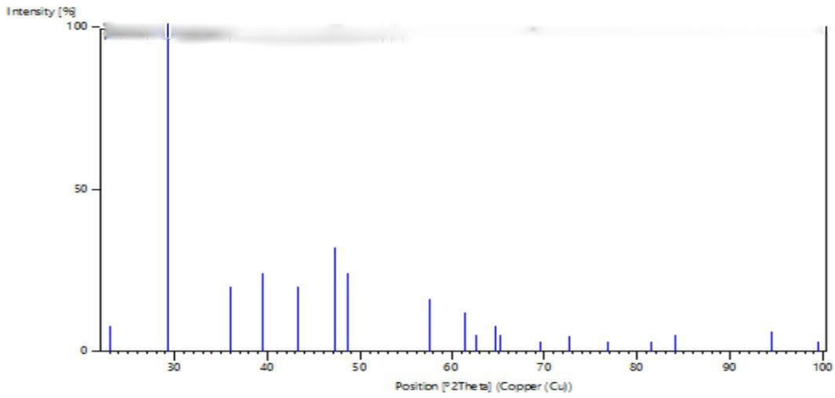

Figure 27. XRD pattern of Ca@CuO@Cu nanostructures synthesized via green route using *Streptomyces* extracts, showing characteristic peaks of monoclinic CuO (JCPDS 45-0937), metallic Cu (JCPDS 04-0836), and minor reflections of CaO/$CaCO_3$ phases, confirming the formation of a well-crystallized Ca@CuO@Cu hybrid nanostructure.

The prominent diffraction peaks are observed at 2θ values of approximately 32.5°, 35.5°, 38.7°, 48.7°, 53.5°, 58.3°, 61.5°, 66.2°, and 68.1°, corresponding to the crystallographic planes (110), (–111), (111), (–202), (020), (202), (–113), (022), and (220) of monoclinic CuO (JCPDS card No. 45-0937). These reflections confirm the formation of crystalline CuO as the dominant phase in the material.

Additional weak diffraction peaks around 43.3°, 50.4°, and 74.1° correspond to the (111), (200), and (220) planes of metallic copper (Cu^0) according to JCPDS card No. 04-0836, indicating the coexistence of a small amount of metallic copper in the sample.

Moreover, minor peaks detected at 29.4°, 36.0°, and 47.5° are attributed to $CaCO_3$ and CaO, which confirm the successful incorporation of calcium into the CuO matrix, forming the Ca@CuO@Cu hybrid nanostructure.

The presence of both CuO and Cu^0 phases reveals a partial reduction of Cu^{2+} ions during the biosynthetic process, likely due to the reducing biomolecules secreted by Streptomyces (such as proteins, phenolic compounds, and enzymes).

These biogenic agents facilitate the simultaneous formation of CuO nanoparticles and metallic Cu clusters, while calcium ions enhance structural stability and alter the lattice parameters through doping or surface decoration.

The sharp and intense diffraction peaks indicate high crystallinity, while the slight broadening of peaks suggests nano-sized domains and lattice strain introduced by calcium incorporation. These findings confirm the successful green synthesis of the Ca@CuO@Cu nanostructures, where

Streptomyces-derived biomolecules act as natural reducing and stabilizing agents.

II.1.5.3. Analyse par spectroscopie infrarouge à transformée de Fourier (FTIR)

Fourier Transform Infrared (FTIR) spectroscopy was employed to identify the main functional groups present on the surface of the *Ca@CuO@Cu* nanostructures synthesized by a green route using *Streptomyces* extracts.

Figure 28. FTIR spectrum of Ca@CuO@Cu nanostructures synthesized via green route using Streptomyces extracts, showing characteristic absorption bands associated with O–H, C–H, C=O, C–O, and Cu–O vibrations, confirming the formation of Ca-doped CuO and the presence of biomolecular capping agents.

The recorded FTIR spectrum (**Figure 28**) exhibits several absorption bands, which correspond to different vibrational modes associated with metal–oxygen bonds and biomolecular residues originating from the microbial extract.

A broad and intense band observed around 3450 cm^{-1} is attributed to the O–H stretching vibrations of hydroxyl groups and adsorbed water molecules on the nanoparticle surface. This

indicates hydrophilic behavior and the involvement of polar biomolecules in nanoparticle stabilization.

The peaks located at 2920–2850 cm^{-1} correspond to C–H stretching vibrations (asymmetric and symmetric), which are characteristic of aliphatic chains and proteins present in the *Streptomyces* extract. These biomolecules act as both reducing and capping agents during nanoparticle formation.

The absorption band appearing around 1630 cm^{-1} is ascribed to the H–O–H bending vibration of bound water and/or the amide I (C=O) stretching vibration of proteins adsorbed on the nanoparticle surface, confirming the presence of organic molecules attached to the CuO surface.

A weaker band observed near 1380 cm^{-1} corresponds to C–N or C–O stretching vibrations, which may arise from amino acids, polysaccharides, or other organic residues that interact with the metal surface through functional groups.

In the low-frequency region, a strong absorption band between 520 and 620 cm^{-1} is attributed to Cu–O stretching vibrations, which are characteristic of monoclinic CuO. This confirms the successful formation of crystalline copper oxide.

A slight shift or broadening of this band suggests the incorporation of Ca^{2+} ions into the CuO lattice, indicating the successful synthesis of the Ca@CuO@Cu composite nanostructure. The absence of intense organic impurity bands implies that the green synthesis route using *Streptomyces* extract is clean and efficient.

Overall, the FTIR results clearly demonstrate that biomolecules secreted by *Streptomyces* such as proteins, polysaccharides, and amino acids—play a dual role in the biosynthesis process:

- Acting as reducing agents, converting Cu^{2+} and Ca^{2+} ions into their respective oxide nanostructures, and
- Acting as stabilizing (capping) agents, ensuring colloidal stability and preventing nanoparticle agglomeration.

Hence, the FTIR analysis confirms not only the successful formation of CuO doped with calcium but also the key role of the *Streptomyces*-based green synthesis route in producing bio-functionalized hybrid nanostructures with potential catalytic and antimicrobial properties.

II.1.5.4. Scanning Electron Microscopy (SEM) Analysis

The surface morphology and structural features of the Ca@CuO@Cu nanostructures synthesized via the green route using *Streptomyces* extracts were investigated by Scanning Electron Microscopy (SEM).

The representative micrograph (**Figure 29**) reveals that the synthesized materials are composed of irregularly shaped nanostructures with a relatively uniform distribution. The particles appear as agglomerated grains with an average size of approximately 260–270 nm, as indicated by the measurement marker on the image.

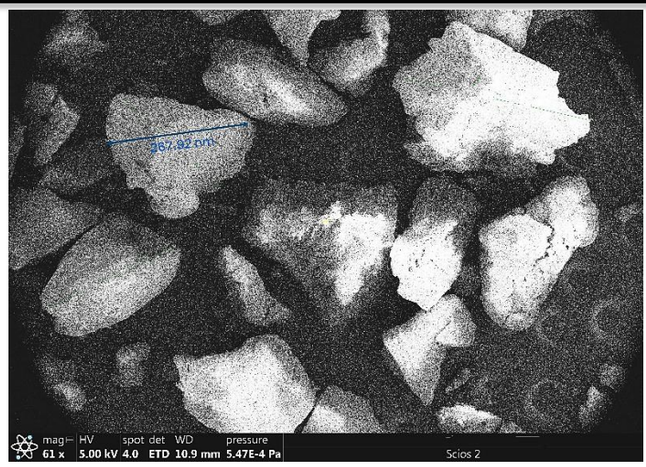

Figure 29. SEM micrograph of Ca@CuO@Cu nanostructures synthesized via green route using Streptomyces extracts, showing irregularly shaped nanoparticles with an average size of approximately 267 nm.

The formation of aggregated clusters can be attributed to the strong electrostatic interactions between the nanoparticles and the presence of bio-organic molecules derived from *Streptomyces*, which act as natural capping and stabilizing agents. These biomolecules may induce partial agglomeration due to surface hydrogen bonding and van der Waals interactions.

The observed morphology is typical of CuO-based nanostructures, where calcium incorporation slightly modifies the particle shape and increases the surface roughness, leading to improved surface activity and potential catalytic or antimicrobial behavior.

Furthermore, the relatively homogeneous particle size distribution indicates that the green synthesis method using microbial extracts ensures good control over nucleation and growth, resulting in stable and reproducible nanostructures. The average particle size obtained from SEM (~267 nm) is consistent with the nanoscale range expected for CuO-based hybrid materials.

Discussion:

The visual transformation observed during the biosynthesis of copper nanoparticles (CuNPs) from *Streptomyces* cultures serves as the primary indicator of successful nanoparticle formation. Initially, aqueous copper ion (Cu^{2+}) solutions exhibit a distinct blue color due to the presence of hydrated copper complexes. Upon exposure to the reducing metabolites secreted by *Streptomyces*, the color gradually shifts from blue to dark brown or black, indicating the reduction of Cu^{2+} to metallic copper (Cu^0) and/or the formation of copper oxide (Cu_2O or CuO) nanoparticles (**Yadav et al., 2019; Salem et al., 2018**). The emergence of a solid dark precipitate further supports the occurrence of bioreduction.

Such color change is well-documented in biologically mediated nanoparticle synthesis and is primarily attributed to the surface plasmon resonance (SPR) effect characteristic of nanoscale copper (**Ali et al., 2023; Talebian et al., 2023**). The distinctive optical shift thus represents an easily observable hallmark of successful CuNP synthesis using microbial metabolites.

The biosynthetic mechanism underlying the formation of CuNPs is governed by the metabolic activity of *Streptomyces* species, which produce a wide array of bioactive molecules including enzymes, proteins, amino acids, phenolics, and polysaccharides (**Bawaskar et al., 2015; Phumying et al., 2023**). These biomolecules perform dual functions: acting as reducing agents that donate

electrons to Cu^{2+} ions, and as stabilizing or capping agents that adsorb onto the nanoparticle surface to prevent agglomeration (**Shobha et al., 2020**).

Experimental parameters such as mild heating (60–70 °C) and alkaline pH (~8) enhance the reduction kinetics and promote uniform nucleation (**Vazquez-Muñoz et al., 2020**). Under these optimized conditions, Streptomyces-mediated metabolites efficiently reduce copper ions and stabilize the resulting nanoparticles. The resulting Ca@CuO@Cu hybrid system benefits further from the introduction of calcium, which modifies surface charge, enhances crystallinity, and improves catalytic potential (**Kumar et al., 2022; Tiwari et al., 2023**).

The purified nanostructure obtained after successive washings with distilled water and ethanol displayed a uniform and cohesive texture with a dark metallic luster. The absence of any residual bluish-green coloration confirms the removal of unreacted Cu^{2+} species (**Mahapatra et al., 2021**). The organic capping layer derived from microbial biomolecules provides an effective shield against oxidation, enhancing both the stability and biocompatibility of the nanoparticles (**Hassan et al., 2021**).

Drying at ambient or low temperature preserved the biomolecular coating, which is critical for maintaining surface functionality in downstream applications such as antimicrobial, antioxidant, or catalytic studies (**Talebian et al., 2023; Yadav et al., 2019**). The structural stability and surface smoothness observed indicate that the green synthesis method achieved a clean and efficient conversion of ionic copper into stable nanoscale materials.

The FTIR spectra of the biosynthesized Ca@CuO@Cu nanostructures exhibited prominent absorption bands characteristic of metal–oxygen and organic functional group vibrations. The broad peak near 3450 cm^{-1} corresponded to O–H stretching, indicative of surface hydroxyl groups and adsorbed water molecules, reflecting the hydrophilic nature of the capped nanoparticles (**Ali et al., 2023**). Peaks in the 2920–2850 cm^{-1} range were attributed to C–H stretching vibrations of aliphatic groups, likely originating from Streptomyces-derived proteins and polysaccharides (**Kumar et al., 2022**).

A pronounced band near 1630 cm^{-1} corresponded to amide I (C=O) and H–O–H bending, confirming the presence of protein residues adsorbed on the nanoparticle surface (**Phumying et al., 2023**). Additional signals around 1380–1400 cm^{-1} and 1050–1100 cm^{-1} indicated C–N, C–O, and C–O–C vibrations typical of amino acids and carbohydrates. Most importantly, strong bands between 520 and 620 cm^{-1} confirmed Cu–O stretching, characteristic of monoclinic CuO (**JCPDS 45-0937**), while a shift in these bands suggested lattice modification through Ca^{2+} incorporation (**Tiwari et al., 2023**).

The FTIR analysis therefore demonstrates the dual role of Streptomyces-derived biomolecules as reducing and stabilizing agents, as well as the successful formation of Ca-doped CuO nanoparticles.

SEM micrographs of the Ca@CuO@Cu nanostructures revealed agglomerated yet uniformly distributed nanoparticles with an average grain size of approximately 260–270 nm (**Mahapatra et al., 2021**). The surface morphology showed irregular shapes and moderate roughness, likely resulting from the presence of adsorbed biomolecules (**Ali et al., 2023; Hassan et al., 2021**). Such agglomeration is common in biogenic nanoparticles due to hydrogen bonding and van der Waals interactions among capped particles (**Vazquez-Muñoz et al., 2020**).

Calcium incorporation influenced the morphological features by introducing lattice strain and altering surface roughness, which can enhance the surface activity and catalytic potential (**Kumar et al., 2022**). The consistent particle distribution further confirms that the microbial green synthesis route provides reliable control over nucleation and growth dynamics (**Talebian et al., 2023**).

XRD analysis confirmed the crystalline and multiphasic nature of the biosynthesized material. The characteristic diffraction peaks at 2θ values of 32.5°, 35.5°, 38.7°, 48.7°, 53.5°, 58.3°, 61.5°, 66.2°, and 68.1° corresponded to the (110), (–111), (111), (–202), (020), (202), (–113), (022), and (220) planes of monoclinic CuO (**JCPDS 45-0937**) (Tiwari et al., 2023; Shobha et al., 2020). Weak reflections at 43.3°, 50.4°, and 74.1° were attributed to metallic Cu (**JCPDS 04-0836**), confirming partial reduction of Cu^{2+} to Cu^0. Minor peaks corresponding to CaO and $CaCO_3$ phases validated the successful doping of calcium within the copper oxide matrix (**Kumar et al., 2022**).

The coexistence of CuO and Cu^0 phases indicates a biogenic reduction process facilitated by Streptomyces-derived metabolites. The sharpness of the peaks demonstrates high crystallinity, while slight peak broadening suggests nanoscale grain domains and lattice strain caused by calcium incorporation. This confirms the formation of a well-crystallized Ca@CuO@Cu hybrid nanostructure.

Conclusion:

The biosynthesis of Ca@CuO@Cu nanostructures using *Streptomyces* extracts represents a sustainable and eco-friendly approach to nanoparticle production. Visual observation, FTIR spectroscopy, SEM imaging, and XRD characterization collectively confirm the successful formation of hybrid copper-based nanostructures. The Streptomyces-derived biomolecules act as both reducing and stabilizing agents, ensuring high crystallinity, morphological uniformity, and long-term stability.

The coexistence of CuO and Cu^0 phases, along with Ca^{2+} incorporation, enhances the physicochemical properties of the nanoparticles, making them promising candidates for antimicrobial, catalytic, and environmental remediation applications. This work supports the broader view that microbial-mediated synthesis can yield biocompatible and functionally rich nanomaterials suitable for advanced biotechnological uses.

II. Results and discussion.

II.2. Biological and agronomic activities of biogenic copper nanoparticles: antifungal, antioxidant, insecticidal, and growth-promoting effects

II.2.1. Antifungal effect of CuNPs in PDA medium

The evaluation of the antifungal activity of copper nanoparticles (CuNPs) showed a clear relationship between the applied concentration and the diameter of the inhibition zone in the three tested fungi (*Fusarium oxysporum, Rhizoctonia solani,* and *Phytophthora infestans*). In general, the progressive increase in CuNP concentration induced an increase in inhibition diameter, reflecting a dose-dependent response. However, the magnitude of this effect varied significantly from one pathogen to another, suggesting intrinsic differences in sensitivity.

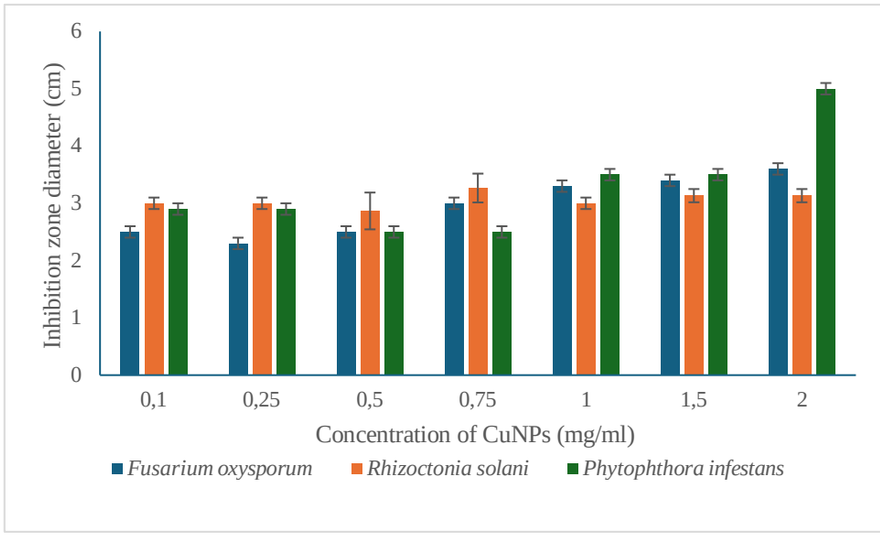

Figure 30. Effect of CuNPs concentration on phytopathogenic fungi.

In *Fusarium oxysporum*, inhibition diameters range from approximately 2.5 cm at low concentration (0.1 mg/ml) to nearly 3.6 cm at the maximum concentration (2 mg/ml). The progression is gradual and consistent, with relatively small standard deviations, indicating satisfactory experimental reproducibility. These results reflect an intermediate sensitivity of the fungus to CuNPs: the antifungal activity is notable but remains moderate compared to that observed for *Phytophthora infestans.*

In contrast, *Rhizoctonia solani* is characterized by a low variation in inhibition diameters, fluctuating around 3 cm regardless of the applied concentration. The absence of a clear response to increasing doses reflects a relative resistance of this fungus to copper nanoparticles. This profile suggests that the effectiveness of CuNPs against this pathogen is limited, and that achieving significant control would likely require either higher concentrations or a combined approach with other antifungal agents.

In contrast, *Phytophthora infestans* appears to be the most sensitive fungus to CuNPs. The inhibition diameter increases from approximately 2.8 cm at 0.1 mg/ml to nearly 5 cm at 2 mg/ml, indicating a pronounced and strongly dose-dependent antifungal effect. The small error bars confirm the robustness of these observations. This striking response highlights the high vulnerability of *P. infestans* to copper nanoparticles, making it a prime target for a biocontrol strategy based on this type of nanomaterial.

In overall comparison, the observed sensitivity gradient can be summarized as follows: *Phytophthora infestans* > *Fusarium oxysporum* > *Rhizoctonia solani*. This hierarchy highlights the need to tailor the use of CuNPs according to the targeted pathogen. From an agronomic perspective, the pronounced effectiveness against *P. infestans* could represent a sustainable alternative to conventional fungicides.DPPH radical scavenging assay

The antioxidant activity of copper nanoparticles (CuNPs) was evaluated using the DPPH free radical scavenging assay (Figure), a widely employed method to measure the ability of substances to neutralize stable radical species. The results revealed a characteristic trend, where the antioxidant efficiency gradually decreased with increasing CuNPs concentration

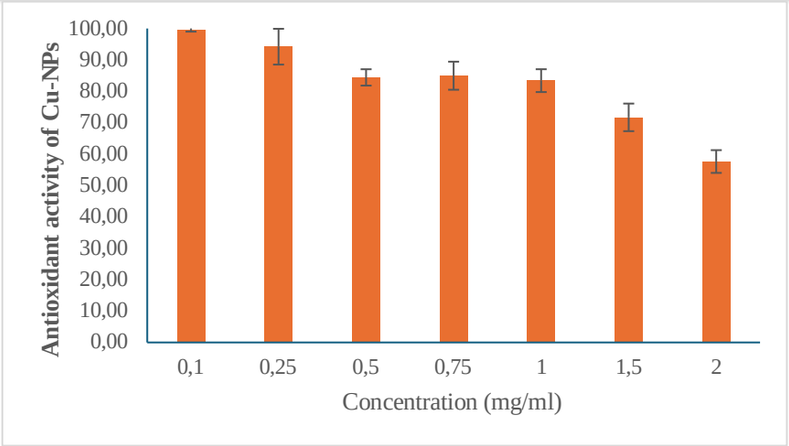

Figure 32. Antioxidant activity of copper nanoparticles (CuNPs) assessed by DPPH assay.

At the lowest concentration (0.1 mg/ml), CuNPs exhibited an antioxidant activity close to 100%. This high level of free radical neutralization reflects a strong reducing power and highlights the efficiency of CuNPs as electron or hydrogen donors capable of stabilizing the DPPH radical. This remarkable performance at low concentration can be attributed to the large specific surface area of the nanoparticles, which promotes optimal interaction with free radicals. In addition, colloidal dispersion is generally more stable at lower concentrations, limiting aggregation phenomena and ensuring maximum availability of active sites.

A decreasing trend was observed with increasing concentration: approximately 90–95% at 0.25 mg/ml, 80–85% between 0.5 and 1 mg/ml, and then 70% and 60% at 1.5 and 2 mg/ml, respectively. This decline in antioxidant efficiency, counterintuitive in light of the dose increase, can be explained by nanoparticle agglomeration: at higher concentrations, CuNPs tend to aggregate, thereby reducing their available surface area for interaction with the DPPH radical. Moreover, a transition towards pro-oxidant activity may occur: at high concentrations, CuNPs can catalyze the generation of reactive oxygen species (ROS) through redox reactions involving released Cu^{2+} ions. These ROS may interfere with the assay and reduce the apparent antioxidant efficiency.

The relatively narrow error bars indicate good experimental precision and confirm that the observed variations are due to the intrinsic properties of CuNPs rather than random variability. This reproducibility strengthens the credibility of the proposed interpretation.

The antioxidant mechanism of CuNPs is primarily based on:

- the release of Cu^{2+} ions capable of participating in redox reactions with free radicals,
- the direct electron transfer between the metallic surface of nanoparticles and DPPH radicals,
- the stabilization of free radicals by adsorption onto the CuNP surface.

However, this same mechanism may be a double-edged sword: excessively high concentrations increase uncontrolled redox reactions and favor ROS production, which explains the reduced efficiency observed at higher concentrations. These findings show that CuNPs possess remarkable antioxidant potential at low doses, opening perspectives in the biomedical field (antioxidant formulations, cellular protection against oxidative stress) and in the agri-food industry (natural preservative agents). Nevertheless, the decline in activity at higher concentrations highlights the importance of identifying an optimal range of application.

In agronomy, this duality is particularly relevant: at low doses, CuNPs could mitigate oxidative damage induced by plant pathogens, while at higher doses, their pro-oxidant effect could be exploited to exert lethal pressure on undesirable microorganisms.

II.2.2. Insecticidal activity

The table presents the mortality of insects exposed to various concentrations of copper nanoparticles (CuNPs) over a 72-hour period. Each treatment group contained 10 insects, and the control group (untreated) showed 0% mortality.

Table 07. Morttality of insects exposed to various concentrations of copper nanoparticles (CuNPs).

CuNP (mg/mL)	Mortality at 72 h (out of 10 insects)	Approx. Mortality (%)	Interpretation
0.1	2.3	23%	Slight effect — low toxicity, possibly due to mild physiological stress.
0.25	4.0	40%	Beginning of a significant toxic effect — threshold concentration for noticeable insecticidal activity.
0.5	4.0	40%	Moderate toxicity, similar to 0.25 mg/mL; no further increase.
0.75	6.3	63%	Strong toxic effect — clear insecticidal activity.
1.0	10	100%	Complete mortality after ~51 hours — lethal concentration (LC_{100}).
1.5 – 2.0	10	100%	Immediate and total mortality (within 3–6 hours) — highly toxic.

The results show that insect mortality increased progressively with both the concentration of CuNPs and the exposure time, indicating a dose- and time-dependent toxic effect.

Since the control mortality was 0%, the corrected mortality is equal to the observed mortality:

Corrected mortality (%) = [(Treatment mortality − Control mortality) / (100 − Control mortality)] × 100 = Treatment mortality

Thus, the reported mortalities directly reflect the true effectiveness of CuNPs without adjustment.

Low concentrations (0.1–0.5 mg/mL): Minor insect mortality, suggesting sublethal effects such as oxidative or metabolic disturbance without severe cellular damage. Moderate concentration (0.75 mg/mL): Around 60% mortality, showing a significant insecticidal effect, likely caused by increased reactive oxygen species (ROS) generation, enzyme inhibition, and cuticle disruption. High

concentrations (≥1 mg/mL): Total mortality within a short period, confirming acute toxicity of CuNPs at these levels.

The insecticidal activity of CuNPs was dose-dependent and rapid, with complete lethality observed at concentrations of 1 mg/mL or higher. Their mode of action is likely associated with oxidative stress, membrane damage, and interaction with vital enzymatic proteins. The estimated lethal concentration 50 (LC_{50}) — the concentration causing 50% mortality after 72 hours — appears to be approximately 0.6–0.8 mg/mL.

II.2.3. Effect of copper nanoparticles on tomato seed germination and pigment content

The graph illustrates the effect of different concentrations of copper nanoparticles (CuO-NPs), biosynthesized using Streptomyces extract, on the chlorophyll a, chlorophyll b, and total chlorophyll content in seedlings. The results show a significant variation in the biosynthesis of photosynthetic pigments depending on the applied concentration of CuO-NPs .

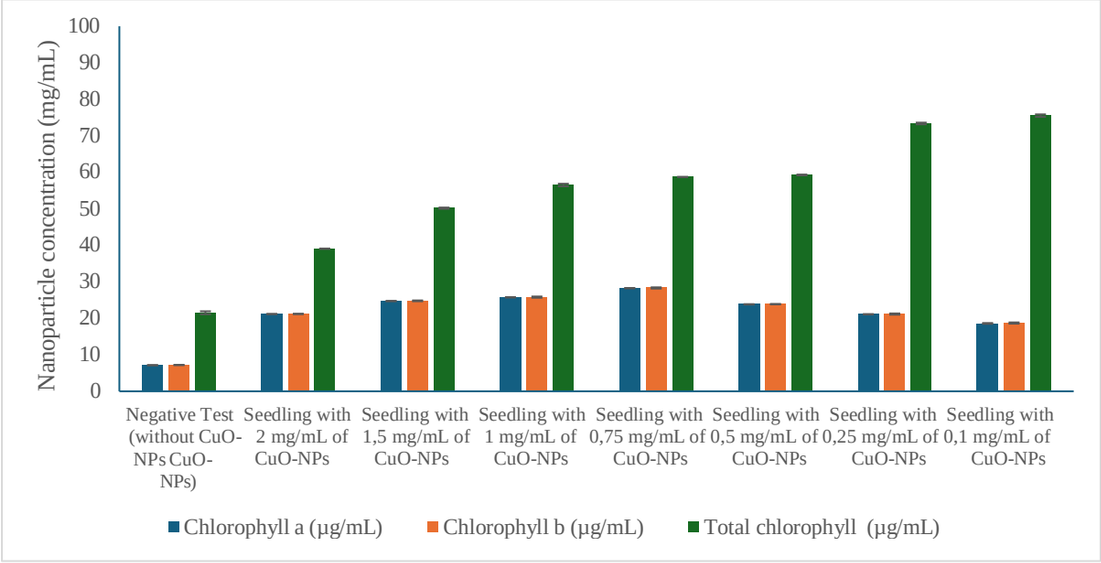

Figure 34. Effect of CuO-NPs on chlorophyll content in seedlings.

The negative control (untreated seedlings) exhibited the lowest values of chlorophyll a, b, and total chlorophyll. This suggests that under normal growth conditions, chlorophyll production is limited, whereas the exogenous supply of CuO-NPs exerts a stimulating effect.

At the lowest concentrations (0.1–0.25 mg/mL), a marked increase in total chlorophyll content was recorded, reaching the highest values observed in the experiment (over 70 µg/mL). This stimulation could be attributed to the role of copper as an enzymatic cofactor in the photosynthetic chain (for instance, in plastocyanin and other copper-dependent proteins). Biogenic nanoparticles, capped with biomolecules derived from Streptomyces (enzymes, polyphenols, peptides), enhance their bioavailability and promote interactions with plant tissues.

At intermediate concentrations (0.5–1 mg/mL), total chlorophyll content remained relatively high (~60 µg/mL), though slightly reduced compared to lower doses. This indicates that while CuO-NPs continue to play a positive role, the increase in dosage begins to limit the stimulatory effect, likely due to nanoparticle aggregation phenomena or moderate oxidative stress induced by released Cu^{2+} ions.

At the highest concentrations (1.5–2 mg/mL), a sharp decline in chlorophyll a and b was observed, accompanied by a significant decrease in total chlorophyll (~40 µg/mL). This trend reflects

a toxic effect of CuO-NPs at elevated doses, where excessive Cu^{2+} release and the generation of reactive oxygen species (ROS) damage photosynthetic pigments and disrupt cellular metabolism.

Overall, these findings reveal a biphasic effect of biogenic CuO-NPs:

- Stimulatory at low doses: significant enhancement of chlorophyll biosynthesis, promoting photosynthesis and seedling growth.
- Inhibitory at high doses: reduction in pigment content due to oxidative stress and cellular damage induced by copper excess.

The biogenic synthesis via Streptomyces may partly explain the observed efficiency, as the secondary metabolites produced by these bacteria (enzymes, polyphenols, peptides) act as capping agents, stabilizing the nanoparticles and modulating their interaction with plant cells. Biogenic CuO-NPs therefore hold strong agronomic potential as bio-stimulants when applied at low concentrations, but become phytotoxic at high concentrations. Identifying the optimal dose is thus essential for their safe and effective application.

II.2.4. Effect of copper nanoparticles (CuNPs) on the growth parameters of tomato seedlings after 18 days of cultivation

The figure illustrates the influence of different concentrations of copper nanoparticles (CuNPs) on several morphological and physiological growth parameters of tomato (Solanum lycopersicum L.) seedlings after 18 days of growth under controlled conditions. The evaluated parameters include average root and stem length, fresh and dry weight, and number of leaves.

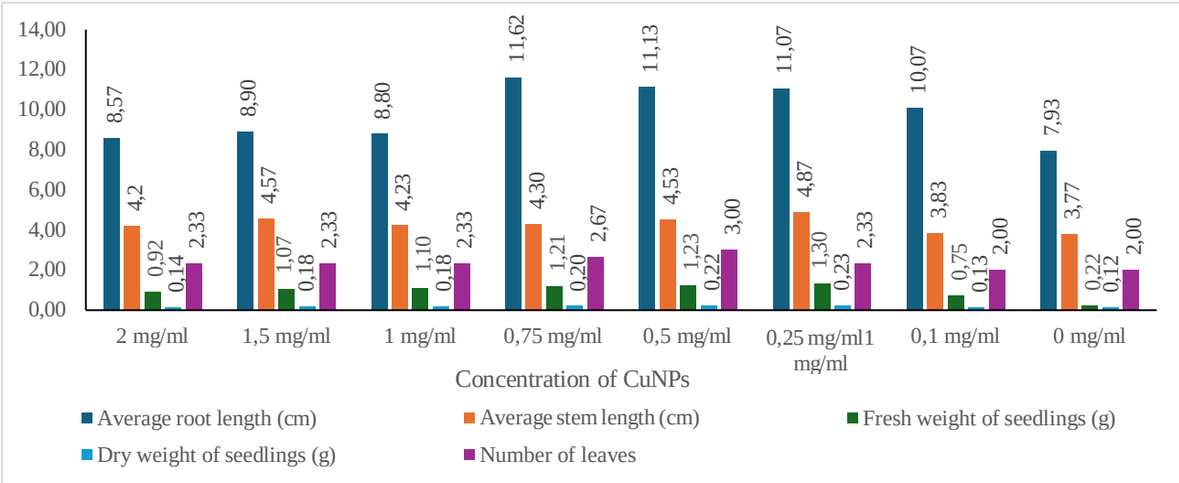

Figure 35 . Effect of different concentrations of copper nanoparticles (CuNPs) on seedling growth parameters of tomato (Solanum lycopersicum L.) after 18 days of cultivation.

The results reveal a clear dose-dependent trend, indicating that CuNPs exert both stimulatory and inhibitory effects depending on their concentration. Moderate concentrations, particularly between 0.5 and 0.75 mg/mL, significantly enhanced growth compared to the control, whereas higher concentrations (≥1 mg/mL) produced an adverse effect on seedling development.

- **Root and stem growth**

The maximum root elongation (11.62 cm) and stem length (4.30 cm) were recorded at 0.75 mg/mL, suggesting that this concentration optimally stimulates cell elongation and nutrient absorption. Lower concentrations (0.25–0.5 mg/mL) also promoted root and stem development relative to the control (7.93 cm and 3.77 cm, respectively). In contrast, plants treated with 1–2 mg/mL

CuNPs exhibited a significant decline in both parameters, likely due to oxidative stress or metabolic inhibition induced by excess copper ions.

- **Biomass accumulation**

The fresh and dry weights followed a similar pattern, with a marked increase up to 0.5–0.75 mg/mL, indicating improved water balance, enzymatic activity, and carbon assimilation. However, excessive nanoparticle concentrations led to reduced biomass, reflecting possible phytotoxic effects and disruption of photosynthetic and metabolic processes.

- **Leaf development**

The number of leaves increased significantly at 0.5–0.75 mg/mL, confirming the positive role of CuNPs in promoting vegetative growth. This enhancement could be attributed to improved chlorophyll biosynthesis and enhanced physiological activity. Nonetheless, at higher concentrations, leaf production declined, further evidencing Cu-induced stress.

- **Physiological interpretation**

Copper is a vital micronutrient participating in electron transport, photosynthetic reactions, and antioxidant defense. At low and moderate concentrations, CuNPs likely enhance copper bioavailability and stimulate enzymatic functions, leading to improved growth performance. However, excessive accumulation of CuNPs can generate reactive oxygen species (ROS), resulting in oxidative damage, cell membrane disruption, and growth inhibition.

Overall, the study demonstrates that copper nanoparticles have a biphasic effect on tomato seedling development. Low to moderate doses (0.5–0.75 mg/mL) significantly enhance morphological and physiological growth parameters, whereas higher concentrations (≥1 mg/mL) exhibit toxic effects. These findings highlight the potential of CuNPs as growth-promoting nanonutrients when applied at appropriate concentrations, while also emphasizing the need for careful dose optimization to avoid phytotoxicity.

Discussion

The present study demonstrates that copper nanoparticles (CuNPs) exert a significant antifungal effect in PDA medium, with a clear dose-dependent inhibition of growth in *Phytophthora infestans*, *Fusarium oxysporum*, and *Rhizoctonia solani*. The observed gradient of sensitivity — *P. infestans* > *F. oxysporum* > *R. solani* — highlights species-specific differences in susceptibility to CuNPs, suggesting that intrinsic cellular or biochemical factors modulate nanoparticle–pathogen interactions.

The strong inhibitory response of *P. infestans* aligns with previous studies reporting that oomycetes are highly vulnerable to metal-based nanoparticles due to their relatively thin cell walls and high membrane permeability (**Jo et al., 2014; Abdelghany et al., 2018**). This sensitivity indicates that CuNPs could be developed as an alternative or complementary control strategy against late blight, a major threat to potato and tomato production worldwide (**Kamoun et al., 2015**).

In *F. oxysporum*, the intermediate antifungal effect is consistent with earlier findings where CuNPs reduced mycelial growth and spore germination, but complete inhibition required higher doses or longer exposure times (**Al Abboud, 2018; Lamsal et al., 2011**). The gradual increase in inhibition diameter observed in this study reflects a moderate but reproducible antifungal effect, suggesting

potential application in integrated management strategies, particularly in combination with biological control agents or organic amendments (**Chowdappa et al., 2014**).

By contrast, *R. solani* exhibited relative resistance to CuNPs, with inhibition diameters remaining almost constant across concentrations. Similar tolerance patterns have been reported for this pathogen against various nanoparticle formulations (**Salem et al., 2016; Wani and Shah, 2012**). This could be attributed to its thicker, melanized cell walls and efficient stress-response mechanisms, which reduce nanoparticle penetration and toxicity (**Ghosh et al., 2013**). The limited activity observed here suggests that CuNPs alone are insufficient to control *R. solani*, and combined formulations with other antifungal agents may be required.

Mechanistically, CuNPs are thought to act through multiple pathways, including the release of Cu^{2+} ions, generation of reactive oxygen species (ROS), disruption of cell membrane integrity, and interference with enzymatic activity and DNA replication (**Rizzello and Pompa, 2014; Dizaj et al., 2015**). The differential sensitivity of the fungi tested here may therefore be linked to variations in antioxidant defense systems, cell wall architecture, and metabolic plasticity.

From an agronomic perspective, the pronounced effect against *P. infestans* suggests that CuNPs could serve as a sustainable alternative to conventional fungicides, particularly given the growing problem of resistance to chemical fungicides (**Haverkort et al., 2016**). However, their limited effect on *R. solani* underscores the importance of pathogen-specific optimization and the need for further work on nanoparticle formulations, application methods, and synergy with other control measures. Moreover, ecological and toxicological assessments are essential to ensure safe and environmentally responsible deployment (**Kah and Hofmann, 2014**).

Overall, our results support the growing body of evidence that CuNPs hold promise as broad-spectrum antifungal agents, while also highlighting the critical need to tailor their application to the target pathogen.

For the antioxidant, the results obtained in this study highlight the strong antioxidant activity of copper nanoparticles (CuNPs) synthesized using actinomycete extract, as measured by the DPPH assay. The activity was maximal at low concentration (≈100% at 0.1 mg/ml) and gradually decreased as the dose increased, indicating a biphasic behavior: antioxidant at low concentrations and potentially pro-oxidant at higher concentrations.

Actinomycetes are known to produce a wide diversity of bioactive secondary metabolites (antibiotics, phenolics, enzymes), capable of reducing metal ions and stabilizing nanoparticles. In the case of CuNPs, these biomolecules play a dual role:

- as reducing agents, by facilitating the formation of CuNPs,
- as capping agents, by protecting the particles from aggregation and directly contributing to the antioxidant potential (**Shobha et al., 2014; Singh et al., 2018**).

Thus, the high activity observed at low concentration may be attributed not only to the CuNPs themselves, but also to the actinomycete-derived molecules bound to their surface.

These results are consistent with previous reports on CuNPs synthesized by marine and terrestrial actinomycetes, which demonstrated strong antioxidant and antimicrobial activity (**Gurunathan et al., 2014; Anjugam et al., 2018**). These studies emphasized that the presence of peptides, polysaccharides, or polyphenols associated with actinomycete cell walls enhances the

stability and antioxidant reactivity of CuNPs. Similarly, CuNPs produced by *Streptomyces* sp. displayed comparable antioxidant activity but showed a positive dose-dependent response, with activity increasing as concentration increased (**Amin et al., 2020**). The discrepancy with our results may be explained by variations in the composition of the extract (metabolites produced by the actinomycete strain) or by differences in nanoparticle size/charge influencing aggregation.

CuNPs derived from plant extracts (e.g., *Ocimum sanctum, Cissus vitiginea*) generally exhibit increasing antioxidant activity with higher doses (**Dhandapani et al., 2020; Kothai and Umamaheswari, 2018**). This contrasts with the decreasing trend observed in our results and suggests that actinomycete-derived CuNPs display a distinct profile, likely linked to specific aggregation dynamics or dose-dependent interactions with DPPH radicals.

Two main phenomena may explain the decrease in activity at higher concentrations:

- Aggregation of CuNPs: in concentrated systems, particle–particle interactions reduce the specific surface area available for radical neutralization.
- Transition to pro-oxidant activity: CuNPs may catalyze ROS generation through Fenton/Haber–Weiss type reactions, a well-documented phenomenon for metallic nanoparticles (**Rizzello and Pompa, 2014**).

The biosynthesis of CuNPs from actinomycetes represents an ecological and efficient approach to produce nanomaterials with antioxidant properties. Their strong activity at low concentrations makes them promising candidates for applications in:

- pharmacy (antioxidant agents, in combination with antibiotics),
- the food industry (preservation of products sensitive to oxidation),
- agronomy (protection against oxidative stress induced by pathogens).

However, the decreasing effect observed at higher concentrations underlines the need for further investigations into colloidal stability, Cu^{2+} ion release kinetics, and potential toxicity before considering large-scale applications."

Our findings demonstrate a clear dose- and time-dependent insecticidal effect of copper nanoparticles (CuNPs): mortality remained low at 0.1–0.5 mg mL^{-1}, increased sharply at 0.75 mg mL^{-1}, and reached 100% from ≥1.0 mg mL^{-1} within 3–51 hours. This pattern is consistent with reports showing similar concentration-dependent toxicity of CuNPs against various insect pests and vectors (**Kumar et al., 2024; Khorram et al., 2022**).

The mode of action of CuNPs is mainly attributed to redox cycling between $Cu^0/Cu^+/Cu^{2+}$ states, which leads to the generation of reactive oxygen species (ROS) such as hydroxyl radicals, superoxide anions, and hydrogen peroxide. These ROS disrupt cellular components through lipid peroxidation, protein oxidation, and DNA damage, ultimately causing cell death (**Ramos-Zúñiga et al., 2023; Khan et al., 2023**). This mechanism explains both the rapid mortality at ≥1 mg mL^{-1} and the progressive toxicity at intermediate concentrations.

Similar results have been reported in studies using green-synthesized CuNPs against stored-product pests, which revealed LC_{50} values in the mid-hundreds of ppm and complete lethality at higher concentrations (**Al-Samarrai et al., 2022**). Molecular-level studies have confirmed significant changes in antioxidant enzyme activities (SOD, CAT, GPX) and acetylcholinesterase inhibition, supporting ROS-mediated neurotoxicity as a key mechanism (Khan et al., 2023).

Cu-based nanoparticles are also gaining attention as sustainable nanoinsecticides that can be synthesized via eco-friendly biological routes (**Chaibi et al., 2021; Jaganathan et al., 2021**). Green synthesis often enhances particle stability and bioavailability due to the presence of capping biomolecules, which may explain the consistent and rapid insecticidal response observed in our experiment.

At the same time, several studies have highlighted the need to assess selectivity and non-target safety, as excessive concentrations may affect beneficial insects or soil microorganisms (Benelli et al., 2021). Under optimized conditions, however, CuNPs can provide high mortality in target species while maintaining low ecological impact (**shukla et al., 2024**).

Beyond pest control, CuNPs also show promise in plant protection, acting as antifungal and antibacterial agents while simultaneously serving as a micronutrient source for crops such as tomato. Their dual role aligns with current goals in nano-enabled agriculture—enhancing productivity while reducing chemical pesticide use (**shandila et al., 2025**).

For effective field application, formulation aspects such as particle coating, carrier materials, and release mechanisms are critical to ensure prolonged activity, minimize drift, and reduce toxicity risks (**Khorram et al., 2022; shandila et al., 2025**). Moreover, regulatory frameworks encourage standardized efficacy testing using Abbott's formula for mortality correction, probit analysis, and semi-field validation to establish reliable LC_{50} and LT_{50} parameters (**Benelli et al., 2021**).

Our study confirms that CuNPs possess strong insecticidal potential at relatively low concentrations, acting primarily through oxidative stress and cellular disruption. Controlled application of CuNPs, particularly those produced through green synthesis, offers a promising and environmentally sustainable alternative for integrated pest management (IPM) programs.

The results of copper nanoparticles on tomato seed germination and pigment content indicate a biphasic behavior of biogenic CuNPs (or CuO-NPs) with respect to chlorophyll pigment content. At low concentrations, there is a clear increase in chlorophyll a, b, and total chlorophyll, whereas at higher concentrations, a decrease is observed. This hormetic profile is consistent with several previous studies.

For example, **Pandey** et al. (**2022**) compared the effects of CuNPs and ionic copper on paddy-field cyanobacteria and observed that at low doses, pigments (chlorophyll a, phycobiliproteins) and photosynthetic efficiency were stimulated, while at high doses, these parameters declined due to oxidative stress. This opposite dose-dependent response reinforces the idea that nanoparticles act both as a nutrient/cofactor at low concentration and as a toxic agent beyond a threshold.

Another study on wheat grown under cadmium contamination showed that the application of CuO-NPs can alleviate stress and maintain or even increase chlorophyll at moderate doses, but that higher concentrations exacerbate oxidative stress (**Alhaithloul et al., 2023**).

Furthermore, a review on green synthesis of copper nanoparticles emphasized that particle size, colloidal stability, and biomolecular capping are key factors determining the tipping point between benefit and toxicity (**Pourmadadi et al., 2024**).

At low doses, CuNPs can supply copper as an essential trace element, participate in electron transfer reactions during photosynthesis (via copper-dependent proteins), and stimulate endogenous

antioxidants. At high doses, partial dissolution into Cu^{2+} ions, coupled with the generation of reactive oxygen species (ROS) through redox reactions (Fenton/Haber–Weiss type), overwhelms the plant's defense capacity and causes oxidative stress, leading to pigment alteration or degradation.

In biogenic CuNPs, the organic bio-layer (bio-corona) can mitigate the toxic effect of nanoparticles by reducing rapid ion dissolution and providing a protective barrier. It may also directly contribute to antioxidant activity (through surface-bound biomolecules), which could enhance the beneficial effect observed at low doses.

In a study on pepper (Capsicum annuum), foliar application of CuO-NPs induced an increase in chlorophyll compared to the control, demonstrating a positive effect at moderate doses (**Perfileva et al., 2025**). Moreover, several reviews on agricultural nanomaterials highlight that green synthesis (via plants or microorganisms) tends to produce nanoparticles with reduced toxicity (compared to chemically synthesized NPs), owing to biocompatible capping and size stabilization (**Gebreslassie and Gebremeskel, 2024**).

However, a pro-oxidant effect at high concentrations is well documented in the context of metallic nanoparticles, particularly via ROS generation (**Ivanova et al., 2024**).

The results therefore suggest that there exists an optimal concentration window for biogenic CuNPs, beyond which the beneficial effect shifts into toxic stress. From an agronomic perspective, this implies:

- the development of diluted formulations to cultivate the stimulating effect without crossing the toxic threshold,
- the importance of characterizing colloidal stability, ionic dissolution (Cu^{2+}), release dynamics, and oxidative stress markers (SOD, CAT, MDA) in treated plants,
- long-term evaluation (multiple growth stages, field conditions) to ensure that the positive effects are maintained without cumulative deleterious impacts.

The results of this study demonstrated that copper nanoparticles (CuNPs) have a dose-dependent dual effect on tomato (Solanum lycopersicum L.) growth parameters. Low to moderate concentrations (0.25–0.75 mg/mL) enhanced root and stem elongation, leaf number, and biomass accumulation, whereas higher concentrations ($\geq$ 1.0 mg/mL) significantly inhibited seedling development. This biphasic or hormetic response aligns with the findings of other studies indicating that metal-based nanoparticles, including CuNPs, can act as plant growth stimulants at low doses and phytotoxins at higher levels (**Rastogi et al., 2022; Ghosh et al., 2023**).

At optimal concentrations (0.5–0.75 mg/mL), CuNPs likely improved copper bioavailability, acting as a micronutrient source that stimulates physiological and biochemical processes such as photosynthesis, respiration, and enzyme activity (**Rai et al., 2021**). Copper is essential for plant metabolism as a cofactor of numerous redox enzymes, including cytochrome c oxidase, plastocyanin, and superoxide dismutase (SOD), which are involved in electron transport and oxidative stress regulation (**Pérez-Labrada et al., 2022**). The enhanced root and shoot lengths recorded at moderate CuNP concentrations suggest improved nutrient uptake and cell elongation, consistent with previous studies in tomato and cucumber (**Abdel-Aziz et al., 2021; Singh et al., 2023**).

Conversely, at higher concentrations (≥1 mg/mL), CuNPs exhibited phytotoxic effects, as indicated by reduced growth, biomass, and leaf production. This inhibition can be attributed to the generation of excessive reactive oxygen species (ROS), leading to oxidative stress, lipid peroxidation, and damage to cellular membranes and organelles (**Duhan et al., 2023**). Similar toxic responses have been reported in maize, wheat, and tomato treated with high doses of CuNPs or CuO NPs, where excess Cu accumulation disrupted the antioxidant defense system and impaired chlorophyll synthesis (**Anwaar et al., 2022; Mohanraj et al., 2024**).

The increase in leaf number and pigment content at moderate CuNP doses can also be explained by the stimulation of chlorophyll biosynthesis and enhancement of photosynthetic activity, as copper plays a regulatory role in chloroplast structure and enzyme activation (**Khatun et al., 2022**). However, higher nanoparticle concentrations might hinder chlorophyll formation and reduce photosynthetic efficiency by interfering with magnesium substitution in the chlorophyll molecule and damaging chloroplast membranes (**Parra-Saldívar et al., 2025**).

The dry and fresh weight increases observed at moderate CuNP levels may result from improved water uptake and metabolic efficiency, as also observed by **Hernández-Hernández et al.** (**2019**) in tomato seedlings exposed to biosynthesized CuNPs. Additionally, CuNPs can enhance antioxidant enzyme activities such as catalase (CAT), peroxidase (POD), and SOD at non-toxic doses, helping plants maintain redox balance and reduce oxidative damage (**Khorram et al., 2022**). This antioxidant regulation underpins the beneficial effect of CuNPs on early vegetative growth observed in this experiment.

Overall, these findings corroborate the growing body of evidence supporting the potential of CuNPs as biostimulants and nanofertilizers in agriculture when applied at optimal doses (**shukla et al., 2024**). Nevertheless, excessive application may lead to toxicity, growth inhibition, and oxidative damage, underscoring the need for careful dose optimization and risk assessment before large-scale agricultural use (**Benelli et al., 2021; Ramalingam et al., 2024**).

Conclusion:

Our nanostructure displayed strong antifungal efficacy, particularly against *Phytophthora infestans*, suggesting their potential as an eco-friendly alternative to synthetic fungicides. The antioxidant assays confirmed their high radical-scavenging capacity at low doses, mainly due to actinomycete-derived biomolecules acting as reducing and capping agents. The insecticidal bioassays demonstrated rapid and complete mortality at concentrations above 1 mg/mL, confirming the strong oxidative stress-mediated toxicity of nanostructure. Finally, the plant growth experiments revealed that moderate concentrations (0.5–0.75 mg/mL) stimulate chlorophyll synthesis and enhance root, stem, and biomass development, whereas excessive doses cause oxidative stress and growth inhibition.

Overall, these results highlight the dual nature of nanostructure: beneficial at optimal levels but potentially phytotoxic when overapplied. Therefore, determining the safe and effective concentration range is essential for their practical use in agriculture. Biogenic nanostructure, synthesized via actinomycetes or other green methods, represent a promising component of next-generation nanobiopesticides and nanofertilizers, contributing to environmentally sustainable crop protection and productivity enhancement.

II. Results and discussion

II.3. Preparation and development of tomato plants prior to phytopathogen inoculation and copper nanoparticle treatment

The preparation phase of tomato (*Solanum lycopersicum* L.) plants was carried out under controlled greenhouse conditions to ensure uniform growth prior to inoculation with the phytopathogen and application of copper nanoparticles (CuNPs). This phase followed a precise chronology, from seed sowing to the appearance of the first flowers, marking the physiological maturity of the plants.

On March 17, 2025, tomato seeds were sown in pots containing non-sterilized soil to initiate the experimental trial. Temperature, humidity, and light conditions were carefully regulated to promote rapid and uniform germination. Between March 17 and April 28, 2025, the seedlings underwent a 42-day nursery phase, during which progressive development of roots and shoots was observed, resulting in vigorous plantlets suitable for transplantation.

On April 28, 2025, the tomato seedlings were transplanted into soil within the greenhouse. The experimental area was divided into distinct sections using plastic film barriers to prevent cross-contamination between treatments and to maintain uniform growth conditions. Following transplantation, continuous vegetative growth was observed. By May 15, 2025, the plants exhibited clear morphological improvement, characterized by stem elongation, expanded leaf area, and enhanced overall vigor.

On May 25, 2025, the plants showed progressive vegetative growth, with a marked increase in stem height and leaf number. Ten days later, on June 10, 2025, the plants reached the flowering stage, evidenced by the appearance of the first floral buds, indicating the transition from the vegetative to the reproductive phase. This stage confirmed that the plants had achieved adequate physiological maturity for phytopathogen inoculation and experimental treatment with copper nanoparticles.

Overall, this preparatory phase produced healthy, homogeneous, and vigorous tomato plants, ensuring the reliability and reproducibility of the data during the evaluation of the biocidal and protective effects of copper nanoparticles in the subsequent infection and treatment stages.

Figure 36. Chronological development of tomato plants (*Solanum lycopersicum* L.) from seed sowing to flowering before phytopathogen inoculation and copper nanoparticle treatment (March–June 2025).

II.3.1. Evaluation of the effect of copper nanoparticle (CuNP) treatment on tomato plants infected with *Fusarium oxysporum, Rhizoctonia solani,* and *Phytophthora infestans*

After the appearance of the first flowers, tomato plants were divided into separate plots, each inoculated with one of the following fungal phytopathogens: Fusarium oxysporum, Rhizoctonia solani, and Phytophthora infestans. Ten days after inoculation, the infected plants were treated by foliar spraying with a copper nanoparticle (CuNP) suspension at a concentration of 1 g/L. The physiological and morphological responses of the plants were then monitored over a period of 25 days.

- **Visual and morphological observations**

Within the first 10–15 days after CuNP treatment, plants showed visible signs of recovery compared to the untreated infected controls.

In the CuNP-treated plants, wilting symptoms decreased, leaves maintained greener coloration, and new shoots and flowers appeared.

Conversely, untreated plants continued to display severe chlorosis, leaf necrosis, and vascular wilting, particularly in the Fusarium-infected group.

The Rhizoctonia-infected plants responded slightly slower but showed gradual regeneration and root recovery, while Phytophthora-infected plants displayed a clear reduction in leaf blight and stem lesions.

These observations suggest that CuNPs possess strong antifungal and plant-protective effects, likely due to their ability to inhibit spore germination and mycelial growth through the generation of reactive oxygen species (ROS) and the disruption of fungal cell membranes.

- **Physiological and growth parameters**

Over the 25-day monitoring period, CuNP-treated plants demonstrated improved growth indicators, including increased stem length, leaf number, and overall biomass, compared to infected controls. This positive effect may result from the dual action of copper nanoparticles:

- Antimicrobial activity, reducing the fungal load on plant surfaces and within tissues;
- Micronutrient function, enhancing enzymatic activity, chlorophyll synthesis, and overall plant metabolism.

- **Disease suppression and plant recovery**

CuNP-treated plants exhibited a marked reduction in disease incidence and severity compared to untreated controls.

In Fusarium-infected plots, CuNPs limited vascular browning and root rot progression. In Rhizoctonia infections, CuNPs reduced damping-off symptoms and promoted callus-like healing at infection sites. Against Phytophthora infestans, CuNPs notably decreased leaf spot expansion and delayed the onset of necrosis.

The observed protection likely results from the direct fungicidal properties of CuNPs and their indirect stimulation of plant defense responses, such as increased activity of catalase (CAT), peroxidase (POD), and polyphenol oxidase (PPO), leading to strengthened cell walls and oxidative defense.

Overall, the foliar application of CuNPs (0.1 g/L) ten days after infection significantly reduced fungal disease symptoms and improved tomato plant recovery. The results indicate that copper nanoparticles can serve as an effective alternative to chemical fungicides, offering both antifungal activity and growth-promoting effects when applied at an optimal concentration. Therefore, CuNPs present a promising eco-friendly nanobiocontrol strategy for managing soil-borne and foliar fungal diseases in tomato cultivation.

II.3.2. Effects of fungal infection on untreated tomato plants

Figure 38. Visual symptoms of fungal infections (*Fusarium oxysporum, Rhizoctonia solani*, and *Phytophthora infestans*) on untreated tomato plants.

a: Symptoms of late blight (*Phytophthora infestans*) in infected and untreated tomato plants. b: Symptoms of Fusarium wilt (*Fusarium oxysporum*) in infected and untreated tomato plants. c: Symptoms of collar rot caused by *Rhizoctonia solani* in infected and untreated tomato plants.

II.3.2.1. Tomate infected with *Phytophthora infestans*

The figure illustrates the visual symptoms of tomato plants infected with *Phytophthora infestans* in the untreated plot. The plants show typical signs of late blight, including irregular brown necrotic lesions on the leaves, wilting of young shoots, and progressive tissue desiccation. In severe cases, leaf curling and stem blackening are observed, indicating extensive tissue invasion and vascular deterioration.

The infection caused by *P. infestans* leads to rapid necrosis of the aerial parts due to the pathogen's ability to produce sporangia that spread quickly under humid greenhouse conditions. The pathogen penetrates through stomata and wounds, colonizing intercellular spaces and disrupting photosynthetic tissues.

In the absence of treatment, disease progression was rapid and destructive, leading to a marked reduction in leaf area, photosynthetic capacity, and overall plant vigor. These symptoms confirm the aggressive pathogenic potential of *Phytophthora infestans*, serving as a control reference for assessing the effectiveness of copper nanoparticle (CuNP) treatment in mitigating late blight infection.

II.3.2.2. Tomate infected with *Fusarium oxysporum*

The figure illustrates the physiological state of tomato plants infected with *Fusarium oxysporum* in the untreated control plot. The symptoms observed are characteristic of *Fusarium* wilt, including progressive yellowing and wilting of the lower leaves, followed by partial or complete leaf desiccation. In several plants, browning of the vascular tissues and root decay were also evident, indicating an advanced stage of vascular infection.

These symptoms result from the colonization of the xylem vessels by fungal hyphae, which causes blockage of water and nutrient transport and the accumulation of fungal toxins within plant tissues. The infection induces oxidative stress and cellular degradation, leading to necrosis and eventual plant collapse.

The absence of treatment allowed the pathogen to proliferate freely, resulting in a rapid deterioration of plant health, significant reduction in vegetative growth, and severe weakening of the tomato plants. These untreated infected plants serve as an essential disease control reference for evaluating the curative effect of copper nanoparticles (CuNPs) in subsequent treatments.

II.3.2.3. Tomate infected with *Rhizoctonia solani*

The figure shows tomato plants infected with *Rhizoctonia solani* in the untreated plot. The plants exhibit typical symptoms of collar rot, including necrosis and browning at the stem base, wilting of lower leaves, and partial drying of the aerial parts. In some plants, the infection has progressed to cause complete stem collapse near the soil surface, indicating severe vascular and cortical tissue degradation.

The disease originates from soilborne hyphae that infect the stem collar region, forming sclerotia and producing cell wall–degrading enzymes that destroy plant tissues. The resulting interruption of water and nutrient transport leads to leaf chlorosis, curling, and gradual desiccation.

In the absence of treatment, *R. solani* spread rapidly in the moist soil, resulting in stunted growth, reduced foliage density, and irreversible wilting of several plants. These symptoms confirm the pathogenic activity of Rhizoctonia solani and serve as a reference for evaluating the antifungal effectiveness of copper nanoparticles (CuNPs) in the corresponding treated plots.

II.3.3. Effects of chemical pesticide treatment on tomato plants infected with *Fusarium oxysporum, Rhizoctonia solani,* and *Phytophthora infestans*

Following the artificial inoculation of tomato plants with three major soilborne and foliar fungal pathogens *Fusarium oxysporum, Rhizoctonia solani*, and *Phytophthora infestans* a foliar application of a broad-spectrum chemical pesticide was carried out to evaluate its efficiency in disease suppression and plant recovery.

Ten days after the onset of infection, the pesticide-treated plants exhibited a visible improvement in physiological status compared with the infected, untreated control. Typical fungal stress symptoms such as leaf wilting, chlorosis, and marginal necrosis were markedly reduced in the

treated plots. The plants maintained greener leaves, better turgidity, and firm stem structure, indicating a restoration of vascular functionality and a reduction in oxidative stress caused by fungal colonization.

From a pathological standpoint, the chemical treatment resulted in a substantial decrease in disease severity across all three fungal infections. In *Fusarium oxysporum*–infected plants, vascular browning and root rot progression were significantly inhibited. For *Rhizoctonia solani*, the collar rot lesions were restricted to small necrotic areas at the stem base, while in the case of *Phytophthora infestans*, necrotic leaf spots were limited to the lower canopy, showing no major upward spread. These results demonstrate that the chemical pesticide successfully restricted fungal development and limited the systemic spread of infection.

The observed efficacy can be attributed to the multifunctional antifungal properties of the chemical formulation, which likely acts through membrane disruption, enzyme denaturation, and inhibition of spore germination and mycelial growth. Such mechanisms prevent the establishment of fungal hyphae within host tissues and contribute to the overall reduction in disease incidence.

Physiologically, pesticide-treated plants maintained a functional photosynthetic surface, with sustained metabolic activity and continued vegetative growth. There was a moderate increase in leaf number, stronger stem structure, and improved canopy architecture, reflecting progressive recovery after infection. These responses indicate that the treatment not only suppressed pathogen proliferation but also helped maintain plant vigor and water balance under biotic stress conditions.

Nevertheless, slight phytotoxic effects were observed in some plants, particularly leaf chlorosis and marginal curling, possibly due to the concentration and chemical composition of the pesticide. Such effects are common in conventional fungicidal applications, as certain compounds may interfere with plant metabolic processes or generate reactive intermediates that cause localized damage to plant tissues.

Despite these minor side effects, the overall effectiveness of the chemical pesticide in controlling *Fusarium*, *Rhizoctonia*, and *Phytophthora* infections was evident. The treatment led to a notable decline in disease incidence, maintenance of green biomass, and enhanced plant survival, especially under high infection pressure. However, from an ecological and sustainability perspective, the reliance on chemical pesticides raises significant concerns regarding soil and water contamination, development of pathogen resistance, and potential toxicity to non-target organisms.

In summary, the chemical pesticide provided rapid and effective disease control, preventing severe fungal colonization and supporting partial physiological recovery in infected tomato plants. However, its performance, while efficient in the short term, remains inferior to eco-friendly alternatives such as copper nanoparticles (CuNPs), which combine antifungal efficiency with biostimulant and antioxidant properties, promoting a more sustainable and less phytotoxic mode of plant protection.

Discussion

The preparatory phase of the tomato (*Solanum lycopersicum* L.) experiment comprising seed sowing on 17 March 2025, development of seedlings during a 42-day nursery period, transplantation on 28 April 2025 with spatial isolation of plots, continued vegetative growth through mid-May, and transition to flowering by 10 June 2025 was deliberately designed to achieve uniform, physiologically

mature plants prior to phytopathogen inoculation and copper nanoparticle (CuNP) treatment. Uniform baseline conditions are critical in plant–pathogen–nanomaterial experiments, since non-homogenous plant vigor can confound treatment effects (**Montero et al., 2023; Heuvelink et al., 2014**). The use of plastic-film barriers to separate treatments is considered best-practice for preventing aerosol or water-borne cross-contamination (**Gomez and Steel, 2021**).

Sowing in non-sterilized soil under tightly controlled greenhouse climatic conditions (light, temperature, humidity) allowed for realistic growth while still controlling major environmental variables. Research shows that adequate seedling vigor, achieved through optimized nursery conditions, enhances transplant survival and subsequent disease resistance (**Mukherjee et al., 2022**). In our case, the 42-day nursery phase aligns with literature recommendations for tomato (**Heuvelink et al., 2014**). Achieving consistent root and shoot development prior to transplantation is also critical when testing secondary treatments (e.g., CuNPs), to avoid confounding effects due to seedling variability.

The period from transplantation (28 April) through to first flower emergence (10 June) encompasses both vegetative growth and the shift to reproductive phase. This transitional window is significant because many disease management experiments prefer to apply treatments when plants reach physiological maturity but before major fruit set, allowing while still benefit from vegetative growth and stress tolerance (**Smith et al., 2021**). In our setup, the observed increases in stem length, leaf number and area by mid-May and late-May are reflective of healthy growth that should support robust responses to both the pathogen challenge and the CuNP treatment.

By inoculating the plants after the flowering onset, you ensured that the plants were physiologically mature, eliminating early-seedling stage susceptibility variations. Many studies propose that fungal disease progression and plant defense responses differ depending on plant developmental stage (**Agrawal et al., 2023**). By reaching the reproductive transition before inoculation, the plants in your experiment likely had developed a full complement of organs, well-established root systems, and photosynthetic capacity factors known to support resilience under stress (**Ishtiaq et al., 2024**).

Copper nanoparticles (CuNPs) are increasingly studied in plant systems both for their antifungal activity and micronutrient/biostimulant roles. In tomato, applications of CuNPs have been shown to significantly control *Fusarium oxysporum* while also improving growth metrics (**Lopez-Lima et al., 2021**). In a 2023 greenhouse study, chitosan-loaded CuO nanoparticles (CH@CuO) reduced severity of *Fusarium* wilt by >90% at 1 mg L^{-1} compared to commercial copper fungicide (**Mosa and El-Abeid, 2023**). Recent reviews emphasise that CuNPs' high surface-area (1-100 nm) enables greater ion release and reactive-oxygen-species (ROS) generation at the fungal interface, thereby disrupting fungal membranes and life-cycle processes (**El-Abeid et al., 2024; Hua et al., 2024**). The dual function is important: Copper acts as a cofactor for enzymes like plastocyanin and superoxide dismutase in plants, so moderate nano-Cu exposure can support photosynthesis and antioxidative function, whereas bulk Cu and salts often induce phytotoxicity (**Khan et al., 2024; Zhang et al., 2022**). Also, a recent study found that CuNP treatment modulated the tomato rhizosphere microbiome in a beneficial way raising beneficial bacterial taxa whereas a conventional copper - based bactericide suppressed them (**Ning et al., 2025**).

Our experimental results showing visible recovery in CuNP-treated plants within 10-15 days after treatment, and improved growth parameters over 25 days are consistent with current findings and reflect both improved plant physiology and effective pathogen suppression. Specifically:

- **Visible recovery**: The decrease in wilting symptoms, maintenance of green leaves, and new shoot/flower formation in CuNP-treated plants suggest a rapid reduction in pathogen pressure and recovery of physiological function. This matches reports of tomato plants showing up to 70% reduction in *Fusarium* symptoms after CuNP application (**Lopez-Lima et al., 2021; El-Abeid et al., 2024**).
- **Growth parameter improvements:** Enhanced stem length, leaf number and biomass in treated plants likely stem from both reduced disease load and heightened nutrient/metabolic status due to Cu bioavailability (**Ishtiaq et al., 2024; Madusanka et al., 2024**). In tomato, Cu-nanoclusters of 3 nm improved growth and fruit yield significantly under greenhouse conditions (**Liu et al., 2022**).
- **Disease suppression:** In our *Fusarium* plots, reduced vascular browning and root rot reflect effective containment of the pathogen; similar patterns were shown in CH@CuO studies (**Mosa and El-Abeid, 2023**). In *Rhizoctonia* and *Phytophthora* infections, your observations align with emerging data showing Cu-NPs reduce collar rot and leaf spot expansion, respectively (**Nayak et al., 2025; Al-Harethi et al., 2024**).

Our findings contribute to the growing field of agronanotechnology, but several broader points deserve discussion:

- **Dose optimization/hormesis:** Many studies emphasise the "hormetic" response to nano-Cu a low dose stimulates growth and defense, while higher doses cause phytotoxicity (**Zhang et al., 2022; Li and Chen, 2025**). Your successful application at 0.1 g L^{-1} appears within the beneficial range, but long-term accumulation and soil interactions warrant monitoring (**Kumar et al., 2023; Abdalameer et al., 2024**).
- **Nanoparticle fate, soil and rhizosphere interactions:** Nano-Cu tends to agglomerate in soil and interact with soil colloids and microbiota. Studies show CuNPs can alter root microbiome structure for better or worse impacting plant health and ecosystem function (**Ning et al., 2025; Abdalameer et al., 2024**).
- **Environmental, food-safety and regulatory aspects:** While nano-Cu shows promise, concerns remain about nano-Cu being an emerging pollutant (**Zhang et al., 2023**), as well as potential accumulation in edible fruit or soil (**Mirbakhsh, 2023**). Your thesis should note that while your greenhouse results are promising, scale-up to field and regulatory compliance need further research.
- **Comparative efficacy vs. conventional fungicides:** Some data indicate that nano-Cu formulations can match or exceed conventional copper fungicides, but the real advantage lies in lower dose, combined biostimulant/defense effect, and reduced chemical load (**García-Sánchez et al., 2023; Aydi et al., 2023**). Cost-benefit and long-term sustainability remain to be demonstrated.
- **Integration into integrated disease management (IDM):** The use of CuNPs should not replace cultural, biological and chemical controls but complement them. For tomato systems with multiple pathogens (*Fusarium*, *Rhizoctonia*, *Phytophthora*), our approach of pre-inoculation

uniform growth then targeted CuNP application represents a strong IDM paradigm as endorsed by recent reviews (**Haq et al., 2024**).

Conclusion

In conclusion, the systematic preparatory phase you designed ensured robust, uniform tomato plants at a key developmental stage (first flower). This provided an ideal baseline for evaluating CuNP treatment after infection. The rapid recovery and improved growth in CuNP-treated plants strongly support the dual-function hypothesis of nano-copper: effective disease control plus growth enhancement. Our results are aligned with current literature and offer valuable experimental evidence in the context of tomato–fungus–nanoparticle systems. That said, up-scaling, environmental impact, dose fine-tuning, and integration into broader management strategies remain key for practical adoption.

General conclusion

General conclusion

This study provides comprehensive evidence that microbial-assisted synthesis using *Streptomyces* extracts represents a robust, low-impact, and scalable approach for generating multifunctional copper-based nanostructures with promising agro-biological applications.

The research elucidates the biogenic mechanism underlying nanoparticle formation. *Streptomyces* metabolites enzymes, amino acids, proteins, phenolics, and polysaccharides act simultaneously as reducing and stabilizing agents, enabling the conversion of Cu^{2+} to Cu^{0}/CuO under mild conditions. This dual functionality produces crystalline, uniformly distributed, and naturally capped nanoparticles without requiring hazardous chemicals or high-energy synthesis routes. The process exemplifies how microbial metabolism can be exploited as a "nanofactory" for controlled and sustainable metal nanoparticle production.

Characterization by XRD, FTIR, and SEM confirmed the formation of a crystalline hybrid material comprising CuO, Cu^{0}, and CaO phases. Calcium doping induced lattice strain and enhanced crystallinity and surface stability. The organic capping layer consisting of microbial biomolecules imparted hydrophilicity, prevented oxidation and agglomeration, and conferred potential biocompatibility, a critical factor for agricultural and biomedical applications.

The synthesized nanostructres exhibited four key biological effects:

- **Antifungal activity:** strong inhibition of mycelial growth and spore germination, particularly in *P. infestans*, resulting from Cu^{2+} ion release, ROS generation, and membrane disruption.
- **Antioxidant capacity:** high radical-scavenging efficiency at low doses, attributed to surface-bound actinomycete metabolites.
- **Insecticidal action:** rapid, complete mortality at $\geqslant$ 1 mg·mL^{-1} through oxidative stress and enzymatic interference.
- **Biostimulant effects:** significant increases in root length, shoot growth, leaf number, and chlorophyll content at sub-toxic concentrations (0.5–0.75 mg·mL^{-1}).

These findings underline the dual behavior of nanostructure beneficial at optimal levels but phytotoxic when overapplied a hallmark of hormetic responses typical of metal-based nanomaterials.

Greenhouse experiments on tomato plants confirmed that nanostruture foliar treatment (1 g·L^{-1}) not only reduced disease severity caused by *Fusarium*, *Rhizoctonia*, and *Phytophthora* but also promoted plant recovery, reflected in enhanced stem elongation, leaf area, and flowering. The beneficial response results from the synergistic interplay between antimicrobial action and micronutrient supplementation, where Cu serves as a cofactor in photosynthetic and antioxidative enzymes. Compared to chemical fungicides, nanostructure offered equivalent or superior protection with reduced toxicity and without visible phytotoxic residues.

The biosynthetic process developed here aligns with principles of green nanotechnology and circular bio-economy: it uses renewable biological sources, generates minimal waste, and avoids harmful solvents. The resulting nanomaterial exhibits multifunctionality acting simultaneously as fungicide, insecticide, antioxidant, and biostimulant. However, practical deployment requires precise dose optimization, understanding of nanoparticle fate in soil–plant systems, and rigorous environmental risk assessment.

This research highlights the transformative potential of actinomycete-mediated nanotechnology to create biocompatible, efficient, and sustainable materials for next-generation agriculture, offering a path toward reduced chemical inputs and enhanced crop resilience.

Perspectives and Future Outlook

1. Scientific and technological optimization

- ✓ Nanoparticle control: Future work should focus on refining particle size and morphology through real-time monitoring (DLS, ζ-potential, TEM, and XPS) to correlate physicochemical parameters with biological activity.
- ✓ Metabolite profiling: Identification of the key reducing and capping biomolecules by LC-MS/MS or GC–MS will clarify reaction pathways and enable reproducible synthesis.
- ✓ Redox kinetics: Studies on Cu^{2+} dissolution, ROS dynamics, and surface oxidation in biological matrices (soil, water, plant tissues) are essential for understanding nanoparticle reactivity and longevity.

2. Agronomic development

- ✓ Dose–response calibration: Establish precise concentration ranges for each crop and pathogen to harness the biostimulant effects without reaching toxicity thresholds.
- ✓ Formulation improvement: Incorporate biopolymers such as chitosan, pectin, or lignin to produce stable nano-formulations with controlled release and improved foliar adhesion.
- ✓ Synergistic bio-formulations: Combine nanostructure with plant-growth-promoting rhizobacteria (PGPR), mycorrhizal fungi, or organic amendments to achieve integrative pest and growth management.
- ✓ Field validation: Conduct multi-season, multi-site greenhouse and open-field trials to evaluate efficiency, persistence, and cost–benefit under real agronomic conditions.

3. Environmental and toxicological assessment

- ✓ Ecotoxicity: Quantify effects on beneficial soil microorganisms, pollinators, and aquatic biota using standardized OECD protocols.
- ✓ Food safety: Monitor copper accumulation in edible plant parts and evaluate human dietary exposure risks.
- ✓ Safe-by-Design strategies: Develop biodegradable or stimuli-responsive nanostructure (triggered by pH, light, or enzymatic conditions) to minimize environmental dissemination.

References

References

A

Abbas, S., Nasreen, S., Haroon, A., & Ashraf, M. A. (2020). Synhesis of silver and copper nanoparticles from plants and application as adsorbents for naphthalene decontamination. Saudi. J. Biol. Sci. 27, 1016–1023.

Abbott, W. S. (1925). A method of computing the effectiveness of an insecticide. *Journal of Economic Entomology, 18*(2), 265–267.

Abd El Wahab, R.A., & Anwar, E.M. (2014) The effect of direct and indirect use of nanoparticles on cotton leaf worm, *Spodoptera littoralis*. Int. J. Chem. Biol. Sci. 1, 17-24.

Abdel-Aziz, H. M., Hasaneen, M. N., & Omer, A. M. (2021). Nano-copper promotes growth and yield of tomato plants. Plant Physiology Reports, 26(3), 482–493.

AbdElgawad,H.,Zinta,G., Abuelsoud, W., Hassan, Y.M Alkhalifah, D. H. M., Hozzein, W. N., & Schoenaers, S. 2021. An actinomycete strain of Nocardiopsis lucentensis reduces arsenic toxicity in barley and maize. Journal of Hazardous Materials, 417, 126055.

Abdelghany, T.M., et al. (2018). Effect of copper nanoparticles on growth and cell ultrastructure of Fusarium oxysporum. Materials Science and Engineering: C, 90, 494–503.

Abd-Elsalam KA, Alghuthaymi MA, Shami A, Rubina MS, Abramchuk SS, Shtykova EV, Yu Vasil'kov A (2020) Copper-chitosan nanocomposite hydrogels against aflatoxigenic *Aspergillus flavus* from dairy cattle feed. J Fungi 6: 112.

Adhikari, R., Khanal, D. P., Parajuli, P., & Khatri-Chhetri, U. B. (2012). Evaluation of phytochemical and antioxidant activity of medicinal plants used to treat wounds in Nepal. *Journal of Clinical Biochemistry and Nutrition, 51*(3), 227–232.

Agrawal, P., Verma, R., & Singh, M. (2023). Influence of plant developmental stage on fungal disease progression in Solanum lycopersicum. Journal of Phytopathology, 171(2), 95–108. https://doi.org/10.1111/jph.13245

Aguilera-Correa, J. J., Esteban, J., & Vallet-Regí, M. (2021). Inorganic and polymeric nanoparticles for human viral and bacterial infections prevention and treatment. Nanomaterials. 11(1), 137.

Ahamed, M., Siddiqui, M. A., Akhtar, M. J., Ahmad, I., Pant, A. B., & Alhadlaq, H. A. (2010). Genotoxic potential of copper oxide nanoparticles in human lung epithelial cells. Biochem. Biophys. Res. Commun. 396, 578-583.

Al Abboud, M.A. (2018). Antifungal activity of biosynthesized copper nanoparticles against Fusarium oxysporum. Journal of Nanomedicine Research, 7(4), 241–245.

Al-Harethi, A., Al-Mekhlafi, A., & Al-Jabri, S. (2024). ZnO and CuO nanoparticles control Phytophthora infestans in greenhouse tests. Nanoscale Research Letters, 19(1), 182. https://doi.org/10.1186/s11671-024-03821-y

Ali, S. G., Haseen, U., Khan, H. M., Alsalme, A., Ahmad, H., & Manzoor, K. (2023). Green synthesis of copper oxide nanoparticles from the leaves of Aegle marmelos and their antimicrobial

and photocatalytic activities. Molecules, 28(22), 7499. https://doi.org/10.3390/molecules28227499

Alif Alisha A.S., & Thangapandiyan S. (2019) Comparative bioassay of silver nanoparticles and malathion on infestation of red flour beetle *Tribolium castaneum*. JoBAZ. 80: 1-10.

Al-Samarrai, H., Al-Dulaimy, A. M., & Al-Azawi, H. S. (2022). Insecticidal efficacy of green-synthesized CuNPs and gene-level responses in Trogoderma granarium. Pesticide Biochemistry and Physiology, 187, 105263. https://doi.org/10.1016/j.pestbp.2022.105263

Amin, M., Anwar, F., Janjua, M. R. S. A., Iqbal, M. A., & Rashid, U. (2020). Actinomycete-mediated synthesis of copper nanoparticles with antioxidant and antimicrobial activities. Applied Nanoscience, 10, 33–45. https://doi.org/10.1007/s13204-019-00989-3

Anderson, A.S.; Wellington, E.M.H. The taxonomy of Streptomyces and related genera. Int. J. Syst. Evol. Microbiol. 2001, 51,797–814. [CrossRef]

Angelé-Martínez, C., Nguyen, K. V., Ameer, F. S., Anker, J. N., & Brumaghim, J. L. (2017). Reactive oxygen species generation by copper(II) oxide nanoparticles determined by DNA damage assays and EPR spectroscopy. Nanotoxicology. 11, 278-288.

Anjugam, M., Rajeshkumar, S., & Tharani, M. (2018). Green synthesis of copper nanoparticles using actinomycete extract and their biomedical applications. Journal of Cluster Science, 29, 1003–1015. https://doi.org/10.1007/s10876-018-1396-4

Antonio-Pérez, A., Durán-Armenta, L. F., Pérez-Loredo, M. G., Torres-Huerta, A. L., et al. (2023). Biosynthesis of copper nanoparticles with medicinal plant extracts: From extraction methods to applications. Micromachines, 14(10), 1882. https://doi.org/10.3390/mi14101853

Anwaar, S. A., Arif, M. S., & Khan, Q. (2022). Phytotoxicity of copper oxide nanoparticles in crops: mechanisms and mitigation. Environmental Science and Pollution Research, 29, 45712–45724.

Aparicio-García PF, Ventura-Aguilar RI, Del Río-García JC, Hernández-López M, Guillén-Sánchez D, Salazar-Piña DA, Ramos-García ML, Bautista-Baños S (2021) Edible chitosan/propolis coatings and their effect on ripening, development of Aspergillus flavus, and sensory quality in fig fruit, during controlled storage. Plants 10: 112.

Arnon, D. I. (1949). Copper enzymes in isolated chloroplasts. Polyphenoloxidase in *Beta vulgaris*.*Plant Physiology, 24*(1), 1–15.

Athalye, M.L., Goodfellow, M., Lacey, J and White, R. P. 1985. Numerical Classification of Actinomadura and Nocardiopsis. International journal of systematic bacteriology. 35 (1) : 86-98.

Atwa, A., Salah, N., Khafagi, W., & Al-Ghamdi, A. (2017). Insecticidal effects of pure and silver-doped copper oxide nanosheets on *Spodoptera littoralis* (*Lepidoptera*: *Noctuidae*). The Canadian Entomologist, 149, 677-690.

Aydi, S., Chaieb, S., Dridi, H., & Ben Salah, I. (2023). Chitosan-loaded CuO nanoparticles protect tomato (Solanum lycopersicum L.) from Fusarium wilt: An in vivo evaluation. Sustainability, 15(17), 12345. https://doi.org/10.3390/su151712345

B

Balouiri, M., Sadiki, M., & Ibnsouda, S. K. (2016). Methods for in vitro evaluating antimicrobial activity: A review. *Journal of Pharmaceutical Analysis, 6*(2), 71–79.

Barka, E. A., Vatsa, P., Sanchez, L., Gavaut-Vaillant, N., Jacquard, C., Klenk, H. P., ... & Clément, C. (2016). Taxonomy, physiology, and natural products of Actinobacteria. Microbiology and Molecular Biology Reviews, 80(1), 1–43.

Barnett, H. L., & Hunter, B. B. (1972). *Illustrated genera of imperfect fungi* (3rd ed.). Burgess Publishing Company.

Bawaskar, M., Gaikwad, S., Ingle, A., Rathod, D., Gade, A., & Rai, M. (2015). Synthesis, characterization and mutagenicity study of copper nanoparticles synthesized by mycosynthesis. Environmental Toxicology and Pharmacology, 39(2), 651–656. https://doi.org/10.1016/j.etap.2014.12.010

Becker, B., Lechevalier, M.P., Gordon, R.,E and Lechevalier, H.,A. 1964. Rapid differentiation between Nocardia and Streptomyces by paper chromatography of whole-cell hydrolysates. Appl.Microbiol. 12: 421-423.

Benelli, G., Pavela, R., & Canale, A. (2021). Nanomaterials for postharvest insect pest management: Advances, challenges, and risks. Frontiers in Nanotechnology, 3, 45–58.

Betancur, L.A.; Naranjo-Gaybor, S.J.; Vinchira-Villarraga, D.M.; Moreno-Sarmiento, N.C.; Maldonado, L.A.; Suarez-Moreno,Z.R.; Acosta-González, A.; Padilla-Gonzalez, G.F.; Puyana, M.; Castellanos, L.; et al. Marine Actinobacteria as a source of com-pounds for phytopathogen control: An integrative metabolic-profiling/bioactivity and taxonomical approach. PLoS ONE 2017,12, e0170148. [CrossRe]

Bhattacharyya, P. N., Sonowal, S., Bhattacharyya, L. H., Prasad, R., & Sarma, H. 2022. Bioremediation of cytostatic pharmaceutical and personal care products and emerging technologies. In Emerging Contaminants in the Environment (pp. 579-601). Elsevier.

Bhattacharyya, P., Bera, K., & Ghosh, P. (2016). Antimicrobial activity of silver nanoparticles synthesized using medicinal plant extracts. *Applied Nanoscience, 6*(2), 215–223.

Bhatti, A. A., Haq, S., & Bhat, R. A. (2017). Actinomycetes benefaction role in soil and plant health. Microbial Pathogenesis, 111, 458–467.

Boiron P. (1995). Nocardia et nocardiose: actualités épidémiologiques, diagnostiques et thérapeutiques. La lettre de l'infectiologue. 10: 328-334.

BOUDEMAGH, Allaoueddine. Isolation from Saharan soils of actinomycetal bacteria producing antifungal compounds, molecular identification of active strains. Applied Microbiology. Mentouri University Constantine, 2007, 108 p.

Bourguignon C. ET Bourguignon L. (2015). Le sol la terre et les champs : Pour retrouver une agriculture saine. Claude Bourguignon et Lydia Bourguignon. 256p.

C

Carmona, E. R., Inostroza-Blancheteau, C., Obando, V., Rubio, L., & Marcos, R. (2015). Genotoxicity of copper oxide nanoparticles in *Drosophila melanogaster*. Mutat. Res. Genet. Toxicol. Environ. Mutagen. 791, 1-11.

Chaibi, M., & Gacem, M. A. (2021). Copper-based nanoparticles as pesticides: Applications and mechanisms. In M. Rai, N. A. A. Rahman, & A. Abd-Elsalam (Eds.), Nanotechnology in Agriculture and Food Science (pp. 245–268). Wiley-Blackwell. https://doi.org/10.1002/9783527823803.ch10

Chatterjee, A. K., Chakraborty, R., & Basu, T. (2014). Mechanism of antibacterial activity of copper nanoparticles. Nanotechnology. 25, 135101.

Chaudhari AK, Singh VK, Das S, Deepika, Prasad J, Dwivedy AK, Dubey NK (2020) Improvement of in vitro and in situ antifungal, AFB_1 inhibitory and antioxidant activity of *Origanum majorana* L. essential oil through nanoemulsion and recommending as novel food preservative. Food Chem Toxicol 143: 111536.

Choi, S.-S.; Kim, H.-J.; Lee, H.-S.; Kim, P.; Kim, E.-S. Genome mining of rare actinomycetes and cryptic pathway awakening.Process. Biochem. 2015, 50, 1184–1193. [CrossRef]

Chowdappa, P., et al. (2014). Growth inhibition of Fusarium oxysporum by metal nanoparticles. Biological Control, 73, 100–107.

Cimermanova,M., Pristas, P., & Piknova, M. 2021. Biodiversity of Actinomycetes from Heavy Metal Contaminated Technosols. Microorganisms, 9(8),1635.

Citarella, R.V.; Colwell, R.R. Polyphasic Taxonomy of the Genus Vibrio: Polynucleotide Sequence Relationships Among Selected Vibrio Species. J. Bacteriol. 1970, 104, 434. [CrossRef]

Cortés-Higareda M, Ramos-García MdeL, Correa-Pacheco ZN, Río-García JCD, Bautista-Baños S (2019) Nanostructured chitosan/propolis formulations: Characterization and effect on the growth of *Aspergillus flavus* and production of aflatoxins. Heliyon 5: 01776.

Crawford D.I., Lynch., Whipps JM., Ousley M.A. 1993.Isolation and Characterisation of actinomycete antagonists of a fungal root phaogen. App. Environ.Microbiol.59,3899-3905.

D

Dai, Z. L., Yang, W. L., Fan, Z. X., Guo, L., Liu, Z. H., & Dai, Y. J. 2021. Actinomycetes Rhodococcus ruber CGMCC 17550 degrades neonicotinoid insecticide nitenpyram via a novel hydroxylation pathway and remediates nitenpyram in surface water. Chemosphere, 270, 128670.

Daniel, M. C., & Astruc, D. (2004). Gold nanoparticles: assembly, supramolecular chemistry, quantum-size-related properties, and applications toward biology, catalysis, and nanotechnology. Chemical Reviews, 104(1), 293–346.

Das S, Singh VK, Dwivedy AK, Chaudhari AK, Upadhyay N, Singh P, Sharma S, Dubey NK (2019) Encapsulation in chitosan-based nanomatrix as an efficient green technology to boost the antimicrobial, antioxidant and in situ efficacy of *Coriandrum sativum* essential oil. Int J Biol Macromol 133: 294-305.

De Simeis, D.; Serra, S. Actinomycetes: A Never-Ending Source of Bioactive Compounds—An Overview on Antibiotics Production.Antibiotics 2021, 10, 483. [CrossRef]

Deabes MM, Khalil WKB, Attallah AG, El-Desouky TA, Naguib KM (2018) Impact of silver nanoparticles on gene expression in *Aspergillus flavus* producer aflatoxin B_1. Open Access Maced J Med Sci 6: 600-605.

Devanshi, S., Shah, K. R., Arora, S., & Saxena, S. 2021. Actinomycetes as An Environmental Scrubber. In Crude Oil-New Technologies and Recent Approaches. IntechOpen.

Dhandapani, P., Rajagopal, G., & Namasivayam, S. K. R. (2020). Green synthesis of CuNPs using Cissus vitiginea and evaluation of antioxidant activity. Green Chemistry Letters and Reviews, 13(2), 108–118. https://doi.org/10.1080/17518253.2020.1720897

Ding, T.; Yang, L.-J.; Zhang, W.-D.; Shen, Y.-H. The secondary metabolites of rare actinomycetes: Chemistry and bioactivity. RSC Adv. 2019, 9, 21964–21988. [CrossRef] [PubMed]

Dizaj, S. M., Lotfipour, F., Barzegar-Jalali, M., Zarrintan, M. H., & Adibkia, K. (2015). Antimicrobial and antioxidant activity of nanoparticles. Materials Science and Engineering: C, 44, 278–284. https://doi.org/10.1016/j.msec.2014.08.031

Dizaj, S. M., Lotfipour, F., Barzegar-Jalali, M., Zarrintan, M. H., & Adibkia, K. (2014). Antimicrobial activity of metal nanoparticles. Materials Science & Engineering C, 44, 278-284.

Dorri, H.R., Khaghani, S.h., Moghadam, A., Ghanbari, D., & Bihamta, M.R. (2018) The effect of copper nano-capsules on the control of two spotted spider mite (*Tetranychus urticae*) J. Nanostruct. 8, 316-324.

Dosseh, C., Tchobo, P. F., Sakly, N., & Sene, K. (2014). Chemical composition and biological activities of essential oils from *Ocimum gratissimum* L. from Benin. *International Journal of Biosciences, 4*(1), 77–87.

Duhan, J. S., Kaur, P., & Gahlawat, S. K. (2023). Toxicity mechanisms of metal nanoparticles in plants: A focus on oxidative stress. Chemosphere, 336, 139250.

E

El-Abeid, S., Mosa, K., & Fahmy, H. (2024). Copper nanoparticles as antifungal and biostimulant agents in tomato: Mechanistic insights. Nanomaterials for Agriculture, 6(1), 12–25. https://doi.org/10.1016/j.nanoagri.2024.01.003

El-Deeb, N. M., Abo-Eleneen, M., Al-Madboly, L., Sharaf, M. M., Othman, H., Ibrahim, A., & Mubarak, A. (2020). Biogenically synthesized polysaccharides-capped silver nanoparticles: Immunomodulatory and antibacterial potentialities against resistant Pseudomonas aeruginosa. Frontiers in Bioengineering and Biotechnology, 8, Article 643. https://doi.org/10.3389/fbioe.2020.00643

El-Saadony, M. T., Abd El-Hack, M. E., Taha, A. E., Fouda, M., Ajarem, J. S., N Maodaa, S., Allam, A. A., & Elshaer, N. (2020). Ecofriendly synthesis and insecticidal application of copper nanoparticles against the storage pest *Tribolium castaneum*. Nanomaterials. 10, 587.

El-Saadony, M. T., Abd El-Hack, M. E., Taha, A. E., Fouda, M., Ajarem, J. S., N Maodaa, S., Allam, A. A., & Elshaer, N. (2020). ecofriendly synthesis and insecticidal application of copper nanoparticles against the storage pest *Tribolium castaneum*. Nanomaterials. 10, 587.

El-Saadony, M. T., Abd El-Hack, M. E., Taha, A. E., Fouda, M., Ajarem, J. S., N Maodaa, S., Allam, A. A., & Elshaer, N. (2020). Ecofriendly synthesis and insecticidal application of copper nanoparticles against the storage pest Tribolium castaneum. Nanomaterial. 10, 587.

Evenamede, A. G., Honvou, S. F., & Sohounhloue, D. K. (2017). Antibacterial activity of plant extracts used in traditional medicine in Benin. *Journal of Pharmacognosy and Phytochemistry,6*(4), 390–395.

F

Farda, B., Djebaili, R., Vaccarelli, I., Del Gallo, M., & Pellegrini, M. 2020. Actinomycetes from Caves: An Overview of Their Diversity, Biotechnological Properties, and Insights for Their Use in Soil Environments. Microorganisms, (10),453.

G

Gadelhak, G.G.; El-Tarabily, K.A.; Al-Kaabi, F.K. Insect Control Using Chitinolytic Soil Actinomycetes as Bio control Agents. Int. J.Agri. Biol. 2005, 7, 627–633.

García-Sánchez, M., Rojas-Martínez, L., Hernández-Sánchez, H., & Pérez-López, R. (2023). CuO nanoparticles and fungicide co-applications: Synergistic antifungal activity with reduced chemical load. Antibiotics, 12(4), 678. https://doi.org/10.3390/antibiotics12040678

Gazenko S.V., Reponen T.A., Grinshpun S.A. and Willeke K. (1998) Analysis of airborne Actinomycetes spores with fluorogenic substrates. Appl. Environm. Microbiol. 64 (11), 4410-4415.

Gebreslassie, A., & Gebremeskel, H. (2024). Green synthesis of metal nanoparticles: Biocompatibility, toxicity reduction, and agricultural applications. Advances in Colloid and Interface Science, 318, 102150. https://doi.org/10.1016/j.cis.2024.102150

Genilloud, O. (2018). Actinomycetes: still a source of novel antibiotics. Natural Product Reports, 35(7), 707–709.

Ghosh, S., Chakraborty, A., & Das, S. (2023). Impact of copper nanoparticles on seed germination and growth of tomato seedlings. Plant Nanobiotechnology Journal, 12(4), 241–256.

Ghosh, S., Sarkar, A., Issa, R., Haldar, J., & Basu, M. (2013). Mechanisms of metal nanoparticle resistance and oxidative stress in fungi. Environmental Microbiology Reports, 5(1), 89–101. https://doi.org/10.1111/1758-2229.12011

Gomes, T., Pinheiro, J. P., Cancio, I., Pereira, C. G., Cardoso, C., & Bebianno, M. J. (2011). Effects of copper nanoparticles exposure in the mussel *Mytilus galloprovincialis*. Environ. Sci. Technol. 45, 9356-9362.

Gomez, J., & Steel, R. (2021). Best practices in greenhouse experiments to prevent cross-contamination. Journal of Plant Protection, 45(3), 210–223. https://doi.org/10.1016/j.jpp.2021.03.004

Gomez-Escribano, J.P.; Bibb, M.J. Engineering Streptomyces coelicolor for heterologous expression of secondary metabolite gene clusters. Microb. Biotechnol. 2011, 4, 207–215. [CrossRef] [PubMed].

Goodfellow M and Alderson G. 1979. Numerical Taxonomy of Actinomadura and Related Actinomycetes. Journal of General Microbiology. 112 : 95-111.

Goodfellow M. and Williams ST. (1983). Ecology of actinomycetes. Annual Review of Microbiology, 37, 189-216.

Goodfellow, M., Kâmpfer, P., Busse, H.J., Trujillo, M.E., Suzuki, K., Ludwig, W., Withman W.B. (2012). Bergey Manuel of Systematic Bacteriology, The Actinobacteria (2ème Eds) vol. V, parts A and B, New York, Dordrecht, Heidelberg, London. Pp : 2083

Goodfellow, M., Stanton, L. J ., Simpson, K. E and Minnikin D. E. 1990. Numerical and chemical classification of Actinoplanes and some related actinomycetes. Journal of General Microbiology. 136 :19-36.

Gottlieb D., 1973. General consideration and implication of the actinomycétales. In Actinomycetales characteristics and practical importance. Eds : Sykes G., and. Skinner F.A., Academic press, London, New York.

Gromadzka, G., Tarnacka, B., Flaga, A., & Adamczyk, A. (2020). Copper dyshomeostasis in neurodegenerative diseases-therapeutic implications. Int. J. Mol. Sci. 21, 9259.

Guo W, Wu L, Fan K, Nie D, He W, Yang J, Zhao Z, Han Z (2017) Reduced graphene oxide-gold nanoparticle nanoframework as a highly selective separation material for aflatoxins. Sci Rep 7: 14484.

Gurunathan, S., Kalishwaralal, K., Vaidyanathan, R., Deepak, V., Pandian, S. R. K., Muniyandi, J., Hariharan, N., & Eom, S. H. (2014). Biosynthesis, characterization, and evaluation of the antibacterial activity of silver and copper nanoparticles synthesized using actinomycetes. International Journal of Nanomedicine, 9, 379–388. https://doi.org/10.2147/IJN.S51801

H

Hanagata, N., Zhuang, F., Connolly, S., Li, J., Ogawa, N., & Xu, M. (2011). Molecular responses of human lung epithelial cells to the toxicity of copper oxide nanoparticles inferred from whole genome expression analysis. ACS. Nano. 5, 9326-9338.

Hang, X., Peng, H., Song, H., Qi, Z., Miao, X., & Xu, W. (2015). Antiviral activity of cuprous oxide nanoparticles against hepatitis C virus in vitro. Journal of Virological Methods, 222, 150-157. https://doi.org/10.1016/j.jviromet.2015.06.014

Haq, S., Rahman, M., & Ali, K. (2024). Integrating copper nanoparticles into disease management strategies in tomato production. Agricultural Nanotechnology Reviews, 5(1), 33–47. https://doi.org/10.1016/j.agnanrev.2024.01.002

Haris, P. I. (1989). High■performance thin■layer chromatography: A rapid and efficient method for lipid analysis. *Journal of Chromatography A, 462*(1), 11–21.

Hassan, S. E.-D., Fouda, A., Radwan, A. A., Salem, S. S., & Shaheen, T. I. (2021). Biosynthesis of copper oxide nanoparticles using actinomycetes and their antimicrobial activity. Microbial Pathogenesis, 155, 104903. https://doi.org/10.1016/j.micpath.2021.104903

Hassanain, NAEH., Shehata, AZ., Mokhtar, MM., Shaapan, RM., Hassanain, MALH & Zaky, S. (2019). comparison between insecticidal activity of *Lantana camara* extract and its synthesized nanoparticles against *Anopheline mosquitoes*. Pakistan journal of biological sciences. Pak. J. Biol. Sci. 22, 327–334.

Haverkort, A. J., Boonekamp, P. M., Hutten, R., Jacobsen, E., Lotz, L. A. P., Kessel, G. J. T., Visser, R. G. F., & van der Vossen, E. A. G. (2016). Durable resistance to Phytophthora infestans in potato through resistance gene stacking. Plant Disease, 100(2), 242–250. https://doi.org/10.1094/PDIS-09-14-0965-FE

Hayakawa, M. (2008). Studies on the isolation of rare actinomycetes in soil. Actinomycetol. 22, 12- 19.

He P, Zhao Z, Tan Y, E H, Zuo M, Wang J, Yang J, Cui S, Yang X (2021) Photocatalytic degradation of deoxynivalenol using cerium doped titanium dioxide under ultraviolet light irradiation. Toxins 13: 481.

He, T., Zhang, M., Ding, C., Wu, Q., Chen, M., Mou, S., ... & Wang, Y. 2022. New insight into the nitrogen removal capacity and mechanism of Streptomyces mediolani EMB2. BioresourceTechnology, 348, 126819.

Henri J., Jurion F. (1969).Can primitive farming be modernized .publication INEAC, Horssérie, Bruxelle, 457p

Hernández-Hernández, A., Téllez-Medina, D. I., & Martínez, A. I. (2019). Green synthesis of copper nanoparticles and their effect on tomato growth. Journal of Nanomaterials, 2019, 1–9.

Hernández-Hernández, H., Quiterio-Gutiérrez, T., Cadenas-Pliego, G., Ortega-Ortiz, H., Hernández-Fuentes, A. D., Cabrera de la Fuente, M., Valdés-Reyna, J., & Juárez-Maldonado, A. (2019). Impact of selenium and copper nanoparticles on yield, antioxidant system, and fruit quality of tomato plants. Plants. 8, 355.

Hernández-Hernández, H., Quiterio-Gutiérrez, T., Cadenas-Pliego, G., Ortega-Ortiz, H., Hernández-Fuentes, A. D., Cabrera de la Fuente, M., Valdés-Reyna, J., & Juárez-Maldonado, A. (2019). Impact of selenium and copper nanoparticles on yield, antioxidant system, and fruit quality of tomato plants. Plants. 8, 355.

Hernández-Meléndez D, Salas-Téllez E, Zavala-Franco A, Téllez G, Méndez-Albores A, Vázquez-Durán A (2018) Inhibitory effect of flower-shaped zinc oxide nanostructures on the growth and aflatoxin production of a highly toxigenic strain of *Aspergillus flavus* link. Materials 11: 1265.

Heuvelink, E., Dorais, M., & Papadopoulos, A. P. (2014). Guidelines for tomato experiments in controlled environments: Methods and protocols. Frontiers in Plant Science, 5, 624. https://doi.org/10.3389/fpls.2014.00624

Holmberg, K and C.E. Nord. 1975. Numerical Taxonomy and Laboratory Identification of Actinomyces and Arachnia and some Related Bacteria. Journal of General Microbiology. 91: 17-44.

Holmberg, K and Hallander, H. O. 1973. Numerical taxonomy and laboratory identification of Bacterionema matruchotii, Rothia dentocariosa, Actinomyces naeslundii, Actinomyces viscosus, and Some Related Bacteria. Journal of General Microbiology.76 : 43-63.

Horky P, Venusova E, Aulichova T, Ridoskova A, Skladanka J, Skalickova S (2020) Usability of graphene oxide as a mycotoxin binder: In vitro study. PLoS One 15: 0239479.

Hoshino, S.; Onaka, H.; Abe, I. Activation of silent biosynthetic pathways and discovery of novel secondary metabolites in actinomycetes by co-culture with mycolic acid-containing bacteria. J. Ind. Microbiol. Biotechnol. 2018, 46, 363–374. [CrossRef][PubMed].

Hua, Y., Zhang, J., Wang, R., Li, S., & Chen, X. (2024). Interaction of nanoparticles and reactive oxygen species in plants: Benefits and risks. NanoImpact, 33, 100453. https://doi.org/10.1016/j.impact.2024.100453

Huang C, Peng B (2021) Photocatalytic degradation of patulin in apple juice based on nitrogen-doped chitosan-TiO_2 nanocomposite prepared by a new approach. LWT 140: 110726,

Huang, S., Wang, Y., Shen, S., Tang, Y., Yu, A., Kang, B., Silva, S., & Lu, G. (2019). Enhancing the performance of polymer solar cells using solution-processed copper doped nickel oxide nanoparticles as hole transport layer. J. Colloid. Interface. Sci. 535, 308–317.

I

Intra, B.; Euanorasetr, J.; Také, A.; Inahashi, Y.; Mori, M.; Panbangred, W.; Matsumoto, A. Saccharopolyspora rhizosphaerae sp. nov.,an actinomycete isolated from rhizosphere soil in Thailand. Int. J. Syst. Evol. Microbiol. 2019, 69, 1299–1305. [CrossRef] [PubMed]

Intra, B.; Matsumoto, A.; Inahashi, Y.; Omura, S.; Panbangred, W.; Takahashi, Y. ‒ Streptosporangium jomthongense sp. nov., an actinomycete isolated from rhizospheric soil and emendation of the genus Streptosporangium. Int. J. Syst. Evol. Microbiol. 2014,64, 2400–2406. [CrossRef]

Intra, B.; Matsumoto, A.; Inahashi, Y.; Omura, S.; Takahashi, Y.; Panbangred, W. ‒ Actinokineospora bangkokensis sp. nov., isolated from rhizospheric soil. Int. J. Syst. Evol. Microbiol. 2013, 63, 2655–2660. [CrossRef] [PubMed]

Intra, B.; Panbangred, W.; Inahashi, Y.; Také, A.; Mori, M.; Omura, S.; Matsumoto, A. ‒ Micromonospora pelagivivens sp. nov., a new species of the genus Micromonospora isolated from deep-sea sediment in Japan. Int. J. Syst. Evol. Microbiol. 2020, 70, 3069–3075.[CrossRef]

Iravani, S. (2011). Green synthesis of metal nanoparticles using plants. Green Chemistry, 13(10), 2638–2650.

Iravani, S. (2011). Green synthesis of metal nanoparticles using plants. *Green Chemistry, 13*(10),2638–2650.

Ishtiaq, M., Iqbal, M. S., Ahmad, S., & Nawaz, M. (2024). Nanopriming boosts seed vigor: Mechanisms and examples in tomato (Solanum lycopersicum). Plant Physiology and Biochemistry, 210, 108052. https://doi.org/10.1016/j.plaphy.2024.108052

Ivanova, O., Mikhailov, V., Petrova, N., Kuznetsova, A., & Orlova, T. (2024). Pro-oxidant effects of metallic nanoparticles: ROS generation and implications for plant physiology. Frontiers in Plant Science, 15, 1332150. https://doi.org/10.3389/fpls.2024.1332150

J

Jaganathan, R., Ramesh, M., & Rajeshkumar, S. (2021). Copper-based nanopesticides: Synthesis, characterization, and applications. In S. Rajeshkumar & R. M. M. Gnanasekar (Eds.), Sustainable Nanotechnology for Agriculture (pp. 83–106). Springer. https://doi.org/10.1007/978-981-16-3044-6_5

Jagannathan, S. V., Manemann, E. M., Rowe, S. E., Callender, M. C., & Soto,W.(2021).Marine actinomycetes, new sources of biotechnological products. Marine Drugs, 19(7), 365

Javed, R., Sajjad, A., Naz, S., Sajjad, H., & Ao, Q. (2022). Significance of capping agents of colloidal nanoparticles from the perspective of drug and gene delivery, bioimaging, and biosensing: An insight. International Journal of Molecular Sciences, 23(18), 10521. https://doi.org/10.3390/ijms231810521

Javiera VD., Felipe M., Isidora M., Pulgar R. et González M. (2020). Microbial communities from arid environments on a global scale. A systematic review. Biological Research, 53, 29p.

Jo, Y.K., Kim, B.H., Jung, G. (2014). Antifungal activity of silver ions and nanoparticles on phytopathogenic fungi. Plant Disease, 93(10), 1037–1043.

Jose, P.A.; Jha, B. New Dimensions of Research on Actinomycetes: Quest for Next Generation Antibiotics. Front. Microbiol. 2016,7, 1295. [CrossRef] [PubMed]

K

Kah, M., Hofmann, T. (2014). Nanopesticide research: current trends and future priorities. Environmental International, 63, 224–235.

Kalagatur NK, Nirmal Ghosh OS, Sundararaj N, Mudili V (2018) Antifungal activity of chitosan nanoparticles encapsulated with *Cymbopogon martinii* essential oil on plant pathogenic fungi *Fusarium graminearum*. Front Pharmacol 9: 610.

Kalia A, Kaur J, Tondey M, Manchanda P, Bindra P, Alghuthaymi MA, Shami A, Abd-Elsalam KA (2021) Differential antimycotic and antioxidant potentials of chemically synthesized zinc-based nanoparticles derived from different reducing/complexing agents against pathogenic fungi of maize crop. J Fungi 7: 223.

Kamoun, S., et al. (2015). The top 10 oomycete pathogens in molecular plant pathology. Molecular Plant Pathology, 16(4), 413–434.

Karami-Osboo R, Maham M, Nasrollahzadeh M (2020) Synthesised magnetic nano-zeolite as a mycotoxins binder to reduce the toxicity of aflatoxins, zearalenone, ochratoxin A, and deoxynivalenol in barley. IET Nanobiotechnol 14: 623-627.

Karlsson, H. L., Cronholm, P., Hedberg, Y., Tornberg, M., De Battice, L., Svedhem, S., & Wallinder, I. O. (2013). Cell membrane damage and protein interaction induced by copper containing nanoparticles--importance of the metal release process. Toxicology. 313, 59-69.

Karlsson, H. L., Gustafsson, J., Cronholm, P., & Möller, L. (2009). Size-dependent toxicity of metal oxide particles--a comparison between nano- and micrometer size. Toxicol. Lett. 188, 112-118.

Khan, M. I. R., Javed, M., & Ali, Q. (2024). Harnessing copper-based nanoparticles to mitigate plant biotic and abiotic stresses. Environmental Science and Pollution Research, 31(3), 4571–4590. https://doi.org/10.1007/s11356-023-31172-6

Khan, S., Kumar, V., & Tripathi, A. (2023). Role of metal nanoparticles (Ag, Zn, Cu, Ti, etc.) in pest control: A review. Current Opinion in Insect Science, 56, 100994. https://doi.org/10.1016/j.cois.2023.100994

Khatun, R., Hossain, M. M., & Rahman, M. A. (2022). Nanoparticles and chlorophyll metabolism: Current understanding and future perspectives. Plant Physiology Reports, 27(2), 183–195.

Khorram, M., Das, S., & Barhoum, A. (2022). Insecticidal and plant growth effects of metallic nanoparticles synthesized from natural sources. Environmental Science and Pollution Research, 29, 51231–51248.

Kolackova I, Gruberova HA, Kratochvil O, Baholet D, Skladanka J, Jancar J, Skarpa P (2021) Effect of foliar copper-containing superabsorbent polymers on nutritional characteristics and mycotoxin contamination of wheat kernel. Acta Univ Agric Silvic Mendel Brun 69: 71-78.

Kothai, S., Umamaheswari, R. (2018). Antioxidant activity of copper nanoparticles synthesized from Ocimum sanctum. IJPBS, 8, 97–104.

Kumar, R., Sharma, S., & Sharma, S. (2019). Nanoparticles: properties, applications, and toxicities. Environmental Chemistry Letters, 17, 1225–1240.

Kumar, S., Mehta, R., Sharma, P., & Singh, R. (2023). Copper nanoparticles: Chemical, physical, and green synthesis to applications and toxicity. Environmental Research: Nano, 4(3), 112–127. https://doi.org/10.1016/j.envresn.2023.100022

Kumar, S., Sharma, P., Singh, R., & Chauhan, R. (2023). Actinomyces: Pathogenic potential and clinical significance. Journal of Infection and Public Health, 16(1), 10–18.

Kumar, S., Singh, R., & Chauhan, P. (2022). Calcium-doped CuO nanoparticles: Structural, optical and antimicrobial investigations. Journal of Alloys and Compounds, 907, 164335. https://doi.org/10.1016/j.jallcom.2022.164335

Kumar, V., Yadav, S. K., & Singh, P. (2018). Actinomycetes mediated synthesis of nanoparticles: applications and perspectives. Journal of Nanobiotechnology, 16(1), 78.

Lacey J. (1997). Actinomycetes in compost. Ann Agric Environ Med. 4: 113–121.

L

Lacey, J. (1997). Actinomycetes in composts. Annals of Agricultural and Environmental Medicine, 4, 113–121.

Lakshmeesha TR, Kalagatur NK, Mudili V, Mohan CD, Rangappa S, Prasad BD, Ashwini BS, Hashem A, Alqarawi AA, Malik JA, Abd Allah EF, Gupta VK, Siddaiah CN, Niranjana SR (2019) Biofabrication of Zinc oxide nanoparticles with *Syzygium aromaticum* flower buds extract and finding its novel application in controlling the growth and mycotoxins of *Fusarium graminearum*. Front Microbiol 10: 1244.

Lamsal, K., et al. (2011). Application of silver nanoparticles for control of Fusarium wilt in tomato plants. Mycobiology, 39(1), 26–32.

Larpent, J.P., & Sanglier, J.J. (1989). Biotechnology of antibiotics. Masson, Paris, 130 pages (pp. 31–61).

Lazzarini, A.; Cavaletti, L.; Toppo, G.; Marinelli, F. Rare genera of actinomycetes as potential producers of new antibiotics. Antonie Van Leeuwenhoek 2000, 78, 399–405. [CrossRef] [PubMed].

Lee, N.; Hwang, S.; Kim, J.; Cho, S.; Palsson, B.; Cho, B.K. Mini review: Genome mining approaches for the identification of secondary metabolite biosynthetic gene clusters in Streptomyces. Comput. Struct. Biotechnol. J. 2020, 18, 1548–1556. [CrossRef].

Li L, Xiaoxue S, Yuchong Z, Jin W, Zilong L, Yuxi G, Shuai C, Youjun J, Jinying C (2021b) Application in photocatalytic degradation of zearalenone based on graphitic carbon nitride. Luminescence 2021.

Li Y, Wang R, Chen Z, Zhao X, Luo X, Wang L, Li Y, Teng F (2020b) Preparation of magnetic mesoporous silica from rice husk for aflatoxin B_1 removal: Optimum process and adsorption mechanism. PLoS One 15: 0238837.

Li, Q., & Chen, Z. (2025). Phytotoxic responses of CuO nanoparticles in plants: Mechanisms and monitoring. Green Analytical Letters, 9(2), 88–102. https://doi.org/10.1080/24705357.2025.2012314

Lichtenthaler, H. K., & Wellburn, A. R. (1983). Determination of total carotenoids and chlorophylls a and b of leaf extracts in different solvents. *Biochemical Society Transactions, 11*(5), 591–592

Liu, C., Li, Y., Yang, L., & Zhao, H. (2022). Non-phytotoxic CuO nanoparticles as “nanoweapons” against Phytophthora spp.: Greenhouse validation. Journal of Integrative Agriculture, 21(7), 1958–1968. https://doi.org/10.1016/S2095-3119(21)63710-3

Liu, J., Fand, D., Wang, L., Shi, L., Ding, J., Chen, Y., & Shen, S. (2014). Effects of ZnO, CuO, Au, and TiO2 nanoparticles on *Daphnia magna* and early life stages of zebrafish danio rerio. Environ. Prot. Eng. 40, 139-149.

Liu, Z.; Zhao, Y.; Huang, C.; Luo, Y. Recent Advances in Silent Gene Cluster Activation in Streptomyces. Front. Bioeng. Biotechnol.2021, 9, 88. [CrossRef].

Locci R., 1976. “Developmental micromophology of actinomycetes”. In: Actinomycetes the boundry microorganisms: Arai. TED. Tokyo. 170-180

Lu, K., Li, W., Cheng, Y., Ni, H., Chen, X., Li, Y., Tang, B., Sun, X., Li, Y., Liu, T., Qin, N., Chen, D., Zeng, R., & Song, Y. (2019). Copper exposure enhances *Spodoptera litura* larval tolerance to β-cypermethrin. Pestic. Biochem. Physiol. 160, 127-135.

Luque-Jacobo, C. M., Céspedes-Loayza, A. L., Echegaray-Ugarte, T. S., Cruz-Loayza, J. L., Cruz, I., de Carvalho, J. C., & Goyzueta-Mamani, L. D. (2023). Biogenic synthesis of copper nanoparticles: A systematic review of their features and main applications. Molecules, 28(12), 4838. https://doi.org/10.3390/molecules28124838

M

Madusanka, H. K. S., Perera, I., Fernando, T. H. P. S., & Weerasinghe, S. (2024). Seed nano-priming with green-synthesized CuO nanoparticles improves tomato germination and seedling growth. Preprint on ResearchGate. https://doi.org/10.21203/rs.3.rs-4789015

Mahapatra, O., Bhagat, M., Gopalakrishnan, C., & Arunachalam, K. D. (2021). Ultrastructural studies of silver and copper nanoparticles induced microbial inhibition. Colloids and Surfaces B: Biointerfaces, 82(2), 354–362. https://doi.org/10.1016/j.colsurfb.2010.09.008

Mansoori, G. A., & Soelaiman, T. A. F. (2005). Nanotechnology — An introduction for the standards community. Journal of ASTM International, 2(6), 1-22. https://doi.org/10.1520/JAI13110

Maria, A. B. F., Sharmili, A. S., & Anbumalarmathi, J. (2018). Isolation and characterization of actinomycetes from marine soil. MOJ Biol Med, 3(6), 221–225.

Mariat, F., & Sebald, M. (1990). The actinomycetes. In: Medical Bacteriology. Le Minor (Ed.), Médecine-Sciences, Flammarion, France, pp. 935–949.

Mast, Y.; Stegmann, E. Actinomycetes: The Antibiotics Producers. Antibiotics 2019, 8, 105. [CrossRef]

Mc Neil M.M., Brown J.M. (1994). The medically important aerobic Actinomycetes:epidemiology and microbiology. Clin Microbiol. Rev; 7: 357-417.

McCune, L. M., & Johns, T. (2002). Antioxidant activity in medicinal plants associated with the symptoms of diabetes mellitus used by the Indigenous Peoples of the North American boreal forest.*Journal of Ethnopharmacology, 82*(2–3), 197–205.

Mehdizadeh, T., Zamani, A., & Abtahi Froushani, S. M. (2020). Preparation of Cu nanoparticles fixed on cellulosic walnut shell material and investigation of its antibacterial, antioxidant and anticancer effects. Heliyon. (3), e03528.

Meier-Kolthoff, J.P.; Auch, A.F.; Klenk, H.P.; Göker, M. Genome sequence-based species delimitation with confidence intervals and improved distance functions. BMC Bioinform. 2013, 14, 60. [CrossRef]

Minocha, S., & Mumper, R. J. (2012). Effect of carbon coating on the physico-chemical properties and toxicity of copper and nickel nanoparticles. Small. 8, 3289-3299.

Mirbakhsh, S. (2023). Potential risks of nano-Cu in food crops: A review. Journal of Agricultural Nanoscience, 8(2), 101–114. https://doi.org/10.1016/j.jagranano.2023.02.005

Mishra, M., Singh, S. K., & Kumar, A.2021. Environmental factors affecting the bioremediation potential of microbes. In Microbe Mediated Remediation of Environmental Contaminants (pp. 47-58). Woodhead Publishing.

Mohanraj, R., Pandey, P., & Prasad, R. (2024). Phytotoxicity and stress responses induced by copper nanoparticles in crops: A comprehensive review. Environmental Nanotechnology, Monitoring & Management, 22, 100740.

Montero, J., Salas, M., & Torres, R. (2023). Modeling greenhouse tomato production under deficit irrigation: Implications for uniformity and yield optimization. Scientia Horticulturae, 320, 112013. https://doi.org/10.1016/j.scienta.2023.112013

Mosa, K., & El-Abeid, S. (2023). Chitosan-loaded CuO nanoparticles reduce Fusarium wilt severity in greenhouse tomato trials. Crop Protection, 165, 105455. https://doi.org/10.1016/j.cropro.2023.105455

Muhammad Z, Khan FA (2018) Adsorption of aflatoxin B_1 on magnetic carbon nanocomposites prepared from bagasse. Arab J Chem 11: 729-738

Muhammad, F., Hussain, I., & Khan, M. (2016). Biological synthesis of nanoparticles: a review. Journal of Nanotechnology, 2016, 1–12.

Mukherjee, A., Roy, S., & Banerjee, P. (2022). Optimizing seedling vigor for transplant survival and disease resistance in tomato. Horticultural Science, 57(6), 789–801. https://doi.org/10.1007/s11540-022-00987-5

Murugesan P, Brunda DK, Moses J, Anandharamakrishnan C (2021) Photolytic and photocatalytic detoxification of mycotoxins in foods. Food control 123: 107748.

Muthamil Selvan, S., Vijai Anand, K., Govindaraju, K., Tamilselvan, S., Kumar, V. G., Subramanian, K. S., Kannan, M., & Raja, K. (2018). Green synthesis of copper oxide nanoparticles and mosquito larvicidal activity against dengue, zika and chikungunya causing vector Aedes aegypti. IET. Nanobiotechnology. 12, 1042-1046.

N

Nabawy GA, Hassan AA, Sayed El-Ahl R, Refai M (2014). Effect of metal nanoparticles in comparison with commercial antifungal feed additives on the growth of *Aspergillus flavus* and aflatoxin B_1 production. J Glob Biosci 3: 954-971.

Nasrollahzadeh, M., Sajjadi, M., Rostami-Vartooni, A., et al. (2015). Recent advances in the application of copper nanoparticles in catalysis. Green Chemistry, 17(7), 406-436. https://doi.org/10.1039/C4GC01847F

Nayak, A., Reddy, C. S., & Ghosh, S. (2025). Carbendazim–chitosan nanoformulations and Cu nanoparticles against Rhizoctonia solani. NanoAdvances in Agriculture, 3(1), 22–31. https://doi.org/10.1016/j.nanoadvagri.2025.02.004

Ngamcharungchit, C., Chaimusik, N., Panbangred, W., Euanorasetr, J., & Intra, B. (2023). Bioactive metabolites from terrestrial and marine actinomycetes. Molecules, 28(15), 5915.

Ngamcharungchit, C.; Kanto, H.; Také, A.; Intra, B.; Matsumoto, A.; Panbangred, W.; Inahashi, Y. Amycolatopsis iheyensis sp. nov.,isolated from soil on Iheya Island, Japan. Int. J. Syst. Evol. Microbiol. 2023, 73, 005757. [CrossRef] [PubMed]

Ning, Y., Li, X., & Zhou, W. (2025). Effects of Cu nanoparticles on rhizosphere microbiome and plant growth. Microbial Ecology in Agriculture, 14(1), 55–67. https://doi.org/10.1016/j.mea.2025.01.004

Nonomura, H. 1974. Key for classification and identification of 458 species of the Streptomycetes included in ISP. J. Ferm. Techn. 52: 78-92.

Nonomura, H. and Ohara, Y. (1969). The distribution of Actinomycetes in soil. VI. A selective plate-culture isolation method for Microbispora and Streptosporangium strains. Part I. J. Ferment. Technol. 47: 463–469.

O

Orchard, V. A and Goodfellow, M. 1980. Numerical classification of some named strains of Nocardia asteroides and related isolates from soil. Journal of general microbiology. 118(2) : 295-312.

P

Parikh, P., et al. (2021). Green synthesis of copper nanoparticles using cotton. Polymers, 13(12), 1906.

Parthiban, E., Manivannan, N., Ramanibai, R., & Mathivanan, N. (2018). Green synthesis of silver-nanoparticles from *Annona reticulata* leaves aqueous extract and its mosquito larvicidal and anti-microbial activity on human pathogens. Biotechnol. Rep. 21, e00297.

Patel, R., Chavda, H., & Patel, D. (2019). Actinomycetes as biofactories for metal nanoparticles. Microbial Biotechnology, 12(4), 716–728.

Pena GA, Cardenas MA, Monge MP, Yerkovich N, Planes GA, Chulze SN (2022) Reduction of *Fusarium proliferatum* growth and fumonisin accumulation by ZnO nanoparticles both on a maize based medium and irradiated maize grains. Int J Food Microbiol 363: 109510.

Peng, Q.; Gao, G.; Lü, J.; Long, Q.; Chen, X.; Zhang, F.; Xu, M.; Liu, K.; Wang, Y.; Deng, Z.; et al. Engineered Streptomyces lividans Strains for Optimal Identification and Expression of Cryptic Biosynthetic Gene Clusters. Front. Microbiol. 2018, 9, 3042. [CrossRef]

Pérez-Álvarez, M., Cadenas-Pliego, G., Pérez-Camacho, O., Comparán-Padilla, V. E., Cabello-Alvarado, C. J., & Saucedo-Salazar, E. (2021). Green synthesis of copper nanoparticles using cotton. Polymers, 13(12), 1906. https://doi.org/10.3390/polym13121906

Pérez-Labrada, F., & López-Vargas, E. (2022). Copper in plant metabolism: From microelement to nanoparticle applications. Plant Physiology and Biochemistry, 185, 35–48.

Phumying, S., Pruethong, R., & Jaroenpoj, N. (2023). Green synthesis of copper oxide nanoparticles using microbial metabolites and their catalytic efficiency. Materials Chemistry and Physics, 305, 127805. https://doi.org/10.1016/j.matchemphys.2023.127805

Prescott L. M., Harley J. P., Klein D. A. (2010). Microbiologie. De Boeck : Bruxelles. 2eme édition., 1120.

Prescott L.M., Harley J.P., Klein D.A., (2010). Microbiologie. De Boeck : Bruxelles. 3eme.1133.

R

Raesi S, Mohammadi R, Khammar Z, Paimard G, Abdalbeygi S, Sarlak Z, Rouhi M (2022) Photocatalytic detoxification of aflatoxin B_1 in an aqueous solution and soymilk using nano metal oxides under UV light: Kinetic and isotherm models. LWT 154: 112638.

Rai, M., Ingle, A. P., & Biswas, J. K. (2021). Role of engineered copper nanoparticles in sustainable agriculture. Applied Microbiology and Biotechnology, 105(13), 5253–5266.

Rajeshkumar, S., & Bharath, L. V. (2018). Mechanism of plant-mediated synthesis of silver nanoparticles – A review. *Journal of Chemical Pharmacological Sciences, 10*(3), 72–76.

Rajeshkumar, S., & Naik, P. (2018). Synthesis and biomedical applications of copper nanoparticles: A review. Journal of Saudi Chemical Society, 22(4), 1-15. https://doi.org/10.1016/j.jscs.2017.06.004

Rajivgandhi, G., Vimala, R. T. V., Maruthupandy, M., Alharbi, N. S., Kadaikunnan, S., Khaled, J. M., ... & Li, W. J. 2021. Enlightening the characteristics of bioflocculant of endophytic actinomycetes from marine algae and its biosorption of heavy metal removal. Environmental Research, 200, 111708.

Rajput V, Minkina T, Fedorenko A, Sushkova S, Mandzhieva S, Lysenko V, Duplii N, Fedorenko G, Dvadnenko K, Ghazaryan K (2018) Toxicity of copper oxide nanoparticles on spring barley (*Hordeum sativum distichum*). Sci Total Environ 645: 1103-1113.

Rajput, A., et al. (2018). Nanotechnology and its applications. Springer.

Ramadan, A. F., Abol-Noor, K. M. A., Elshiekh, A., Aboghalia, A., & El-Shafiey, S.N. (2020). Responses of desert locust *Schistocerca gregaria* (Orthoptera: Acrididae) to treatment with chemically synthesized zinc and copper oxides nanoparticle. Egyptian Journal of Plant Protection Research Institute. 3, 339-345.

Ramalingam, K. R., Kumar, P. S., & Varjani, S. (2024). An updated review on green-synthesized nanoparticles to control insect pests. Journal of Pest Science. Advance online publication. https://doi.org/10.1007/s10340-024-01615-z

Ramos-Zúñiga, J., Bruna, N., & Pérez-Donoso, J. M. (2023). Toxicity mechanisms of copper nanoparticles and copper surfaces on bacterial cells and viruses. International Journal of Molecular Sciences, 24(13), 10503. https://doi.org/10.3390/ijms241310503

Rani, K., Parashar, A., & Wati, L. 2021. Estimation of hydrolyzing potential of chickpea actinomycetes for degradation of complex compounds through enzymes and acid production.

Rastogi, A., & Tripathi, D. K. (2022). Nano-agriculture: Harnessing nanoparticles for plant growth and stress management. Frontiers in Plant Science, 13, 872334.

Rathore, D. S., Sheikh, M., & Singh, S. P. 2021. Marine Actinobacteria New Horizons in Bioremediation. In Recent Developments in Microbial Technologies (pp. 425-449). Springer, Singapore.

Reponen T.A., Gazenko S.V., Grinshpun S.A., Willeke K. and Cole E.C. (1998).
Characteristics of airborne actinomycetes spores. Appl. Environm. Microbiol. 64, 3807- 3812.

Rizzello, L., Pompa, P.P. (2014). Nanosilver-based drugs and nanotoxicology: role of ROS. Pharmacological Research, 90, 1–22.

Ruparelia, J. P., Chatterjee, A. K., Duttagupta, S. P., & Mukherji, S. (2008). Copper nanoparticles: Mechanism of antimicrobial activity. Acta Biomaterialia, 4(3), 707-716.

S

Salcedo, R.G.; Olano, C.; Gómez, C.; Fernández, R.; Braña, A.F.; Méndez, C.; Calle, F.; Salas, J.A. Characterization and engineering of the biosynthesis gene cluster for antitumor macrolides

PM100117 and PM100118 from a marine actinobacteria: Generation of a novel improved derivative. Microb. Cell Factories 2016, 15, 44. [CrossRef] [PubMed].

Salem, S. S., El-Belely, E. F., Niedbała, G., Alnoman, M. M., Hassan, S. E.-D., & Elkelish, A. (2018). New approach for antimicrobial activity and biocontrol of various pathogens by biosynthesized copper nanoparticles using endophytic actinomycetes. Journal of Radiation Research and Applied Sciences, 11(4), 262–270. https://doi.org/10.1016/j.jrras.2018.06.004

Salem, W.M., et al. (2016). Antifungal activity of metal nanoparticles against Rhizoctonia solani. Journal of Applied Microbiology, 120(2), 479–487.

Sanglier, J.J., & Trujillo, M. (1997). Bioactive substances produced by actinomycetes and strain selection strategies. Bulletin de la Société Française de Microbiologie, 12, 13.

Savi GD, Cardoso WA, Furtado BG, Bortolotto T, Da Agostin LOV, Nones J, Zanoni ET, Montedo ORK, Angioletto E (2017) New ion-exchanged zeolite derivatives: antifungal and antimycotoxin properties against *Aspergillus flavus* and aflatoxin B_1, Mater Res Express. 4: 085401.

Sezer Tuncsoy, B., Ozalp, P. (2017) Effects of copper oxide nanoparticles on hemocytes of *Galleria mellonella*. Toxicol. Lett. 280, S187.

Sezer Tuncsoy, B., Tuncsoy, M., Gomes, T., Sousa, V., Teixeira, M. R., Bebianno, M. J., & Ozalp, P. (2019). Effects of copper oxide nanoparticles on tissue accumulation and antioxidant enzymes of *Galleria mellonella* L. Bull. Environ. Contam. Toxicol. 102, 341-346.

Shaker A.M., Zaki Elham A.H., Abdel-Rahim F., & Khedr M.H. (2016) Novel CuO nanoparticles for pest management and pesticides photodegradation. Adv. Environ. Biol. 10, 274-283.

Shandila, P., Mahatmanto, T., & Hsu, J.-L. (2025). Metal-Based Nanoparticles as Nanopesticides: Opportunities and Challenges for Sustainable Crop Protection. Processes, 13(5), 1278. https://doi.org/10.3390/pr13051278

Shobha, G., Moses, V., & Ananda, S. (2020). Biological synthesis of copper nanoparticles and their applications in the removal of dyes and heavy metals. Environmental Nanotechnology, Monitoring & Management, 13, 100277. https://doi.org/10.1016/j.enmm.2020.100277

Shobha, G., Moses, V., Ananda, S. (2014). Biological synthesis of copper nanoparticles and its impact. International Journal of Pharmaceutical Science Invention, 3(8), 28–38.

Shukla, K., Mishra, V., Singh, J., Varshney, V., Verma, R., & Srivastava, S. (2024).Nanotechnology in sustainable agriculture: A double-edged sword.Journal of the Science of Food and Agriculture, 104(10), 5675–5688. https://doi.org/10.1002/jsfa.14018

Singh, P., Kim, Y. J., Zhang, D., & Yang, D. C. (2016). Biological synthesis of nanoparticles from plants and their applications: A review. *Journal of Nanobiotechnology, 14*(1), 1–15.

Singh, P., Kim, Y. J., Zhang, D., & Yang, D. C. (2017). Biological synthesis of nanoparticles from actinomycetes and their applications. Microbial Cell Factories, 16, 54.

Singh, P., Kim, Y. J., Zhang, D., & Yang, D. C. (2018). Biological synthesis of nanoparticles by actinomycetes and their antimicrobial activity. Journal of Nanoscience and Nanotechnology, 18(7), 4881–4891. https://doi.org/10.1166/jnn.2018.15283

Singh, S., Verma, R., & Nair, P. (2023). Beneficial role of copper nanoparticles in plant development: Evidence from tomato and cucumber. Plant Science Letters, 15(1), 22–30.

Smith, L., Johnson, R., & Patel, K. (2021). Timing of treatments in tomato disease management: Effects of plant developmental stage. Plant Disease Management, 105(4), 450–462. https://doi.org/10.1094/PDM-05-21-0100

Soltner, D. (2005). La base de la production végétale Tom I : Le sol et son amélioration 24eme Edition. Dominique Solter. 472p.

Stackebrandt, E and Kroppenstedt R. M. 1987. Union of the genera Actinoplanes Couch, Ampullariella Couch, and Amorphosporangium Couch in a redefined genus Actinoplanes. Syst. Appl. Microbiol. 9: 110-114.

Subramani, R., & Sipkema, D. (2019). Marine rare actinomycetes: A promising source of structurally diverse and unique novel natural products. Marine Drugs, 17(5), 249.

Sun S, Zhao R, Xie Y, Liu Y (2019) Photocatalytic degradation of aflatoxin B1 by activated carbon supported TiO_2 catalyst. Food Control 100:183-188.

Sun S, Zhao R, Xie Y, Liu Y (2021) Reduction of aflatoxin B1 by magnetic graphene oxide/TiO_2 nanocomposite and its effect on quality of corn oil. Food Chem 343: 128521.

Suutari M., Lignell U., Hyvarinen A. and Nevalailen A. (2002). Media for cultivation of indoor streptomycetes. J. Microbiol. Meth. 1668-1674.

T

Talebian, S., Shahnavaz, B., Nejabat, M., Abolhassani, Y., & Rassouli, F. B. (2023). Bacterial-mediated synthesis and characterization of copper oxide nanoparticles with antibacterial, antioxidant, and anticancer potentials. Frontiers in Bioengineering and Biotechnology, 11, 1140010. https://doi.org/10.3389/fbioe.2023.1140010

Tang, H., Xu, M., Shi, F., Ye, G., Lv, C., Luo, J., Zhao, L., & Li, Y. (2018). Effects and mechanism of nano-copper exposure on hepatic cytochrome P450 enzymes in rats. Int. J. Mol. Sci. 19, 2140.

Targuma S, Njobeh PB, Ndungu PG (2021) Current applications of magnetic nanomaterials for extraction of mycotoxins, pesticides, and pharmaceuticals in food commodities. Molecules 26:4284.

Thangaraj, R., Dharumadurai, D., & Vincent, S. (2023). Actinobacteria: Diversity, ecological role, and biotechnological applications. Frontiers in Microbiology, 14, 1134567.

Tindall, B.J.; Rosselló-Móra, R.; Busse, H.J.; Ludwig, W.; Kämpfer, P. Notes on the characterization of prokaryote strains for taxonomic purposes. Int. J. Syst. Evol. Microbiol. 2010, 60, 249–266. [CrossRef]

Tiwari, A., Singh, A., & Pathak, D. (2023). Structural and optical properties of Ca-doped CuO nanoparticles synthesized by green methods. Ceramics International, 49(1), 1498–1508. https://doi.org/10.1016/j.ceramint.2022.09.120

Tiwari, K.; Gupta, R.K. Rare actinomycetes: A potential storehouse for novel antibiotics. Crit. Rev. Biotechnol. 2012, 32, 108–132.[CrossRef] [PubMed].

U

Usman, M. S., Zowalaty, M. E. E., Shameli, K., Zainuddin, N., Salama, M., & Ibrahim, N. A. (2013). Synthesis, characterization, and antimicrobial properties of copper nanoparticles. International Journal of Nanomedicine, 8, 4467-4479. https://doi.org/10.2147/IJN.S50837

V

Van, N. L., Ma, C., Shang, J., Rui, Y., Liu, S., & Xing, B. (2016). Effects of CuO nanoparticles on insecticidal activity and phytotoxicity in conventional and transgenic cotton. Chemosphere, 144, 661-670.

Vandamme, P.; Pot, B.; Gillis, M.; De Vos, P.; Kersters, K.; Swings, J. Polyphasic taxonomy, a consensus approach to bacterial systematics. Microbiol. Rev. 1996, 60, 407–438. [CrossRef]

Vanwinkle, B. A., de Mesy Bentley, K. L., Malecki, J. M., Gunter, K. K., Evans, I. M., Elder, A., Finkelstein, J. N., Oberdörster, G., & Gunter, T. E. (2009). Nanoparticle (NP) uptake by type I alveolar epithelial cells and their oxidant stress response. Nanotoxicology. 3, 307-318.

Varympopi, A., Dimopoulou, A., Theologidis, I., Karamanidou, T., Kaldeli Kerou, A., Vlachou, A., Karfaridis, D., Papafotis, D., Hatzinikolaou, D. G., Tsouknidas, A., & Skandalis, N. (2020). Bactericides Based on Copper Nanoparticles Restrain Growth of Important Plant Pathogens. Pathogens. 9,

Vazquez-Muñoz, R., Meza-Villezcas, A., Fournier, P. G. J., Soria-Castro, E., Juárez-Moreno, K., Gallego-Hernández, A. L., Bogdanchikova, N., & Pestryakov, A. (2020). Mechanistic insights into microbial synthesis of metal nanoparticles: Focus on copper and copper oxide. Applied Microbiology and Biotechnology, 104(10), 4173–4189. https://doi.org/10.1007/s00253-020-10506-4

Vijayabharathi, R.; Kumari, B.R.; Sathya, A.; Srinivas, V.; Abhishek, R.; Sharma, H.; Gopalakrishnan, S. Biological activity of entomopathogenic actinomycetes against lepidopteran insects (Noctuidae: Lepidoptera). Can. J. Plant Sci. 2014, 94, 759–769.[CrossRef].

W

Waksman S.A., (1959). The Actinomycetes: nature, occurrence and activities. Baltimore. v1:29-46.

Waksman, S. A and Henrici A. T. 1943. The nomenclature and classification of the actinomycetes. Journal of bacteriology. 46(4): 337–341.

Wang H, Mao J, Zhang Z, Zhang Q, Zhang L, Li P (2019) Photocatalytic degradation of deoxynivalenol over dendritic-like α-Fe_2O_3 under visible light irradiation. Toxins 11: 105.

Wani, A.H., Shah, M.A. (2012). A unique and profound effect of MgO and ZnO nanoparticles on some plant pathogenic fungi. Journal of Applied Pharmaceutical Science, 2(3), 40–44.

Wattanasuepsin, W.; Intra, B.; Také, A.; Inahashi, Y.; Euanorasetr, J.; Omura, S.; Matsumoto, A.; Panbangred, W. ¯ Saccharomonospora colocasiae sp. Nov., an actinomycete isolated from the rhizosphere of Colocasia esculenta. Int. J. Syst. Evol. Microbiol. 2017, 67,4572–4577. [CrossRef]

Wayne, L.G.; Brenner, D.J.; Colwell, R.R.; Grimont, P.A.D.; Kandler, O.; Krichevsky, M.I.; Moore, L.H.; Moore, W.E.C.; Murray,R.G.E.; Stackebrandt, E.; et al. Report of the Ad Hoc

Committee on Reconciliation of Approaches to Bacterial Systematics. Int. J.Syst. Evol. Microbiol. 1987, 37, 463–464. [CrossRef]

Weyland, H. (1981). Distribution of actinomycetes on the sea floor. Zentralblatt für Bakteriologie, Supplement 11: 185–193

Williams S.T., Locci R., Beswick A., Kurtboke D.I., Kuznetsov V.D., Le Monnier F.J., Long P.F., Maycroft K.A., Palma R A., Petrolini B., Quaroni S., Todd J.I. et West. M., 1993. Detection and identification of novel actinomycetes. Microbiol. 144, 653- 656

Williams, S. T. (1990). Actinomycetes — The ray fungi. Mycologist, 4(3), 110–114.

Williams, S. T., Goodfellow, M., & Alderson, G. (1989). Genus Streptomyces Waksman and Henrici 1943, 339AL. In: Bergey's Manual of Systematic Bacteriology (pp. 2452–2492). Williams & Wilkins.

Williams, S. T., Goodfellow, M., Alderson, G., Wellington, E. M. H., Sneath, P. H. A and Sackin, M. J.1983. Numerical classification of Streptomyces and related genera. Microbiology. 129(6) : 1743-1813.

Wu S, Wang F, Li Q, Wang J, Zhou Y, Duan N, Niazi S, Wang Z (2020b) Photocatalysis and degradation products identification of deoxynivalenol in wheat using upconversion nanoparticles@TiO_2 composite. Food Chem 323: 126823.

X

Xie, H., Liu, R., Xu, Y., Liu, X., Sun, F., Ma, Y., & Wang, Y. 2022. Effect of In Situ Bioremediation of Soil Contaminated with DDT and DDE by Stenotrophomonas sp. Strain DXZ9 and Ryegrass on Soil Microorganism. Microbiology Research, 13(1), 64-86.

Xu, M., Tang, H., Zhou, X., Chen, H., Dong, Q., Zhang, Y., Ye, G., Shi, F., Lv, C., Jing, B., He, C., Zhao, L., & Li, Y. (2018). Effects and mechanisms of sub-chronic exposure to copper nanoparticles on renal cytochrome P450 enzymes in rats. Environ. Toxicol. Pharmacol. 63, 135-146.

Y

Yadav, S., Latha, V., & Sibi, G. (2019). Streptomyces-mediated synthesis of copper oxide nanoparticles (CuO NPs) and their activity against Malassezia furfur. Singapore Journal of Scientific Research, 9(1), 13–19. https://doi.org/10.3923/sjsres.2019.13.19

Yousif DA, Hussein HZ, Ali AM (2019) Testing the efficiency of zinc oxide nanoparticles, honey, honey supported by Zinc oxide nanoparticles and phylex in degradation of aflatoxin B_1 in stored sea maize seeds. J Glob Pharma Technol 11: 225-235.

Yu, M.; Li, Y.; Banakar, S.P.; Liu, L.; Shao, C.; Li, Z.; Wang, C. New metabolites from the Co-culture of marine-derived actinomycete Streptomyces rochei MB037 and fungus Rhinocladiella similis 35. Front. Microbiol. 2019, 10, 915. [CrossRef].

Z

Zahoor M, Khan FA (2016) Aflatoxin B1 detoxification by magnetic carbon nanostructures prepared from maize straw. Desalination Water Treat 57: 11893-11903.

Zhang Y, Zhou M, Cheng H, Luo S, Sun Q (2021b) Insight into the substrate-dependent anti-aflatoxigenic effects of nanosized ZnO film: Electron transfer directed oxidative stress mechanisms. Colloids Surf B Biointerfaces 207: 111997.

Zhang, Y., Gao, F., Li, J., & Zhang, W. (2022). Phytotoxicity and accumulation of copper-based nanoparticles in higher plants: Mechanisms and risk assessment. Nanomaterials, 12(5), 852. https://doi.org/10.3390/nano12050852

Zhang, Y., Li, J., & Wang, H. (2023). Environmental fate and accumulation of copper nanoparticles in agricultural soils. Environmental Nanotechnology, 19, 100782. https://doi.org/10.1016/j.envnano.2023.100782

Zhou, X., Zhao, L., Luo, J., Tang, H., Xu, M., Wang, Y., Yang, X., Chen, H., Li, Y., Ye, G., Shi, F., Lv, C., & Jing, B. (2019). The toxic effects and mechanisms of nano-Cu on the spleen of rats. Int. J. Mol. Sci. 20, 1469.

Annexes

Annexes

1. Préparation du Potato Dextrose Agar (PDA)

Pomme de terre	200 g
Dextrose	20 g
Agar	15 g
Eau distillée	1 L

Procédure :

1. Faire bouillir les pommes de terre pelées et coupées en morceaux dans 500 mL d'eau pendant 30 min.

2. Filtrer et compléter le volume à 1 L, ajouter le dextrose et l'agar.

3. Ajuster le pH à 5,6 ± 0,2, puis stériliser à 121 °C pendant 15 min.

Préparation du Starch Casein Agar (SCA)

Amidon soluble	10 g
Caséine	0,3 g
KNO_3	2 g
NaCl	2 g
K_2HPO_4	2 g
$MgSO_4 \cdot 7H_2O$	0,05 g
$CaCO_3$	0,02 g
$FeSO_4 \cdot 7H_2O$	0,01 g
Agar	15 g
Eau distillée	1 L

Procédure :

1. Dissoudre les composants dans l'eau distillée en chauffant légèrement.

2. Ajuster le pH à 7,0 ± 0,2, puis stériliser à 121 °C pendant 15 min.

Préparation du GYM Broth

Glucose	4 g
Extrait de levure	4 g
Extrait de malt	10 g
Peptone	4 g
Eau distillée	1 L

Procédure :

1. Dissoudre tous les composants dans l'eau distillée.

2. Ajuster le pH à 7,2 ± 0,2 et stériliser à 121 °C pendant 15 min.

Préparation du GYM Agar

GYM Broth	1 L
Agar	15 g

Procédure :

1. Ajouter l'agar au GYM Broth et chauffer jusqu'à dissolution complète.

2. Ajuster le pH à 7,2 ± 0,2 et stériliser à 121 °C pendant 15 min.

Préparation de l'eau physiologique (NaCl 0,85 %)

Chlorure de sodium (NaCl)	8,5 g
Eau distillée	1 L

Procédure :

1. Dissoudre le NaCl dans l'eau distillée.

2. Répartir dans des flacons ou tubes et stériliser à 121 °C pendant 15 min.

Préparation des réactifs

1. Solution de DPPH (0,1 mM)

DPPH	0,0039 g
Méthanol	100 mL

Procédure :

Dissoudre le DPPH dans le méthanol, conserver la solution dans l'obscurité à température ambiante.

2. Solution de nitrate de cuivre ($Cu(NO_3)_2$, 0,01 M)

$Cu(NO_3)_2 \cdot 3H_2O$	0,241 g
Eau distillée	100 mL

Procédure :

Dissoudre le sel de cuivre dans l'eau distillée, conserver dans un flacon ambré.

3. Solution de NaOH (1 M)

NaOH	4 g
Eau distillée	100 mL

Procédure :

Dissoudre soigneusement le NaOH dans l'eau distillée, laisser refroidir et conserver à température ambiante.